

REPORT NO.
NASA-CR-54359
WESTINGHOUSE
WAED 66.39E
JUNE 1966

DEVELOPMENT AND EVALUATION OF MAGNETIC AND ELECTRICAL MATERIALS CAPABLE OF OPERATING IN THE 800° TO 1600°F TEMPERATURE RANGE

Sixth Quarterly Report

edited by
P. E. Kueser et al

prepared for
NATIONAL AERONAUTICS AND SPACE ADMINISTRATION
LEWIS RESEARCH CENTER
UNDER CONTRACT NAS3-6465



Westinghouse Electric Corporation
AEROSPACE ELECTRICAL DIVISION
LIMA, OHIO

FACILITY FORM 802	N67-29988	(THRU)
	(ACCESSION NUMBER)	
	10/63 RS 25	(CODE)
	(PAGES)	
27H	CR-54359-110	17
	(NASA-CR OR TMX OR AD NUMBER)	(CATEGORY)

20 Report No. 66.39E 29C

29C. QR-6 END

9 June 1966 10cy

3 DEVELOPMENT AND EVALUATION OF MAGNETIC AND
ELECTRICAL MATERIALS CAPABLE OF OPERATING
IN THE 800° TO 1600°F TEMPERATURE RANGE 4

Deq

SIXTH QUARTERLY REPORT
(MARCH 1, 1966 - MAY 31, 1966) 6

sponsored by

NATIONAL AERONAUTICS AND SPACE ADMINISTRATION
CONTRACT NAS 3-6465

25

29A

Project Management
NASA - Lewis Research Center
Space Power Systems Division
R. A. Lindberg

Prepared by:

6 P. E. Kueser, et al 9

Manager, NASA Materials Study
and Research Program

Approved by:

N. W. Bucci, Jr.

Manager, Engineering
Development Department

1 Westinghouse Electric Corporation
2 Aerospace Electrical Division 3
Lima, Ohio 3

PREFACE

The work reported here was sponsored by the Space Power Systems Division of the NASA Lewis Research Center under Contract NAS 3-6465. Mr. R. A. Lindberg of NASA has provided the Project Management for the program. His review and suggestions as well as those of Mr. T. A. Moss, also of NASA, are gratefully acknowledged. The Westinghouse Aerospace Electrical Division (WAED) is responsible for the Technical Direction of the program. The Westinghouse Research and Development Center (WR&D) is conducting Tasks 1, 2, and 4 of Program I on Optimized Magnetic Materials for Application in the 1000 to 1200°F Range, the Investigation for Raising the Alpha to Gamma Transformation, and Creep Testing of Rotor Materials. Eitel-McCullough (EIMAC) is responsible for the Bore Seal Development, Task 1 of Program III. All other tasks are being conducted at the Westinghouse Aerospace Electrical Division (WAED).

In a program of this magnitude a large group of engineers and scientists are involved in its progress. An attempt to recognize those who are contributing directly, together with their area of endeavor, follows:

Program I - Magnetic Materials for High-Temperature Operation

Task 1 - Optimized Precipitation Hardened Magnetic Materials
for Application in the 1000 to 1200°F Range

Dr. K. Detert (WR&D); J. W. Toth (WAED)

Task 2 - Investigation for Raising the Alpha to Gamma Transformation
Temperature in Cobalt-Iron Alloys

Dr. K. Detert (WR&D); J. W. Toth (WAED)

Task 3 - Dispersion-Strengthened Magnetic Materials for Application
in the 1200 to 1600°F Range

Dr. R. J. Towner (WAED)

Task 4 - Creep Testing

M. Spewock (WR&D); D. H. Lane (WAED)

Program II High-Temperature Capacitor Feasibility

R. E. Stapleton (WAED)

Program III - Bore Seal Development and Combined Material Investigation
Under a Space Simulated Environment

Task 1 - Bore Seal Development

R. C. McRae, Dr. L. Reed, M. F. Parkman (EIMAC);
J. W. Toth (WAED)

Tasks 2, 3, 4 - Stator and Bore Seal, Transformer and Solenoid

W. L. Grant, H. E. Keneipp, D. H. Lane, R. P. Shumate,
J. W. Toth (WAED)

Dr. A. C. Beiler (WAED) and Dr. G. W. Wiener (WR&D) are acting as consultants on Program I.

SUMMARY

This is the sixth quarterly report on Contract NAS 3-6465 for the Development and Evaluation of Magnetic and Electrical Materials Capable of Operating in the Temperature Range from 800 to 1600°F. Advanced space electric power systems are the area of eventual application.

Program I is directed at developing high-temperature magnetic materials with satisfactory strength for use in the solid rotors of electrical generators. The precipitation strengthened magnetic materials for final evaluation from 15-pound ingots have been selected. They were selected based upon their hardening response and stability. The stability was determined from isothermal aging studies on hardness and coercive force. The final martensitic alloy selected was Fe-12Ni-30Co-3Ta-1W-0.4Al-0.4Ti; and the final cobalt-base alloy was Co-15Ni-5Fe-1.3Al-5Ta-0.2Zr. Dispersion-strengthening has continued on cobalt-iron and cobalt-base alloys. Low-coercive (< 25 oersteds) force has been achieved, a problem area originally expected because of the nature of dispersion-strengthening. Saturation magnetization has been lowered in proportion to the volume of non-magnetic dispersoids. This is as expected. High-strength and creep resistance has been promoted by small interparticle spacings. Coarser particles tend to lower coercive force. These observations on the structure desired for a dispersion-strengthened magnetic material are based on the first phase of the program. The latter two phases will use these as a guide for the final alloy selection. Creep testing has continued on Nivco alloy which is the best, presently-available, magnetic rotor alloy. Six thousand two-hundred hours at 1100°F and a pressure of 1.7×10^{-9} torr has been achieved. Creep strain amounts to 0.66 percent.

Program II will determine the feasibility of high-temperature capacitors using high-quality dielectric materials. A five-layer capacitor of BN with platinum electrodes completed its 250 hour stability test with no significant change in performance. Total capacitance change was only 1.39 percent which occurred in the first 65 hours.

Program III incorporates developments on alkali-metal compatible ceramic-to-metal seals and combinations of material designed into a stator with a bore seal, a transformer, and a solenoid for investigations of compatibility under electrical and magnetic stress at elevated temperature and under high vacuum. Two four-inch bore seals were successfully fabricated joining high-purity beryllia ($> 99.8\%$) to Cb-1Zr using a wetting layer of molybdenum and a Zr-V-Cb

active-metal braze. The stator, transformer, and solenoid continued on test at 1100°F hot-spot temperature in vacuum. Pressures have continued to decrease and are in the 10^{-9} torr range. No changes in performance have been observed in the electrical conductor performance after >4000 hours of testing. Electrical insulation performance on a-c components also has been unaffected, but a slight decrease in resistance has been observed in the energized solenoid indicating that an invariant electrical stress on these materials may influence its performance.

TABLE OF CONTENTS

<u>Section</u>		<u>Page</u>
	PREFACE	ii
	SUMMARY	iv
I	INTRODUCTION	1
II	PROGRAM I - MAGNETIC MATERIALS FOR HIGH-TEMPERATURE OPERATION	3
	A. Task 1 - Optimized Precipitation Hardened Magnetic Materials for Application in the 1000 to 1200° F Range	4
	1. Summary of Technical Progress	4
	2. Discussion	4
	a. Experimental Procedure	6
	b. Results	10
	3. Program for the Next Quarter	55
	B. Task 2 - Investigation for Raising the Alpha to Gamma Transformation Temperature in Cobalt-Iron Alloys	56
	C. Task 3 - Dispersion-Strengthened Magnetic Materials for Application in the 1200 to 1600° F Range	57
	1. Summary of Technical Progress	57
	2. Discussion	58
	a. Processing of Powders Into Extrusions ..	59
	b. Testing of Extrusions	59
	c. Secondary Working	73
	d. Plans for Intermediate Evaluation	74
	3. Program for the Next Quarter	75
	D. Task 4 - Creep Testing	76
	1. Summary of Technical Progress	76
	2. Discussion	76
	3. Program for the Next Quarter	76

TABLE OF CONTENTS - Continued

<u>Section</u>		<u>Page</u>
III	PROGRAM II - HIGH TEMPERATURE CAPACITOR FEASIBILITY	80
	A. Summary of Technical Progress.....	80
	B. Discussion.....	82
	1. Pyrolytic Boron Nitride Multi-Layer Capacitors.....	83
	a. Rectangular Wafer Capacitors.....	83
	b. Tabbed Wafer Capacitors.....	84
	C. Program for the Next Quarter	92
IV	PROGRAM III - BORE SEAL DEVELOPMENT AND COMBINED MATERIAL INVESTIGATIONS UNDER A SPACE-SIMULATED ENVIRONMENT.....	93
	A. Task 1 - Bore Seal Development.....	94
	1. Summary of Technical Progress	94
	2. Discussion.....	96
	a. Properties of Ceramic-to-Metal Seal Components.....	96
	b. Ceramic-to-Metal Joining	101
	c. Model Bore Seal Construction.....	106
	d. Conclusions.....	120
	3. Program for the Next Quarter.....	120
	B. Task 2 - Stator and Bore Seal.....	121
	1. Summary of Technical Progress	121
	2. Discussion.....	121
	a. Stator Installation, Construction and Operation at 1100°F.....	121
	b. Stator Data and Discussion	125
	c. Status of 1300°F Stator Model - 2nd 5000 Hour Test.....	128
	3. Program for the Next Quarter.....	129
	C. Task 2 - Transformer.....	130
	1. Summary of Technical Progress	130
	2. Discussion.....	130
	a. Transformer Installation, Construction and Operation at 1100°F.....	130

TABLE OF CONTENTS - Concluded

<u>Section</u>	<u>Page</u>
IV (Cont.)	
b. Transformer Data and Discussion	133
c. Status of 1300°F Transformer Model - 2nd 5000 Hour Test.....	136
3. Program for the Next Quarter	137
D. Task 4 - Solenoid.....	138
1. Summary of Technical Progress	138
2. Discussion.....	138
a. Solenoid Installation, Construction and Operation at 1100°F.....	138
b. Solenoid Data and Discussion.....	139
c. Status of 1300°F Solenoid Model - 2nd 5000 Hour Test.....	142
3. Program for the Next Quarter	142
REFERENCES.....	143

LIST OF FIGURES

<u>Number</u>	<u>Title</u>	<u>Page</u>
II-1	Hot Hardness vs. Temperature of Alloy 1-A-V-4 After Annealing One Hour at 1832°F (1000°C) and Aging at 1112°F (600°C). Test Load 2.5 kG	18
II-2	Hot Hardness vs. Temperature of Alloy 1-B-V-4 After Annealing One Hour at 1832°F (1000°C) and Aging at 1112°F (600°C). Test Load 2.5 kG	19
II-3	Hardness and Coercive Force of Alloys 1-A-S-1, 1-A-S-2, 1-B-S-1, and 1-B-S-2 at Room Temperature After Aging One Hour at Temperature	20
II-4	Change in Room Temperature Hardness and Coercive Force During Isothermal Aging at 1022°F (550°C) of Alloy 1-A-S-1 Annealed, and Annealed and Five Percent Deformed	23
II-5	Change in Room Temperature Hardness and Coercive Force During Isothermal Aging at 1022°F (550°C) of Alloy 1-A-S-2 Annealed, and Annealed and Five Percent Deformed	24
II-6	Change in Room Temperature Hardness and Coercive Force of Alloys 1-B-S-1 and 1-B-S-2 During Isothermal Aging at 1292°F (700°C)	25
II-7	Microstructure of Alloy 1-A-V-1 (48Fe-15Ni-30Co-2W-4Ta-0.5Al-0.5Ti) After 100 Hours Aging at 1022°F (550°C) 500 X	26
II-8	Microstructure of Alloy 1-A-V-2 (66Fe-10Ni-20Co-3Ta-0.5Al-0.5Ti) After 100 Hours Aging at 1022°F (550°C) 500 X	27
II-9	Microstructure of Alloy 1-A-V-3 (57.5Fe-12Ni-25Co-1W-3.5Ta-0.5Al-0.5Ti) After 100 Hours Aging at 1022°F (550°C) 500 X	28
II-10	Microstructure of Alloy 1-A-V-4 (51Fe-15Ni-30Co-3Ta-0.5Al-0.5Ti) After 100 Hours Aging at 1022°F (550°C) 500 X	29
II-11	Microstructure of Alloy 1-A-V-5 (49Fe-15Ni-30Co-2W-3Ta-0.5Al-0.5Ti) After 100 Hours Aging at 1022°F (550°C) 500 X	30

LIST OF FIGURES - Continued

<u>Number</u>	<u>Title</u>	<u>Page</u>
II-12	Microstructure of Alloy 1-A-V-6 (60Fe-5Ni-5Cr-25Co-1W-3Ta-0.5Al-0.5Ti) After 100 Hours Aging at 1022°F (550°C) 500 X	31
II-13	Microstructure of Alloy 1-B-V-1 (71.7Co-5Fe-15Ni-1.5Ti-1.5Al-0.3Zr-5Ta) After 100 Hours Aging at 1292°F (700°C) 500 X	32
II-14	Microstructure of Alloy 1-B-V-2 (80.5Co-5Fe-10Ni-1.2Al-0.3Zr-3Ta) After 100 Hours Aging at 1292°F (700°C) 500 X	33
II-15	Microstructure of Alloy 1-B-V-3 (76.3Co-5Fe-12Ni-1.0Ti-1.4Al-0.3Zr-4Ta) After 100 Hours Aging at 1292°F (700°C) 500 X	34
II-16	Microstructure of Alloy 1-B-V-4 (73.5Co-5Fe-15Ni-1.2Al-0.3Zr-5Ta) After 100 Hours Aging at 1292°F (700°C) 500 X	35
II-17	Microstructure of Alloy 1-B-V-5 (78.2Co-5Fe-10Ni-1.5Al-0.3Zr-5Ta) After 100 Hours Aging at 1292°F (700°C) 500 X	36
II-18	Microstructure of Alloy 1-B-V-6 (74Co-5Fe-15Ni-1.5Ti-1.2Al-0.3Zr-3Ta) After 100 Hours Aging at 1292°F (700°C) 500 X	37
II-19	Microstructure of Alloy 1-A-S-1 (50.3Fe-15Ni-30Co-1W-3Ta-0.3Al-0.4Ti+0.001B+0.003Zr) After 100 Hours Aging at 1022°F (550°C) 500 X	38
II-20	Microstructure of Alloy 1-A-S-2 (53.2Fe-12Ni-30Co-1W-3Ta-0.4Al-0.4Ti+0.001B+0.003Zr) After 100 Hours Aging at 1022°F (550°C) 500 X	39
II-21	Microstructure of Alloy 1-B-S-1 (73.55Co-5Fe-15Ni-1.25Al-5.0Ta-0.2Zr-0.001B) After 100 Hours Aging at 1292°F (700°C) 500 X	40
II-22	Microstructure of Alloy 1-B-S-2 (73.55Co-5Fe-15Ni-1.25Al-5.0Ta-0.1Zr-0.1Be-0.001B) After 100 Hours Aging at 1292°F (700°C) 500 X	41
II-23	Electron Transmission Micrograph of Alloy 1-A-V-4 (51Fe-15Ni-30Co-3Ta-0.5Al-0.5Ti) After Annealing One Hour at 1832°F (1000°C) 42,000 X.....	43

LIST OF FIGURES - Continued

<u>Number</u>	<u>Title</u>	<u>Page</u>
II-24	Electron Transmission Micrograph of Alloy 1-A-V-4 (51Fe-15Ni-30Co-3Ta-0.5Al-0.5Ti) After Annealing One Hour at 1832°F (1000°C) and 100 Hours Aging at 1022°F (550°C) 31,000 X	44
II-25	Electron Microscope Replica of Alloy 1-A-V-4 (51Fe-15Ni-30Co-3Ta-0.5Al-0.5Ti) After Annealing One Hour at 1832°F (1000°C) and 100 Hours at 1022°F (550°C) 10,500 X	45
II-26	Electron Transmission Micrograph of Alloy 1-B-V-4 (73.5Co-5Fe-15Ni-1.2Al-0.3Zr-5Ta) After Annealing One Hour at 1832°F (1000°C) and Aging 100 Hours at 1292°F (700°C) 14,000 X	46
II-27	Electron Microscope Replica of Alloy 1-B-V-4 (73.5 Co-5Fe-15Ni-1.2Al-0.3Zr-5Ta) After Annealing One Hour at 1832°F (1000°C) and 100 Hours Aging at 1292°F (700°C) 17,500 X	47
II-28	Dynapak As-Extruded Rod of Atomized Powder No. 13, Fe+24.8%Co+1.1%B+3.2%Zr, Showing (Fe,Co) ₂ B Particles (A-light) and ZrO ₂ Particles (B-dark) Dispersed in Fe-Co Recrystallized Matrix, Longitudinal Section, 1000X, Etched in Carapella's Reagent	60
II-29	Hydraulic As-Extruded Rod of Atomized Powder No. 13, Showing Coarser (Fe,Co) ₂ B Particles (A-light) than in Figure II-28 in Fe-Co Recrystallized Matrix, Longitudinal Section, 1000X, Etched in Carapella's Reagent	61
II-30	Yield Strength and Saturation Magnetization at 1200°F of Dispersion-Strengthened Extrusions and Nivco ..	68
II-31	Yield Strength and Saturation Magnetization at 1600°F of Dispersion-Strengthened Extrusions and Nivco ..	69
II-32	Creep, Nivco Heat 10-NO2V-1099, Tested in Vacuum at 1100°F and 37,500 psi (Specimen #2)	77
II-33	Creep, Nivco Heat 10-NO2V-1099, Tested in Vacuum at 1150°F and 25,000 psi and 30,000 psi.	78

LIST OF FIGURES - Continued

<u>Number</u>	<u>Title</u>	<u>Page</u>
II-34	Creep, Nivco Heat 10-NO2V-1099, Tested in Vacuum at 1050°F and 50,000 psi (Specimen #5)	79
III-1	Change in Capacitance vs. Time at 500 Volts/mil in Vacuum (4×10^{-7} to 1.1×10^{-8} torr) at 1100°F for a Five (5) Wafer Pyrolytic Boron Nitride Capacitor.	91
IV-1	Photograph of the Beryllia Rings and Tubes Used In the Two Inch Ceramic-to-Metal Seal Test Assemblies..	97
IV-2	Schematic of Two Inch Ceramic-to-Metal Seal Used In the High Temperature Mechanical and Vacuum Tests.....	99
IV-3	Schematic of High Temperature Leak Detector Apparatus Used On the Two Inch Ceramic-to-Metal Seals..	100
IV-4	Schematic of Ceramic Metallizing Apparatus	102
IV-5	Photograph of Ceramic Metallizing Apparatus	103
IV-6	Schematic of Four Inch Model Bore Seal.....	108
IV-7	Photograph of Thermalox 998 Beryllia Tube After Dye Penetrant Check	109
IV-8	Schematic of Endbell Flange Leveling Fixture for the Four Inch Model Bore Seals	110
IV-9	Sub-Assembly of a Model Four Inch Thermalox 998 BeO-(Cb-1Zr) Bore Seal.....	111
IV-10	Photograph of Four Inch Model Bore Seal in Brazing Fixture	114
IV-11	Time Temperature Brazing Curves of Thermalox 998 - (Cb-1Zr) Model Bore Seals No. 1 and 2	116
IV-12	Photograph of Thermalox 998 - (Cb-1Zr) Brazed Bore Seal No. 1	117
IV-13	Schematic of Four Inch Model BeO - (Cb-1Zr) Bore Seal In Room Temperature Vacuum/Pressure Testing Apparatus	119
IV-14	Cutaway View of Vacuum Furnace Showing the Stator Test Specimen Installed	122
IV-15	Stator Chamber Pressure vs. Endurance Test Time 1100°F Stator Hot Spot	126
IV-16	Stator Conductor Resistance vs. Endurance Test Time at Noted Conductor Hot Spot Temperatures	127

LIST OF FIGURES - Concluded

<u>Number</u>	<u>Title</u>	<u>Page</u>
IV-17	Cutaway View of a Vacuum Furnace Showing Installation of Two Solenoids and a Transformer	131
IV-18	Transformer and Solenoid Chamber Pressure vs. En- durance Test Time	134
IV-19	Transformer Winding Resistance vs. Endurance Test Time	135
IV-20	Solenoid Conductor Resistance vs. Endurance Test Time	140

LIST OF TABLES

<u>Number</u>	<u>Title</u>	<u>Page</u>
II-1	Chemical Analysis of 300 Gram Vacuum Arc Melted Martensitic Alloys 1-A-V-1 to 1-A-V-6 and Cobalt-Base Alloys 1-B-V-1 to 1-B-V-6 (expressed in weight percent)	7
II-2	Chemical Analysis of 300 Gram Vacuum Arc Melted Martensitic Alloys 1-A-V-1 to 1-A-V-6 and Cobalt-Base Alloys 1-B-V-1 to 1-B-V-6 (expressed in atomic percent)	7
II-3	Nominal Composition of Final Alloys Vacuum Induction Melted as 15-Pound Ingots	8
II-4	Chemical Analysis of Final Alloys Vacuum Induction Melted as 15-Pound Ingots (expressed in weight percent)	8
II-5	Composition of Final Alloys Vacuum Induction Melted as 15-Pound Ingots Based on Chemical Analysis (expressed in atomic percent)	8
II-6	Saturation Magnetic Moment of 300 Gram Vacuum Arc Melted Martensitic Alloys 1-A-V-1 to 1-A-V-6 . . .	11
II-7	Magnetic Moment of 300 Gram Vacuum Arc Melted Cobalt-Base Alloys 1-B-V-1 to 1-B-V-6	11
II-8	Coercive Force Measurements on 300 Gram Vacuum Arc Melted Martensitic Alloys 1-A-V-1 to 1-A-V-6 at Different Temperatures	13
II-9	Coercive Force Measurements on 300 Gram Vacuum Arc Melted Cobalt-Base Alloys 1-B-V-1 to 1-B-V-6 at Different Temperatures	13
II-10	Tensile Tests of 300 Gram Vacuum Arc Melted Martensitic Alloys 1-A-V-1 to 1-A-V-6	14
II-11	Tensile Tests of 300 Gram Vacuum Arc Melted Cobalt-Base Alloys 1-B-V-1 to 1-B-V-6	15
II-12	Hot Hardness Measurements on Samples of 300 Gram Vacuum Arc Melted Martensitic Alloys 1-A-V-1 to 1-A-V-6 After Annealing One Hour at 1832°F (1000°C) and Aging One Hour at 1112°F (600°C) . . .	17
II-13	Hot Hardness Measurements on Samples of 300 Gram Vacuum Arc Melted Cobalt-Base Alloys 1-B-V-1 to 1-B-V-6 After Annealing One Hour at 1832°F (1000°C) and Aging One Hour at 1382°F (750°C) . .	17

LIST OF TABLES - Continued

<u>Number</u>	<u>Title</u>	<u>Page</u>
II-14	Maximum Hardness Obtained by the Isochronal Aging of the Final Alloys Vacuum Induction Melted as 15-Pound Ingots	22
II-15	Saturation Magnetic Moment of the Final Alloys Vacuum Induction Melted as 15-Pound Ingots	22
II-16	Phases Detected in Alloy 1-A-V-4, After Aging 100 Hours at 1022°F (550°C) and in Alloy 1-B-V-4, After Aging 100 Hours at 1292°F (700°C) With and Without a Previous Deformation by 50 Percent Cold Rolling	48
II-17	Properties of Martensitic Alloys 1-A-V-1 to 1-A-V-6 and 1-A-S-1 and 1-A-S-2	50
II-18	Properties of Cobalt-Base Alloys 1-B-V-1 to 1-B-V-6 and 1-B-S-1 and 1-B-S-2	53
II-19	X-ray Diffraction Identification of Dispersed Constituent Particles in Extrusions	62
II-20	Comparison of Room Temperature Coercive Force Values of Extrusions Made With a Conventional Hydraulic Press and Dynapak	64
II-21	Comparison of Elevated Temperature Tensile Properties of Extrusions Made With a Conventional Hydraulic Press and Dynapak	66
II-22	Legend for Figures II-30 and II-31	70
II-23	Tensile and Magnetic Properties of Dispersion-Strengthened Rod (as-extruded) at 1200°F and 1600°F	72
III-1	Evaluation Data For Individual Wafers In the Nine (9) Wafer Pyrolytic Boron Nitride Capacitor	85
III-2	Life Test Data - Nine (9) Wafer Pyrolytic Boron Nitride Capacitor	87
III-3	Evaluation Data For Individual Wafers Used In the Five (5) Wafer Pyrolytic Boron Nitride Capacitor	89
III-4	Two Hundred Fifty Hour Life Test Data - Five (5) Wafer Pyrolytic Boron Nitride Capacitor	90

LIST OF TABLES - Concluded

<u>Number</u>	<u>Title</u>	<u>Page</u>
IV-1	Analysis of Beryllia Powder Used in Fabrication of Two Inch by Two Inch Bore Seal Test Assemblies	96
IV-2	Room Temperature Flexural Strength of Several Lots of Thermalox 998 Beryllia Ceramics and Ceramic- to-Metal Seal Assemblies	105
IV-3	Analyses of Beryllia Powder and Fired Ceramics for the Four Inch Beryllia Tubes	107
IV-4	Stator Insulation Performance.....	129
IV-5	Transformer Insulation Performance	136
IV-6	Solenoid Insulation Performance	141

SECTION I

INTRODUCTION

This is the sixth quarterly report on Contract NAS 3-6465 for the Development and Evaluation of Magnetic and Electrical Materials Capable of Operating in the Temperature Range from 800 to 1600°F. The period of performance is from March 1, 1966 through May 30, 1966. The program consists of three Programs with their related tasks as follows:

Program I - Magnetic Materials for High-Temperature Operation

Task 1 - Optimized Precipitation Hardened Magnetic Materials for Application in the 1000 to 1200°F Range

Task 2 - Investigation for Raising the Alpha to Gamma Transformation Temperature in Cobalt-Iron Alloys (completed)

Task 3 - Dispersion-Strengthened Magnetic Materials for Application in the 1200 to 1600°F Range

Task 4 - Creep Testing

Program II - High-Temperature Capacitor Feasibility

Program III - Bore Seal Development and Combined Material Investigation Under a Space Simulated Environment

Task 1 - Bore Seal Development

Task 2 - Stator and Bore Seal

Task 3 - Transformer

Task 4 - Solenoid

In Program I, limitations in magnetic material performance at elevated temperature have been recognized from Contract NAS 3-4162 and the development of materials incorporating improved magnetic and mechanical properties is being pursued. In the 1000 to 1200°F range, precipitation hardening of cobalt-base and martensitic alloys is in progress. Dispersion-strengthened cobalt and cobalt-iron is under evaluation in the 1200 to 1600°F range. In most cases, high-strength compromises the magnetic properties; therefore, a balance between these two variables is sought.

Program II is directed at determining the feasibility of applying high-quality dielectric materials and their processes to a high-temperature (1100°F) capacitor which is lightweight and suitable for static power conditioning apparatus used in space applications.

Program III incorporates development on ceramic-to-metal seals and on combinations of materials previously evaluated under Contract NAS 3-4162 into a stator with a bore seal, a transformer, and a solenoid for investigation of compatibility under electrical and magnetic stress at elevated temperature and high vacuum.

The three Programs will be reported consecutively in Sections II, III, and IV. Section II and Section IV are further divided into their respective tasks. Each task is reported separately and includes a summary of technical progress, a discussion, and the program for the next quarter so the reader may obtain an understanding of each task.

The first, second, third, fourth, and fifth quarterly reports were issued as NASA CR-45354, CR-45355, CR-45356, CR-45357, and CR-45358. These reports are extensively referenced in this report and fully identified in Section V. Other references identified by number in the discussion of each task are contained in Section V. These are identified in Section V by the program and task for which the reference is applicable.

SECTION II

PROGRAM I - MAGNETIC MATERIALS FOR HIGH-TEMPERATURE OPERATION

Program I is directed at improvement and further understanding of magnetic materials suitable for application in the rotor of a generator or motor in advanced space electric power systems.

Task 1 is concerned with precipitation-hardened magnetic materials in the 1000 to 1200°F range. These materials are of the iron-cobalt-nickel ternary system. The two specific areas of interest are the iron and cobalt corners of the ternary system.

Task 2 is a small research investigation for determining the feasibility of raising the alpha to gamma transformation temperature in the iron-cobalt system; thereby increasing the useful magnetic temperature of this system. This investigation is completed and the final results were given in the third quarterly report. Selected alloy additions of 3 to 5 weight percent increased the transformation temperature approximately 9°F(5°C) for each weight percent added. Magnetic saturation was lowered by each addition. If only a 45°F increase in alpha to gamma transformation temperature is desired, at a slight sacrifice in magnetic saturation, several alloying agents are satisfactory.

Task 3 is directed at applying dispersion-strengthening mechanisms to magnetic materials to achieve useful and invariant mechanical and magnetic properties in the 1200 to 1600°F range. Because both variables are influenced differently by particle size and spacing, a compromise is sought thereby tailoring the materials to the need of dynamic electric machines.

Task 4 is a creep program on Nivco alloy (approximately 72 percent cobalt, 23 percent nickel and certain other elements) which will generate 10,000 hour design data in a vacuum environment (1×10^{-6} torr or less). This material represents a presently available magnetic material with the highest useful application temperature for stressed applications.

A. TASK 1 - OPTIMIZED PRECIPITATION HARDENED MAGNETIC MATERIALS FOR APPLICATION IN THE 1000 TO 1200°F RANGE

1. Summary of Technical Progress

- a) Testing of the alloys made in the form of 300 gram buttons has been completed.
- b) Four compositions, two ferritic alloys and two cobalt-base alloys, were derived for melting as 15-pound ingots. These four alloys have been melted and fabricated into sheet and bar. Samples have been made for preliminary tests to check the reproducibility of results predicted from previous alloys of a smaller size.
- c) The preliminary tests including hardness tests, coercive force measurements, and magnetic saturation measurements showed that the reproducibility remained within the expected limits.
- d) Two final alloys have been selected for thorough evaluation by determining the magnetic properties more completely and by studying the aging kinetics. The compositions of these alloys are:

Ferritic alloy 1-A-S-2, Fe-12Ni-30Co-3Ta-1W-0.4Al-0.4Ti
Cobalt-base alloy 1-B-S-1, Co-15Ni-5Fe-1.3Al-5.0Ta-0.2Zr

2. Discussion

The objective of this program is to find and evaluate an alloy composition which displays high-creep strength and useful ferromagnetic properties in the range of 1000 to 1200°F. The target ultimate tensile strength for the alloy at 1100°F is 125,000 psi or better. The target stress to produce 0.4 percent creep strain in 1000 hours at 1100°F is 76,000 psi or greater. The 10,000 hour stress target at 1100°F is 80 to 90 percent of that at 1000 hours. The target magnetic saturation for the developmental alloy is 13,000 gauss or better at 1100°F and a coercive force less than 25 oersteds.

An alloy screening program which defines a range of alloy compositions with an optimum combination of high-strength, high magnetic saturation, low coercive force, and stability of structure has been completed. Based on the results of the screening tests, several 15-pound heats were melted to study alloy mechanical and magnetic properties in more detail.

In the first phase of the screening program, a large variety of alloys were melted by levitation melting in the form of 25 gram buttons. Hardness tests, coercivity measurements, and saturation measurements after a suitable heat treatment as well as dilatometer tests; were conducted to provide representative property and thermal stability data. The results of these tests were reported in the first five quarterly reports. From these results two types of alloys were derived as candidate materials for further study.

A ferritic type alloy which undergoes a martensitic transformation during cooling exhibited very high strength. Its composition range was fixed within the following limits:

Ni: 10 to 15 weight percent, Co: 20 to 30 weight percent,
Cr: up to 5 weight percent by substituting 2 weight percent
Ni with every weight percent of Cr, Ta: 3 to 4 weight percent,
W: 0 to 5 weight percent, Al: 0.0 to 0.5 weight percent,
Ti: 0.0 to 0.5 weight percent, Fe: balance.

A precipitation process in the martensitic matrix produces the high strength during an aging treatment.

A cobalt-base alloy showed remarkable stability of the matrix to 1292°F (700°C) when the composition remained within the following limits:

Ni: 10 to 15 weight percent, Fe: 5 weight percent, Al: 1.0 to 1.5 weight percent, Ti: 0 to 1.5 weight percent, Ta: 2 to 4 weight percent, Zr: 0.2 to 0.3 weight percent, Co: balance.

This alloy is strengthened by a precipitation process which forms a precipitate phase that remains partially coherent in the matrix.

In the second phase of the screening investigation, 12 alloys were melted in the form of 300 gram buttons by vacuum-arc melting. The compositions of the 12 alloys were selected within the limits of composition specified above. Testing of these alloys should demonstrate the degree of reproducibility of results when the melt size is enlarged from 25 grams to 300 grams and a different melting technique is employed. Furthermore, the testing of the larger ingots was extended to measure VHN hardness and coercive force at a higher temperature. Tensile tests were also performed.

The preparation of samples and a portion of the test results obtained on the 300 gram vacuum-arc melted buttons were reported previously in the fifth quarterly report. The remainder of the test results from the 300 gram buttons are given in this report. After evaluating these tests, four alloy compositions were chosen for melting in the form of 15-pound ingots. Two of these heats will serve as sample material for a more detailed evaluation of mechanical and magnetic properties. Preliminary test results obtained on the 15-pound ingots are reported in a later section of this report.

a. EXPERIMENTAL PROCEDURE

The method of melting the 300 gram buttons by non-consumable electrode vacuum-arc melting was reported in the fifth quarterly report. The analyses of the compositions are listed in Table II-1. Table II-2 shows the compositions converted into atomic percent.

The compositions of the final four alloys are given in Tables II-3, II-4, and II-5. Table II-3 shows the nominal composition, Table II-4, the analyzed composition, and Table II-5, the analyzed composition expressed in atomic percent.

The charge used in melting the large ferritic alloy ingots weighed 8000 grams and the charge used in the cobalt-base alloys weighed 8500 grams. The metals used in the charges correspond to those listed in the third quarterly report. The alloying additions were obtained from master alloys as specified in the fifth quarterly report.

The alloy melting was started with the Fe-Ni-Co metals in an induction furnace using a heating coil of three windings operating at 10,000 cycles at a nominal 50 kVA. The molten material was held for about one hour at a vacuum of 2×10^{-4} torr, then one gram of Mischmetal was added. After the pressure returned to 2×10^{-4} torr, the furnace was back-filled with argon to a pressure of 280 mm. The alloying elements were added as required. Nickel-zirconium and iron-boron were the last additions. The same magnesium oxide crucible was used for all melts. The alloys were then cast into an iron tube ten inches long with a two-inch inside diameter. The tube, coated with a zirconia wash, was positioned on a copper plate. A funnel shaped from refractory brick was placed on top of the tube. The top of the ingots formed in this mold

TABLE II-1. Chemical Analysis of 300 Gram Vacuum Arc Melted Martensitic Alloys 1-A-V-1 to 1-A-V-6 and Cobalt-Base Alloys 1-B-V-1 to 1-B-V-6 (expressed in weight percent)

Alloy Number	Fe	Co	Ni	Ta	Ti	Al	W	Cu	C	Cr	Zr
1-A-V-1	47.4	29.2	14.6	4.50	0.49	0.56	2.15	0.005	0.0057	-	-
1-A-V-2	65.5	20.1	9.57	3.56	0.53	0.63	<0.2	0.020	0.0034	-	-
1-A-V-3	57.2	25.0	11.4	4.06	0.52	0.61	1.00	0.005	0.0028	-	-
1-A-V-4	52.2	29.4	14.8	3.48	0.52	0.64	<0.2	0.006	0.0029	-	-
1-A-V-5	48.6	29.8	14.5	3.48	0.54	0.62	2.10	0.005	0.0032	-	-
1-A-V-6	59.8	25.7	4.66	3.56	0.49	0.64	1.18	0.058	0.015	5.19	-
1-B-V-1	5.0	68.0	14.6	5.20	1.66	1.44	0.010	0.29	0.0030	-	0.27
1-B-V-2	4.8	79.2	10.3	3.07	<0.2	1.19	0.008	0.018	0.0036	-	0.27
1-B-V-3	4.9	76.0	11.9	4.05	1.07	1.40	0.029	0.087	0.0039	-	0.26
1-B-V-4	5.1	72.8	14.8	5.19	<0.2	1.25	<0.005	0.018	0.0045	-	0.26
1-B-V-5	5.0	77.0	9.85	5.30	0.2	1.60	0.11	0.023	0.0047	-	0.27
1-B-V-6	4.8	69.0	15.0	3.10	1.66	1.19	0.12	0.013	0.0046	-	0.24

TABLE II-2. Chemical Analysis of 300 Gram Vacuum Arc Melted Martensitic Alloys 1-A-V-1 to 1-A-V-6 and Cobalt-Base Alloys 1-B-V-1 to 1-B-V-6 (expressed in atomic percent)

Alloy Number	Fe	Co	Ni	Ta	Ti	Al	W	Cu	C	Cr	Zr
1-A-V-1	bal	29.49	14.80	1.48	0.61	1.24	0.70	-	-	-	-
1-A-V-2	bal	19.68	9.41	1.14	0.64	1.35	-	-	-	-	-
1-A-V-3	bal	24.84	11.37	1.31	0.64	1.32	0.32	-	-	-	-
1-A-V-4	bal	28.99	14.65	1.12	0.66	1.38	-	-	-	-	-
1-A-V-5	bal	29.85	14.58	1.14	0.67	1.36	0.67	-	-	-	-
1-A-V-6	bal	25.29	4.60	1.14	0.59	1.38	0.37	-	-	5.79	-
1-B-V-1	5.34	bal	14.83	1.71	2.07	3.18	-	-	-	-	0.18
1-B-V-2	5.09	bal	10.39	1.00	-	2.61	-	-	-	-	0.19
1-B-V-3	5.20	bal	12.02	1.33	1.32	3.08	-	-	-	-	0.17
1-B-V-4	5.48	bal	15.12	1.72	-	2.78	-	-	-	-	0.17
1-B-V-5	5.35	bal	10.03	1.75	-	3.55	-	-	-	-	0.18
1-B-V-6	5.02	bal	14.92	1.00	2.02	4.31	-	-	-	-	0.15

TABLE II-3. Nominal Composition of Final Alloys Vacuum Induction Melted as 15-Pound Ingots (expressed in weight percent)

Alloy Number	Fe	Ni	Co	W	Ta	Al	Ti	Zr	Be	B	C	Ce
1-A-S-1	50.3	15	30	1	3	0.3	0.4	0.003	-	0.001	-	-
1-A-S-2	53.2	12	30	1	3	0.4	0.4	0.003	-	0.001	-	-
1-B-S-1	5	15	73.55	-	5.0	1.25	-	0.2	-	0.001	-	-
1-B-S-2	5	15	73.55	-	5.0	1.25	-	0.1	0.1	0.001	-	-

TABLE II-4. Chemical Analysis of Final Alloys Vacuum Induction Melted as 15-Pound Ingots (expressed in weight percent)

Alloy Number	Fe	Ni	Co	W	Ta	Al	Ti	Zr	Be	B	C	Ce
1-A-S-1	50.2	15.3	29.1	0.92	2.90	0.27	0.42	0.006	-	0.002	0.0039	-
1-A-S-2	52.4	12.2	29.5	0.96	2.95	0.38	0.41	0.006	-	0.002	0.0022	-
1-B-S-1	5.8	15.3	71.3	-	4.98	1.28	-	0.21	-	0.003	0.0062	-
1-B-S-2	5.2	15.2	72.4	-	4.98	1.36	-	0.12	0.065	0.002	0.0062	0.006

TABLE II-5. Composition of Final Alloys Vacuum Induction Melted as 15-Pound Ingots Based on Chemical Analysis (expressed in atomic percent)

Alloy Number	Fe	Ni	Co	W	Ta	Al	Ti	Zr	Be	B	C	Ce
1-A-S-1	bal	15.25	28.89	0.29	0.94	0.59	0.51	-	-	-	-	-
1-A-S-2	bal	12.14	29.23	0.30	0.95	0.82	0.50	-	-	-	-	-
1-B-S-1	6.22	15.60	bal	-	1.65	2.84	-	0.14	-	-	-	-
1-B-S-2	5.55	15.43	bal	-	1.64	3.00	-	0.08	0.43	-	-	-

were cut off. After cutting, the ingots weighed 7000 to 7500 grams.

The two-inch diameter rod-shaped ingots were used as consumable electrodes in a vacuum-arc furnace at a pressure of 10^{-4} torr. Melting was performed at the rate of one inch per minute using an applied current of 1600 amperes. The mold had a three-inch inside diameter. A seven inch long melted ingot was obtained. After cutting the ends off, the ingot weighed 5000 grams. The ingots were machined to give a flaw-free finish. The ingots were placed in a furnace at 2102°F (1150°C) and soaked for one hour, then forged into one by two-inch bars. The bars were reheated during forging when the temperature cooled below 1832°F (1000°C). After forging, the bars were 17 inches long and weighed 4500 grams except for alloy 1-B-S-1, which had developed cracks during forging. The end of this bar was cut off. This bar was 11 inches long and weighed 3300 grams.

A four-inch length of each bar was cut off and heated in an argon-filled retort for one hour at 1922°F (1050°C). The pieces were hot rolled to 150-mil thick slabs. The slabs were reheated for 15 minutes after each pass. After the last pass the samples were soaked for one hour at 1922°F (1050°C), then air cooled. The slabs were sandblasted to remove the scale. Samples for magnetic saturation measurements were machined from the hot-rolled slabs. The slabs were then cold-rolled to 70-mil thick strips. Strips of alloy 1-A-S-2, 1-B-S-1, and 1-B-S-2 were pickled in hydrochloric acid. Samples for hardness and coercive force were taken from these strips.

The details of measuring magnetic saturation, coercive force, and room temperature hardness were described in the first and second quarterly reports.

The hot hardness measurements reported here were made at a pressure of 2×10^{-5} torr using a Vickers pyramid indenter. The applied load was 2.5 kG. Samples were held at temperature for one minute after heating to temperature within 15 minutes.

The tensile tests were performed on a hard-beam tensile tester at a strain rate of 5×10^{-5} in/in/sec using flat samples with a gage length of 1-1/4 inches and a cross section of 1/4 inch by 50 mils. Sensitivity was estimated at 5×10^{-5} inches strain and

500 psi stress. When measuring at elevated temperatures the samples were held for 15 minutes at temperature. Test time was about 10 minutes. Annealing was done in helium or argon flushed tube furnaces. Aging was performed in salt baths.

The microstructure for optical microscopy was revealed in the manner described in the second quarterly report. The alloys were polished mechanically. Martensitic alloys were etched electrolytically in ten percent chromic acid solution. The cobalt-base alloys were etched in a solution of 40 ml HCl, 20 ml HNO₃, and 60 ml glycerin at 104°F (40°C).

Electron microscopic studies were done on samples of alloys 1-A-V-4 and 1-B-V-4. Extraction replicas and thin films for electron transmission were prepared after the samples had been rolled to a thickness of 15 mils and heat treated. The electrolyte used in polishing the samples was 20 percent perchloric acid in ethyl alcohol. An applied voltage of 20 volts was used for polishing. In obtaining replicas, samples were etched in the same electrolyte with a lower applied voltage (~10V). Then a 500 Å thick layer of carbon was deposited on the etched surface. The carbon film and attached particles were stripped from the surface after re-submitting the sample to the electropolishing bath. The thinning of samples to obtain foils for electron transmission was done by electropolishing by the window technique between stainless steel plates serving as cathodes. The electrolyte was the same as described above.

A Debye-Scherrer diagram was obtained by conventional X-ray techniques.

b. RESULTS

The test results obtained during the sixth quarter on the 300 gram vacuum-arc melted buttons are reported in the first portion of this section. Preliminary test results obtained on the 15-pound vacuum induction melted buttons are reported in the last part of this section.

(1) Saturation Measurements - 300 Gram Buttons

The results of magnetic saturation measurements made during this quarter on samples from the 300 gram buttons are listed in Tables II-6 and II-7. Saturation of the aged

TABLE II-6. Saturation Magnetic Moment of 300 Gram Vacuum Arc Melted Martensitic Alloys 1-A-V-1 to 1-A-V-6

Alloy Number	Nominal Alloy Composition (weight percent)	Saturation Magnetic Moment (emu/g) ^(a)			
		After Annealing One Hour at 1832°F (1000°C)	After Annealing One Hour at 1832°F (1000°C) and Aging One Hour at 1112°F (600°C)		
		Tested at Room Temperature	Tested at Room Temperature	Tested at 1112°F (600°C)	Tested at 1202°F (650°C)
1-A-V-1	48Fe-15Ni-30Co-2W-4Ta-0.5Al-0.5Ti	181	183	160	149
1-A-V-2	66Fe-10Ni-20Co-3Ta-0.5Al-0.5Ti	208	206	172	165
1-A-V-3	57.5Fe-12Ni-25Co-1W-3.5Ta-0.5Al-0.5Ti	196	196	166	150
1-A-V-4	51Fe-15Ni-30Co-3Ta-0.5Al-0.5Ti	192	195	168	151
1-A-V-5	49Fe-15Ni-30Co-2W-3Ta-0.5Al-0.5Ti	185	187	161	153
1-A-V-6	60Fe-5Ni-5Cr-25Co-1W-3Ta-0.5Al-0.5Ti	184	186	150	139
(a) To convert the saturation magnetic moment to the approximate induction in gauss, multiply the listed value by 100.					

TABLE II-7. Saturation Magnetic Moment of 300 Gram Vacuum Arc Melted Cobalt-Base Alloys 1-B-V-1 to 1-B-V-6

Alloy Number	Nominal Alloy Composition (weight percent)	Saturation Magnetic Moment (emu/g) ^(a)			
		After Annealing One Hour at 2012°F (1100°C)	After Annealing one Hour at 2012°F (1100°C) and Aging One Hour at 1292°F (700°C)		
		Tested at Room Temperature	Tested at Room Temperature	Tested at 1112°F (600°C)	Tested at 1202°F (650°C)
1-B-V-1	71.7Co-5Fe-15Ni-1.5Ti-1.5Al-0.3Zr-5Ta	123	119	91	87
1-B-V-2	80.5Co-5Fe-10Ni-1.2Al-0.3Zr-3Ta	144	144	114	108
1-B-V-3	76.3Co-5Fe-12Ni-1.0Ti-1.4Al-0.3Zr-4Ta	132	130	102	97
1-B-V-4	73.5Co-5Fe-15Ni-1.2Al-0.3Zr-5Ta	133	134	106	101
1-B-V-5	78.2Co-5Fe-10Ni-1.5Al-0.3Zr-5Ta	135	135	105	100
1-B-V-6	74Co-5Fe-15Ni-1.5Ti-1.2Al-0.3Zr-3Ta	130	128	100	94
(a) To convert the saturation magnetic moment to the approximate induction in gauss, multiply the listed value by 110.					

samples was measured at room temperature, 1112°F (600°C), and at 1202°F (650°C). Samples of the ferritic alloys were annealed for one hour at 1832°F (1000°C); then aged for one hour at 1112°F (600°C) before testing. The cobalt-base alloys were annealed for one hour at 2012°F (1100°C) and aged for one hour at 1292°F (700°C) before testing.

(2) Aging Tests - 300 Gram Buttons

Results obtained from coercive force measurements on samples of the 300 gram buttons are shown in Tables II-8 and II-9. Coercive force was measured at several temperatures. Two samples were taken from each of the ferritic alloys for measurements. One sample was aged for one hour at 1112°F (600°C), the other sample was subjected to isothermal aging for 100 hours at 1022°F (550°C) before testing. Two samples were also taken from the cobalt-base alloys. One sample was aged for one hour at 1382°F (750°C) before testing; the other sample was subjected to isothermal aging for 100 hours at 1292°F (700°C) before testing. In the case of the isothermally aged samples, coercive force was re-measured at room temperature after measurements at higher temperatures. The results indicate a very slight reduction of coercive force value due to the tests at temperature.

(3) Tensile and Hot Hardness Tests - 300 Gram Buttons

Results of tensile tests which were obtained on samples from the 300 gram buttons are shown in Tables II-10 and II-11. The ferritic samples were annealed one hour at 1832°F (1000°C); then machined to size and aged for one hour at 1112°F (600°C) before testing. Cobalt-base alloys were annealed one hour at 1832°F (1000°C); then machined to size and aged for one hour at 1382°F (750°C) before testing. The hardness of each sample was measured at room temperature before the test. This value is also shown in Tables II-10 and II-11. The tables list yield stress at 0.2 percent plastic elongation, the ultimate tensile stress, the uniform elongation, and the reduction of area at fracture.

TABLE II-8. Coercive Force Measurements on 300 Gram Vacuum Arc Melted Martensitic Alloys 1-A-V-1 to 1-A-V-6 at Different Temperatures

Alloy Number	Nominal Alloy Composition (weight percent)	Coercive Force (Oersteds)				
		Annealed One Hour at 1832°F (1000°C); Then Aged One Hour at 1112°F (600°C) Before Testing				
		Test Temperature				
		Room Temp.	1022°F (550°C)	1112°F (600°C)	1202°F (650°C)	Room ^(a) Temp.
1-A-V-1	48Fe-15Ni-30Co-2W-4Ta-0.5Al-0.5Ti	42.5	--	39.0	31.0	--
1-A-V-2	66Fe-10Ni-20Co-3Ta-0.5Al-0.5Ti	24.0	--	17.6	15.8	--
1-A-V-3	57.5Fe-12Ni-25Co-1W-3.5Ta-0.5Al-0.5Ti	32.8	--	25.0	22.5	--
1-A-V-4	51Fe-15Ni-30Co-3Ta-0.5Al-0.5Ti	37.0	--	30.0	26.0	--
1-A-V-5	49Fe-15Ni-30Co-2W-3Ta-0.5Al-0.5Ti	43.0	--	37.0	31.0	--
1-A-V-6	60Fe-5Ni-5Cr-25Co-1W-3Ta-0.5Al-0.5Ti	37.0	--	24.5	20.0	--
Annealed One Hour at 1832°F (1000°C); Then Aged 100 Hours at 1022°F (550°C) Before Testing						
1-A-V-1	48Fe-15Ni-30Co-2W-4Ta-0.5Al-0.5Ti	62.5	56.0	51.0	48.0	63.0
1-A-V-2	66Fe-10Ni-20Co-3Ta-0.5Al-0.5Ti	30.0	22.0	20.0	20.0	28.0
1-A-V-3	57.5Fe-12Ni-25Co-1W-3.5Ta-0.5Al-0.5Ti	42.5	33.0	30.0	29.0	41.5
1-A-V-4	51Fe-15Ni-30Co-3Ta-0.5Al-0.5Ti	48.5	48.0	45.5	42.0	48.0
1-A-V-5	49Fe-15Ni-30Co-2W-3Ta-0.5Al-0.5Ti	62.5	58.0	53.0	48.5	62.0
1-A-V-6	60Fe-5Ni-5Cr-25Co-1W-3Ta-0.5Al-0.5Ti	37.0	22.0	20.0	18.1	32.0
(a) Room temperature results shown in the last column were measured after elevated temperature measurements were made.						

TABLE II-9. Coercive Force Measurements on 300 Gram Vacuum Arc Melted Cobalt-Base Alloys 1-B-V-1 to 1-B-V-6 at Different Temperatures

Alloy Number	Nominal Alloy Composition (weight percent)	Coercive Force (Oersteds)				
		Annealed One Hour at 1832°F (1000°C); Then Aged One Hour at 1382°F (750°C) Before Testing				
		Test Temperature				
		Room Temp.	1022°F (550°C)	1112°F (600°C)	1202°F (650°C)	Room ^(a) Temp.
1-B-V-1	71.7Co-5Fe-15Ni-1.5Ti-1.5Al-0.3Zr-5Ta	3.4	2.2	1.6	1.5	--
1-B-V-2	80.5Co-5Fe-10Ni-1.2Al-0.3Zr-3Ta	3.0	1.4	1.2	0.95	--
1-B-V-3	76.3Co-5Fe-12Ni-1.0Ti-1.4Al-0.3Zr-4Ta	2.8	1.5	1.0	0.85	--
1-B-V-4	73.5Co-5Fe-15Ni-1.2Al-0.3Zr-5Ta	2.9	1.4	0.90	0.65	--
1-B-V-5	78.2Co-5Fe-10Ni-1.5Al-0.3Zr-5Ta	2.6	1.3	0.88	0.77	--
1-B-V-6	74Co-5Fe-15Ni-1.5Ti-1.2Al-0.3Zr-3Ta	2.8	1.5	0.99	0.88	--
Annealed One Hour at 1832°F (1000°C); Then Aged 100 Hours at 1292°F (700°C) Before Testing						
1-B-V-1	71.7Co-5Fe-15Ni-1.5Ti-1.5Al-0.3Zr-5Ta	26.0	11.0	9.2	8.3	25.0
1-B-V-2	80.5Co-5Fe-10Ni-1.2Al-0.3Zr-3Ta	6.7	3.4	2.5	2.3	6.3
1-B-V-3	76.3Co-5Fe-12Ni-1.0Ti-1.4Al-0.3Zr-4Ta	12.4	5.6	4.8	3.7	12.2
1-B-V-4	73.5Co-5Fe-15Ni-1.2Al-0.3Zr-5Ta	10.6	5.0	3.4	2.8	10.3
1-B-V-5	78.2Co-5Fe-10Ni-1.5Al-0.3Zr-5Ta	9.3	4.2	4.3	2.7	9.0
1-B-V-6	74Co-5Fe-15Ni-1.5Ti-1.2Al-0.3Zr-3Ta	14.2	6.5	5.0	4.1	13.6
(a) Room temperature results shown in the last column were measured after elevated temperature measurements were made.						

TABLE II-10. Tensile Tests(a) of 300 Gram Vacuum Arc Melted Martensitic Alloys 1-A-V-1 to 1-A-V-6

Alloy Number	Nominal Alloy Composition (weight percent)	Room Temperature Hardness 50 k G Load (VHN)	Test Temperature °F °C		0.2% Yield Strength (psi)	Ultimate Tensile Strength (psi)	Uniform Elongation (percent)	Reduction of Area (percent)
1-A-V-1	48Fe-15Ni-30Co-2W-4Ta-0.5Al-0.5Ti	747	77	25	71 650(b)	-	-	(c)
1-A-V-2	66Fe-10Ni-20Co-3Ta-0.5Al-0.5Ti	547	77	25	153 000(b)	-	-	(c)
1-A-V-3	57.5Fe-12Ni-25Co-1W-3.5Ta-0.5Al-0.5Ti	642	77	25	148 000(b)	-	-	(c)
1-A-V-4	51Fe-15Ni-30Co-3Ta-0.5Al-0.5Ti	687	77	25	140 500(b)	-	-	(c)
1-A-V-5	49Fe-15Ni-30Co-2W-3Ta-0.5Al-0.5Ti	685	77	25	131 800(b)	-	-	(c)
1-A-V-6	60Fe-5Ni-5Cr-25Co-1W-3Ta-0.5Al-0.5Ti	503	77	25	229 650	239 850	2.11	16.26
1-A-V-1	48Fe-15Ni-30Co-2W-4Ta-0.5Al-0.5Ti	747	1112	600	147 600	158 750	1.00	4.0
1-A-V-2	66Fe-10Ni-20Co-3Ta-0.5Al-0.5Ti	540	1112	600	101 200	115 050	1.93	43.9
1-A-V-3	57.5Fe-12Ni-25Co-1W-3.5Ta-0.5Al-0.5Ti	636	1112	600	115 300	129 050	1.43	30.6
1-A-V-4	51Fe-15Ni-30Co-3Ta-0.5Al-0.5Ti	685	1112	600	115 750	133 850	1.60	4.0
1-A-V-5	49Fe-15Ni-30Co-2W-3Ta-0.5Al-0.5Ti	723	1112	600	130 250	152 800	1.30	5.6
1-A-V-6	60Fe-5Ni-5Cr-25Co-1W-3Ta-0.5Al-0.5Ti	510	1112	600	97 950	104 650	1.06	76.4
(a) Samples were annealed one hour at 1832°F (1000°C), machined to size and then aged one hour at 1112°F (600°C) before testing.								
(b) Fracture stress								
(c) Broke at radius of fillet in a brittle manner								

TABLE II-11. Tensile Tests(a) of 300 Gram Vacuum Arc Melted Cobalt-Base Alloys 1-B-V-1 to 1-B-V-6

Alloy Number	Nominal Alloy Composition (weight percent)	Room Temperature Hardness 50 kG Load (VHN)	Test Temperature °F °C		0.2% Yield Strength (psi)	Ultimate Tensile Strength (psi)	Uniform Elongation (percent)	Reduction of Area (percent)
1-B-V-1	71.7Co-5Fe-15Ni-1.5Ti-1.5Al-0.3Zr-5Ta	365	77	25	120 800	178 000	19.3	41.6
1-B-V-2	80.5Co-5Fe-10Ni-1.2Al-0.3Zr-3Ta	230	77	25	68 800	115 200	36.5	54.1
1-B-V-3	76.3Co-5Fe-12Ni-1.0Ti-1.4Al-0.3Zr-4Ta	317	77	25	106 800	160 000	22.7	42.7
1-B-V-4	73.5Co-5Fe-15Ni-1.2Al-0.3Zr-5Ta	327	77	25	110 800	158 800	19.7	41.0
1-B-V-5	78.2Co-5Fe-10Ni-1.5Al-0.3Zr-5Ta	313	77	25	110 000	155 600	22.3	49.3
1-B-V-6	74Co-5Fe-15Ni-1.5Ti-1.2Al-0.3Zr-3Ta	323	77	25	111 200	166 800	23.3	42.7
1-B-V-1	71.7Co-5Fe-15Ni-1.5Ti-1.5Al-0.3Zr-5Ta	361	1112	600	102 400	141 600	12.2	29.1
1-B-V-2	80.5Co-5Fe-10Ni-1.2Al-0.3Zr-3Ta	226	1112	600	46 400	84 000	14.9	17.0
1-B-V-3	76.3Co-5Fe-12Ni-1.0Ti-1.4Al-0.3Zr-4Ta	317	1112	600	91 200	127 600	13.9	35.4
1-B-V-4	73.5Co-5Fe-15Ni-1.2Al-0.3Zr-5Ta	325	1112	600	93 200	128 400	11.5	32.3
1-B-V-5	78.2Co-5Fe-10Ni-1.5Al-0.3Zr-5Ta	316	1112	600	89 200	122 000	11.9	28.0
1-B-V-6	74Co-5Fe-15Ni-1.5Ti-1.2Al-0.3Zr-3Ta	320	1112	600	92 400	126 000	13.0	25.0
(a) Samples were annealed one hour at 1832°F (1000°C), machined to size and aged for one hour at 1382°F (750°C) before testing.								

Tests were performed at room temperature and at 1112°F (600°C). Samples were held for 15 minutes at temperature before the start of testing. Tests at 1112°F (600°C) were conducted in argon. In the room temperature tests tensile specimens of the ferritic alloys with the exception of alloy 1-A-V-6 failed in a brittle manner at the radius of the fillet before 0.2 percent plastic elongation was reached. The stress at fracture is listed in those cases. Ferritic tensile specimens showed some necking when tested in 1112°F (600°C). The cobalt-base samples were quite ductile at both test temperatures.

Hot-hardness values for samples from the 300 gram buttons are shown in Tables II-12 and II-13. Samples of the ferritic alloys were annealed one hour at 1832°F (1000°C) and then aged for one hour at 1112°F (600°C) before testing. Samples of the cobalt-base alloys were annealed one hour at 1832°F (1000°C) and aged for one hour at 1382°F (750°C) prior to testing. The temperature dependence of hardness of alloys 1-A-V-4 and 1-B-V-4 is shown in Figures II-1 and II-2. The values of hardness listed in Tables II-12 and II-13 should be regarded as relative values. Comparison of Vickers hardness numbers for alloy 1-A-V-4 at room temperature shows values of 680 and 615 at 50 kG and 2.5 kG loads respectively.

(4) Aging Tests - 15-Pound Ingots

Results of the isochronal aging of samples made from the four final alloys are plotted in Figure II-3. The two ferritic samples (1-A-S-1 and 1-A-S-2) were annealed one hour at 1832°F (1000°C). The isochronal aging sequence started at 932°F (500°C). Aging time was one hour with 90°F (50°C) increments in temperature. The highest isochronal aging temperature for the ferritic alloys was 1202°F (650°C). Both cobalt-base samples (1-B-S-1 and 1-B-S-2) were annealed one hour at 1832°F (1000°C). The isochronal aging sequence started at 1202°F (650°C), with an aging time of one hour. The temperature was then successively increased in increments of 90°F (50°C) to 1472°F (800°C) which was the highest aging temperature applied to the cobalt-base alloys.

TABLE II-12. Hot Hardness Measurements^(a) on Samples of 300 Gram Vacuum Arc Melted Martensitic Alloys 1-A-V-1 to 1-A-V-6 After Annealing One Hour at 1832°F (1000°C) and Aging One Hour at 1112°F (600°C)

Alloy Number	Nominal Alloy Composition (weight percent)	Hot Hardness (VHN)	
		Test Temperature	
		1112°F (600°C)	1202°F (650°C)
1-A-V-1	48Fe-15Ni-30Co-2W-4Ta-0.5Al-0.5Ti	340	267
1-A-V-2	66Fe-10Ni-20Co-3Ta-0.5Al-0.5Ti	268	193
1-A-V-3	57.5Fe-12Ni-25Co-1W-3.5Ta-0.5Al-0.5Ti	322	252
1-A-V-4	51Fe-15Ni-30Co-3Ta-0.5Al-0.5Ti	338	215
1-A-V-5	49Fe-15Ni-30Co-2W-3Ta-0.5Al-0.5Ti	355	250
1-A-V-6	60Fe-5Ni-5Cr-25Co-1W-3Ta-0.5Al-0.5Ti	242	157
(a) All measurements were made under vacuum of 2×10^{-5} torr at a load of 2.5 kG.			

TABLE II-13. Hot Hardness Measurements^(a) on Samples of 300 Gram Vacuum Arc Melted Cobalt-Base Alloys 1-B-V-1 to 1-B-V-6 After Annealing One Hour at 1832°F (1000°C) and Aging One Hour at 1382°F (750°C)

Alloy Number	Nominal Alloy Composition (weight percent)	Hot Hardness (VHN)	
		Test Temperature	
		1112°F (600°C)	1202°F (650°C)
1-B-V-1	71.7Co-5Fe-15Ni-1.5Ti-1.5Al-0.3Zr-5Ta	192	270
1-B-V-2	80.5Co-5Fe-10Ni-1.2Al-0.3Zr-3Ta	106	132
1-B-V-3	76.3Co-5Fe-12Ni-1.0Ti-1.4Al-0.3Zr-4Ta	246	249
1-B-V-4	73.5Co-5Fe-15Ni-1.2Al-0.3Zr-5Ta	292	257
1-B-V-5	78.2Co-5Fe-10Ni-1.5Al-0.3Zr-5Ta	229	242
1-B-V-6	74Co-5Fe-15Ni-1.5Ti-1.2Al-0.3Zr-3Ta	156	248
(a) All measurements were made under vacuum of 2×10^{-5} torr at a load of 2.5 kG.			

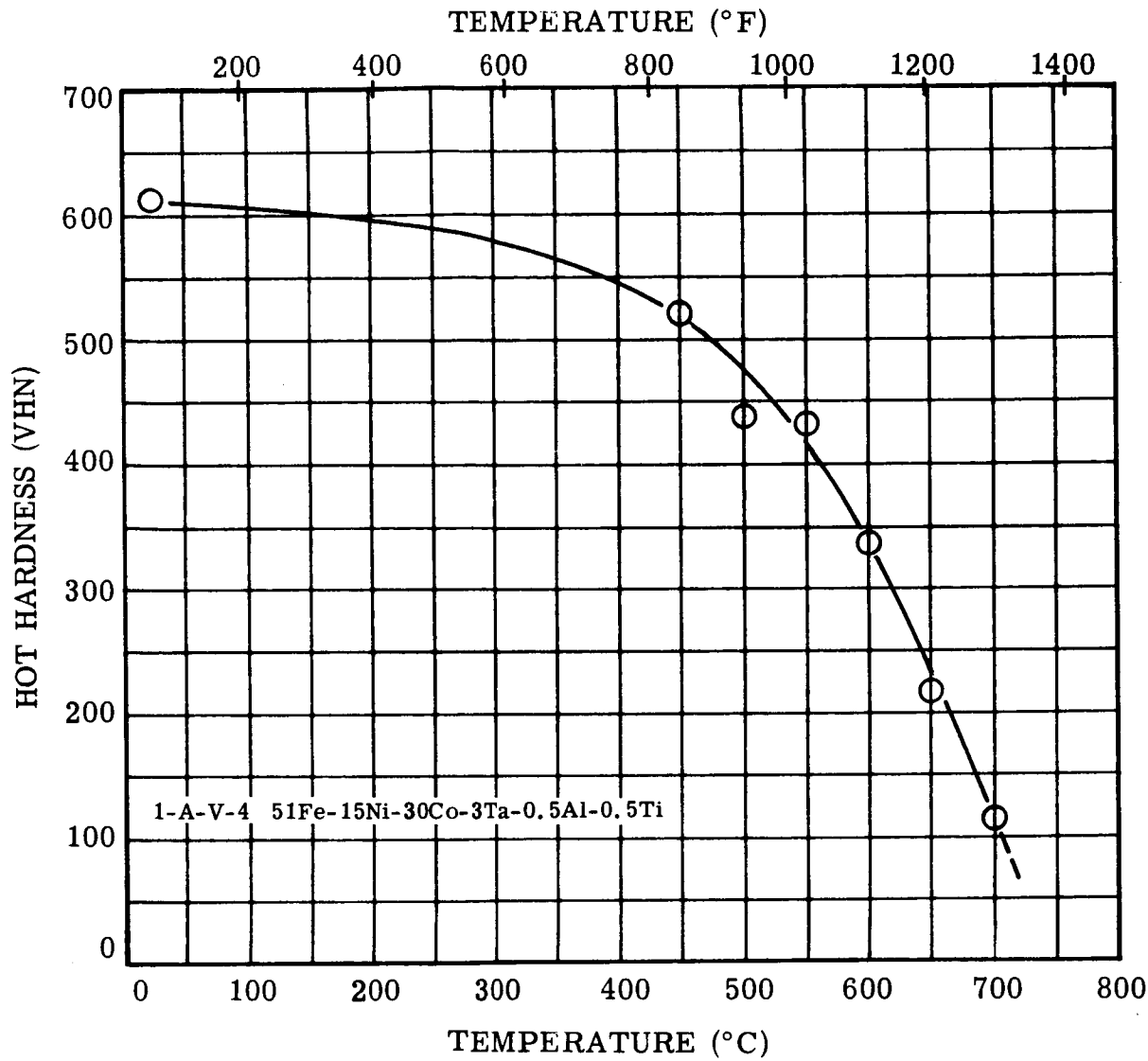


FIGURE II-1. Hot Hardness Versus Temperature of Alloy 1-A-V-4 After Annealing One Hour at 1832°F (1000°C) and Aging at 1112°F (600°C). Test Load 2.5kG.

Figure II-1. Hot Hardness vs. Temperature of Alloy 1-A-V-4

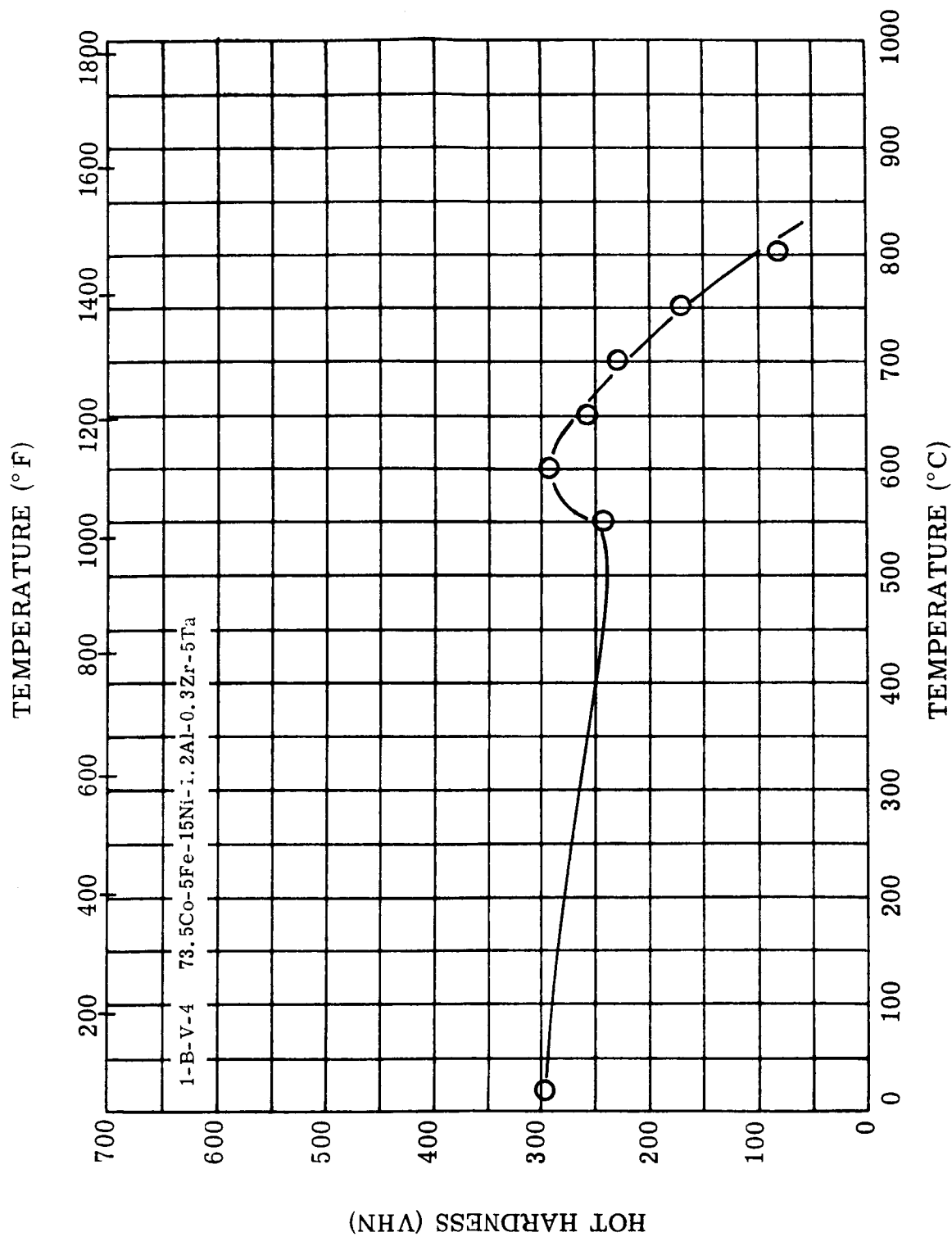


Figure II-2. Hot Hardness vs. Temperature of Alloy 1-B-V-4

FIGURE II-2. Hot Hardness vs. Temperature of Alloy 1-B-V-4 After Annealing One Hour at 1832°F (1000°C) and Aging at 1112°F (600°C). Test Load 2.5 kG.

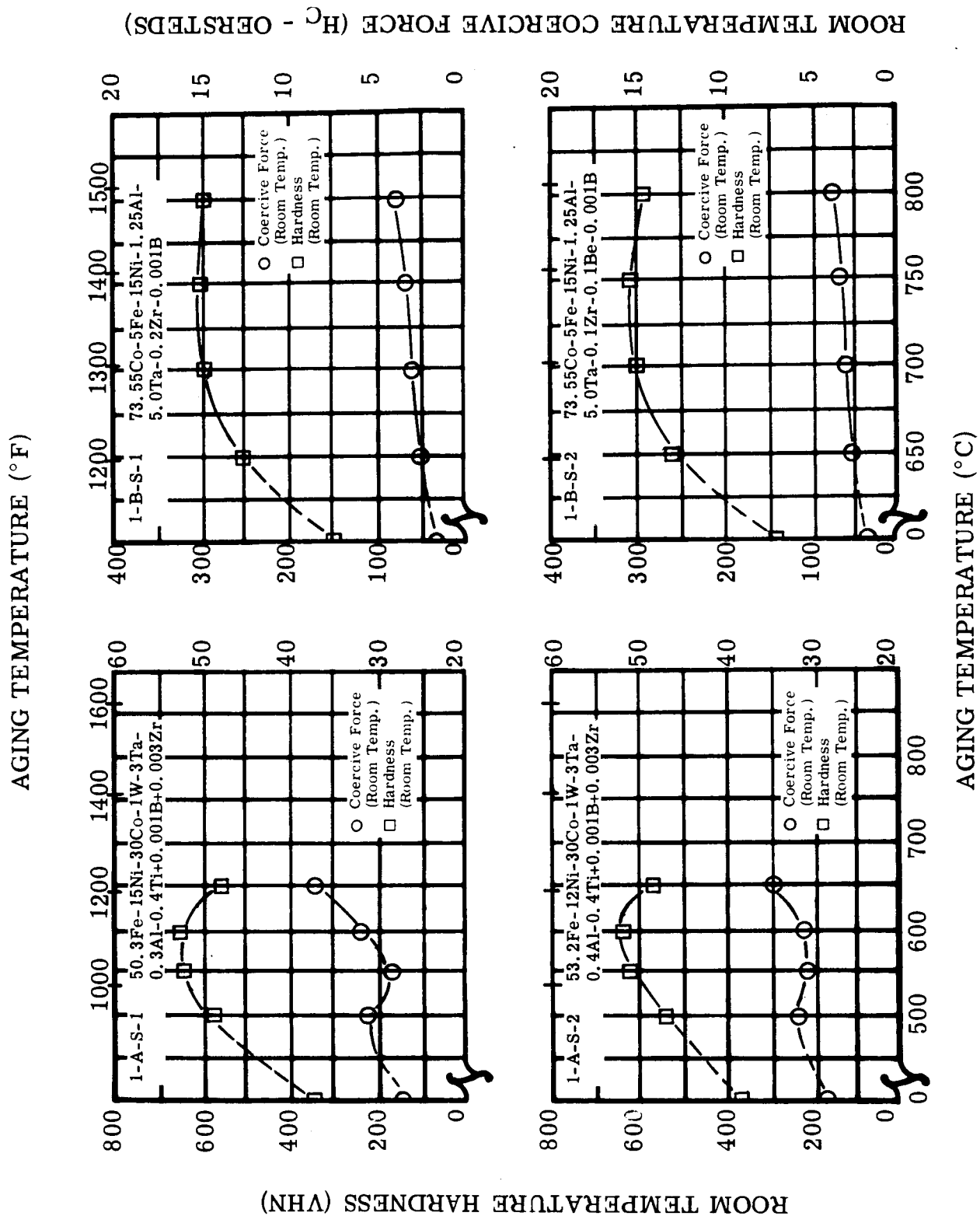


Figure II-3. Hardness and Coercive Force of Alloys 1-A-S-1, 1-A-S-2, 1-B-S-1, and 1-B-S-2

FIGURE II-3. Hardness and Coercive Force of Alloys 1-A-S-1, 1-A-S-2, 1-B-S-1, and 1-B-S-2 at Room Temperature After Aging One Hour at Temperature

The maximum values of room temperature hardness measured during the isochronal aging sequence are listed in Table II-14 together with the aging temperature, where maximum hardness was attained. The room temperature coercivity is listed for the same aging temperature. Results of the isothermal aging tests of the final alloys are plotted in Figures II-4, II-5, and II-6. The samples for isothermal aging tests were annealed one hour at 1832°F (1000°C) before testing.

Two samples were taken from each of the ferritic alloys. One sample was aged at 1012°F (550°C) after annealing; the other sample was five percent cold reduced after annealing. Then aging at 1012°F (550°C) was started. The results are compared for alloy 1-A-S-1 in Figure II-4 and alloy 1-A-S-2 in Figure II-5. Five percent reduction by cold rolling had reduced the value of coercive force between 10 and 15 oersteds. After isothermal aging 100 hours, the value of coercive force increased, but the value of the five percent cold rolled sample was still 10 oersteds lower. The change of hardness was not influenced by cold working. The influence of the small plastic strain is similar to the behavior observed in 15 percent nickel maraging steel. Results of isothermal aging at 1292°F (700°C) of the cobalt-base alloys are plotted in Figure II-6. The results of magnetic saturation measurements on the final four alloys are listed in Table II-15.

(5) Microstructure

Optical micrographs were made of the microstructure of all the alloys after 100 hours isothermal aging. These are shown in Figures II-7 through II-22. The micrographs of the ferritic alloys melted as 300 gram buttons are shown in Figures II-7 through II-12. One notices the presence of coarser particles of a second phase in all the alloys. However, the second phase content of alloy 1-A-V-4 and 1-A-V-5 appears rather small. These particles probably originated during solidification or from annealing treatment before the last aging treatment. In micrographs of cobalt-base alloys made from 300 gram buttons, shown in Figures II-13 through II-18, one notices the existence of particles of a second phase, probably present since solidification. A faint grain

TABLE II-14. Maximum Hardness Obtained by the Isochronal Aging of the Final Alloys Vacuum Induction Melted as 15-Pound Ingots (a)

Alloy Number	Nominal Alloy Composition (weight percent)	Aging Temperature At Which Maximum Room Temperature Hardness Was Obtained		Total Aging Time ^(b) (hours)	Maximum Room Temperature Hardness (VHN)	Room Temperature Coercivity At Maximum Hardness (oersteds)
		°F	°C			
1-A-S-1	50.3Fe-15Ni-30Co-1W-3Ta-0.3Al-0.4Ti+0.001B+0.003Zr	1112	600	4	664	32
1-A-S-2	53.2Fe-12Ni-30Co-1W-3Ta-0.4Al-0.4Ti+0.001B+0.003Zr	1112	600	4	643	31
1-B-S-1	73.55Co-5Fe-15Ni-1.25Al-5.0Ta-0.2Zr-0.001B	1382	750	6	311	3.3
1-B-S-2	73.55Co-5Fe-15Ni-1.25Al-5.0Ta-0.1Zr-0.1Be-0.001B	1382	750	6	313	3.1

(a) See Figure II-3

(b) Total aging time may be determined by adding one hour aging time for each 90°F (50°C) increment in temperature starting at 932°F (500°C).

TABLE II-15. Saturation Magnetic Moment of the Final Alloys Vacuum Induction Melted as 15-Pound Ingots

Alloy Number	Nominal Alloy Composition (weight percent)	Treatment Before Testing	Saturation Magnetic Moment (emu/g) ^(a)	Treatment Before Testing	Saturation Magnetic Moment (emu/g)	
			Tested at Room Temperature		Tested at Room Temperature	Tested at 1112°F (600°C)
1-A-S-1	50.3Fe-15Ni-30Co-1W-3Ta-0.3Al-0.4Ti+0.001B+0.003Zr	Annealed one hour at 1832°F (1000°C)	192	Annealed then aged one hour at 1112°F (600°C)	195	162
1-A-S-2	53.2Fe-12Ni-30Co-1W-3Ta-0.4Al-0.4Ti+0.001B+0.003Zr		197		200	171
1-B-S-1	73.55Co-5Fe-15Ni-1.25Al-5.0Ta-0.2Zr-0.001B	Annealed one hour at 2012°F (1100°C)	138	Annealed then aged one hour at 1292°F (700°C)	135	104
1-B-S-2	73.55Co-5Fe-15Ni-1.25Al-5.0Ta-0.1Zr-0.1Be-0.001B		132		134	102

(a) To convert the saturation magnetic moment to the approximate induction in gauss, multiply the listed values for alloys 1-A-S-1 and 1-A-S-2 by 100 and alloys 1-B-S-1 and 1-B-S-2 by 110.

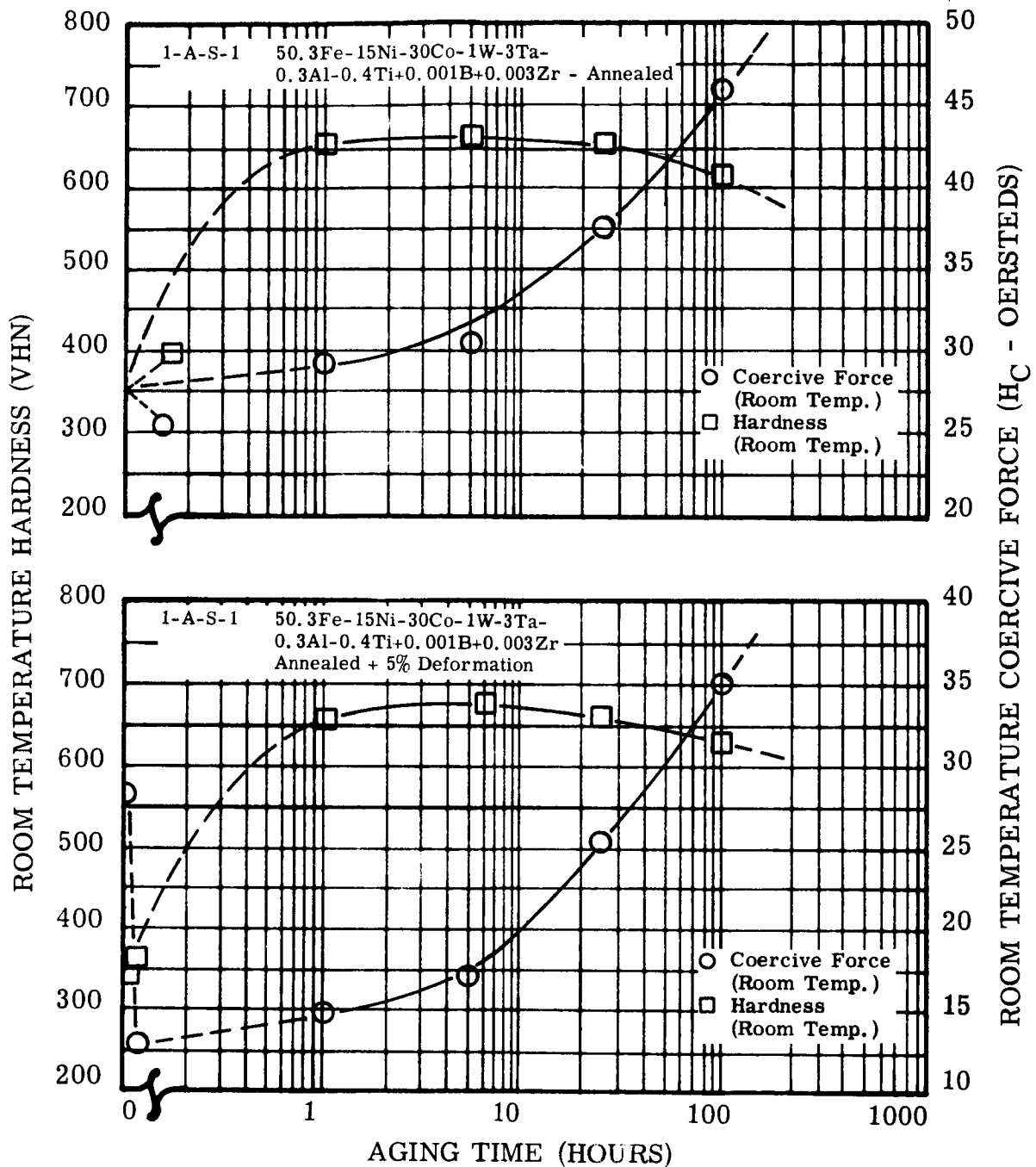


FIGURE II-4. Change in Room Temperature Hardness and Coercive Force During Isothermal Aging at 1022°F (550°C) of Alloy 1-A-S-1 Annealed, and Annealed and Five Percent Deformed

Figure II-4. Hardness and Coercive Force of Alloy 1-A-S-1 During Isothermal Aging

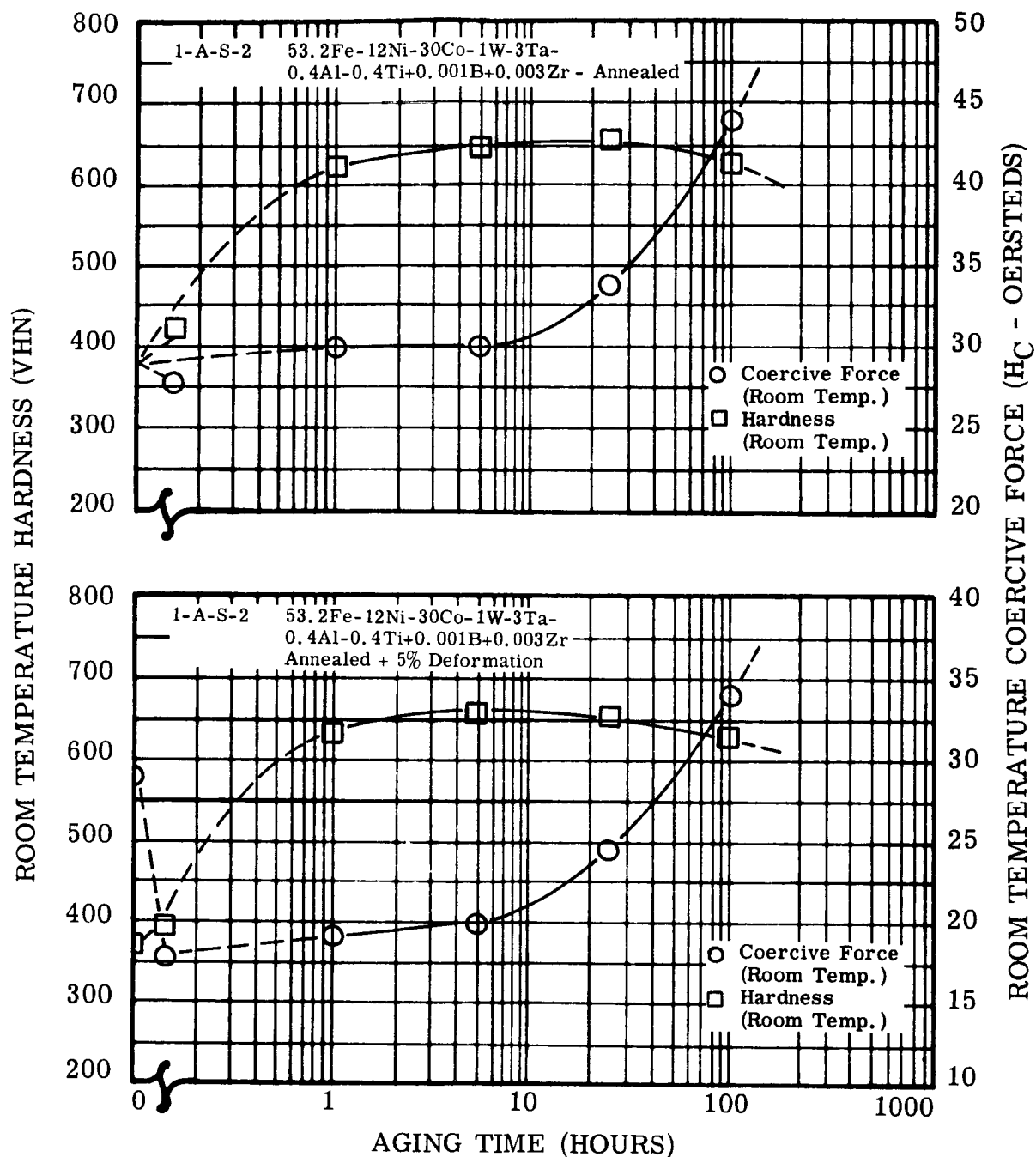


FIGURE II-5. Change in Room Temperature Hardness and Coercive Force During Isothermal Aging at 1022°F (550°C) of Alloy 1-A-S-2 Annealed, and Annealed and Five Percent Deformed

Figure II-5. Hardness and Coercive Force of Alloy 1-A-S-2 During Isothermal Aging

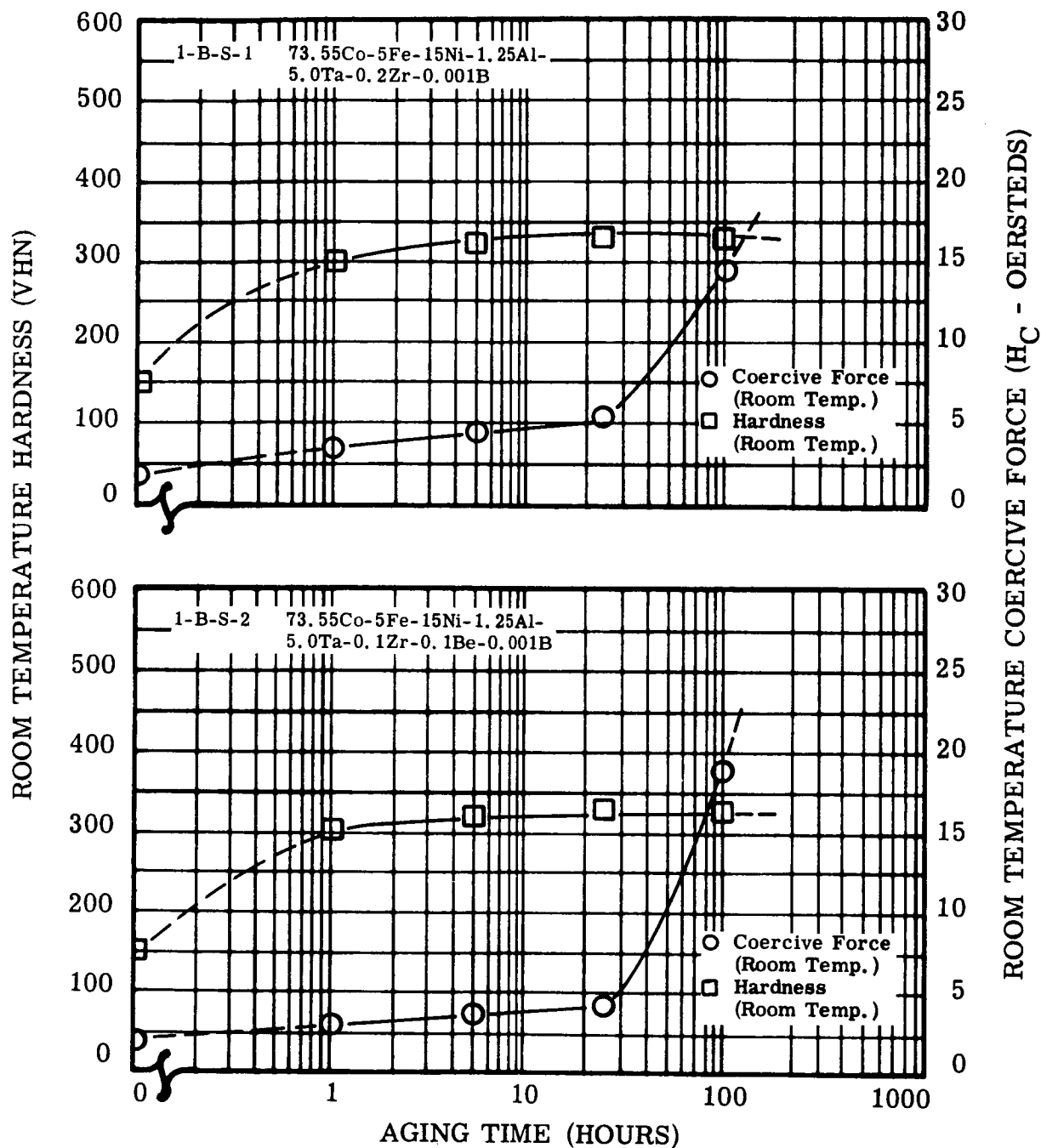
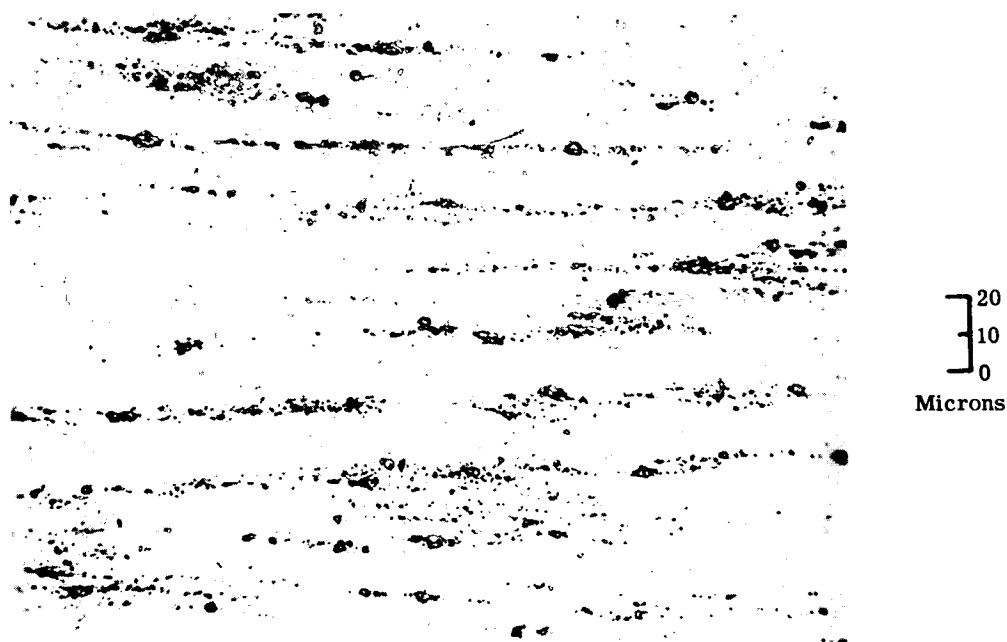


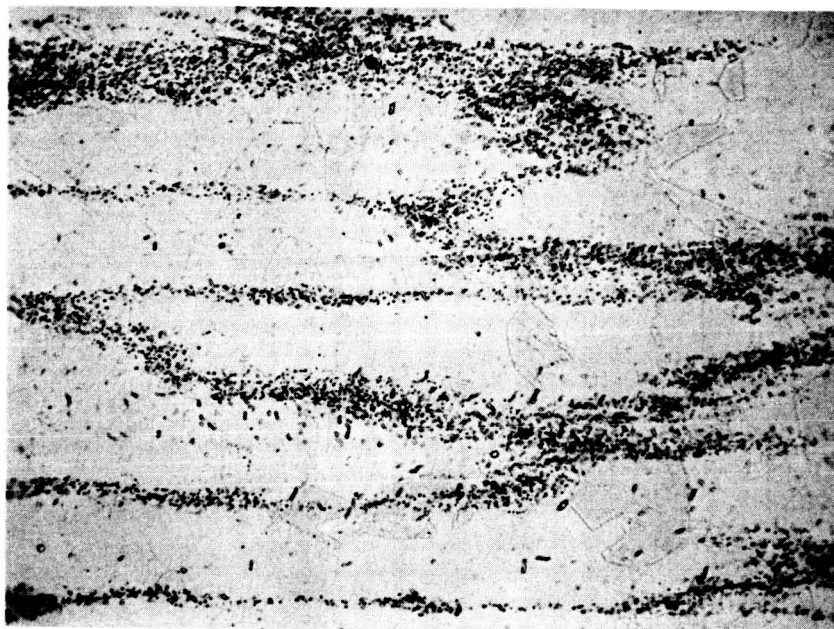
FIGURE II-6. Change in Room Temperature Hardness and Coercive Force of Alloys 1-B-S-1 and 1-B-S-2 During Isothermal Aging at 1292°F (700°C)

Figure II-6. Hardness and Coercive Force of Alloys 1-B-S-1 and 1-B-S-2 During Isothermal Aging



Electrolytically etched in 10 percent chromic acid.

FIGURE II-7. Microstructure of Alloy 1-A-V-1 (48Fe-15Ni-30Co-2W-4Ta-0.5Al-0.5Ti) After 100 Hours Aging at 1022° F (550°C) 500X



20
10
0
Microns

Electrolytically etched in 10 percent chromic acid.

FIGURE II-8. Microstructure of Alloy 1-A-V-2 (66Fe-10Ni-20Co-3Ta-0.5Al-0.5Ti) After 100 Hours Aging at 1022°F (550°C) 500X



Electrolytically etched in 10 percent chromic acid.

FIGURE II-9. Microstructure of Alloy 1-A-V-3 (57.5Fe-12Ni-25Co-1W-3.5Ta-0.5Al-0.5Ti) After 100 Hours Aging at 1022°F (550°C) 500 X



20
10
0
Microns

Electrolytically etched in 10 percent chromic acid.

FIGURE II-10. Microstructure of Alloy 1-A-V-4 (51Fe-15Ni-30Co-3Ta-0.5Al-0.5Ti) After 100 Hours Aging at 1022°F (550°C) 500 X



20
10
0
Microns

Electrolytically etched in 10 percent chromic acid.

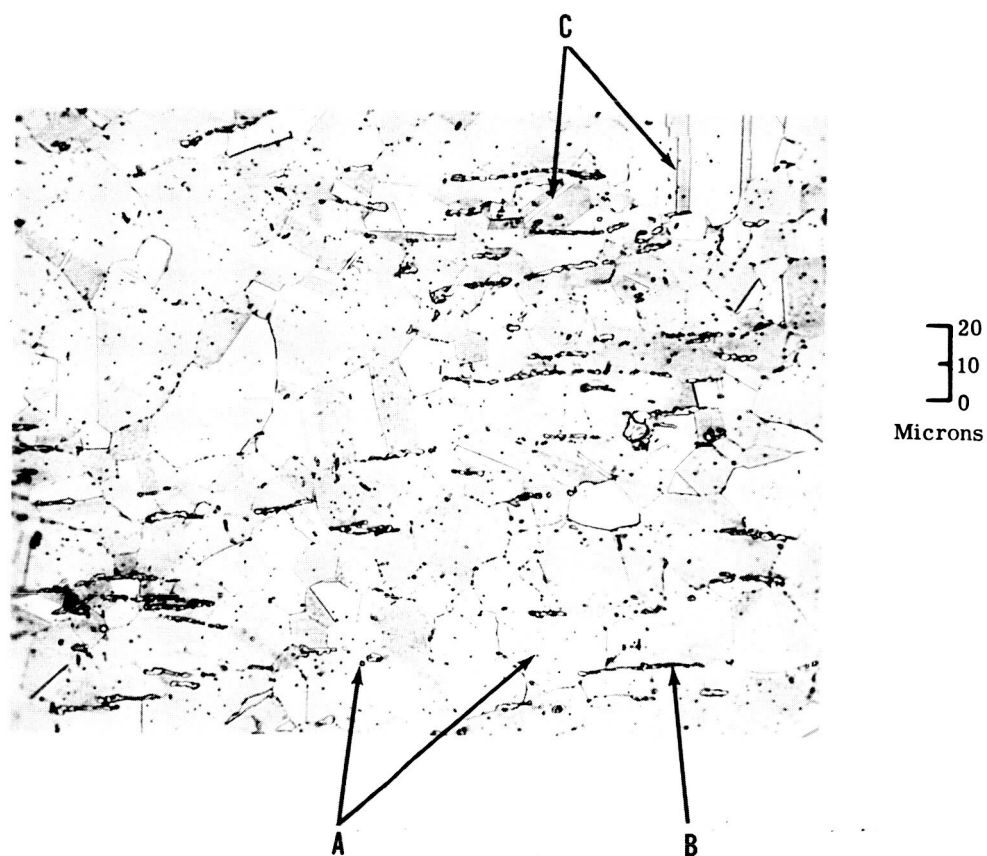
FIGURE II-11. Microstructure of Alloy 1-A-V-5 (49Fe-15Ni-30Co-2W-3Ta-0.5Al-0.5Ti) After 100 Hours Aging at 1022°F (550°C) 500 X



20
10
0
Microns

Electrolytically etched in 10 percent chromic acid.

FIGURE II-12. Microstructure of Alloy 1-A-V-6 (60Fe-5Ni-5Cr-25Co-1W-3Ta-0.5Al-0.5Ti) After 100 Hours Aging at 1022°F (550°C) 500 X

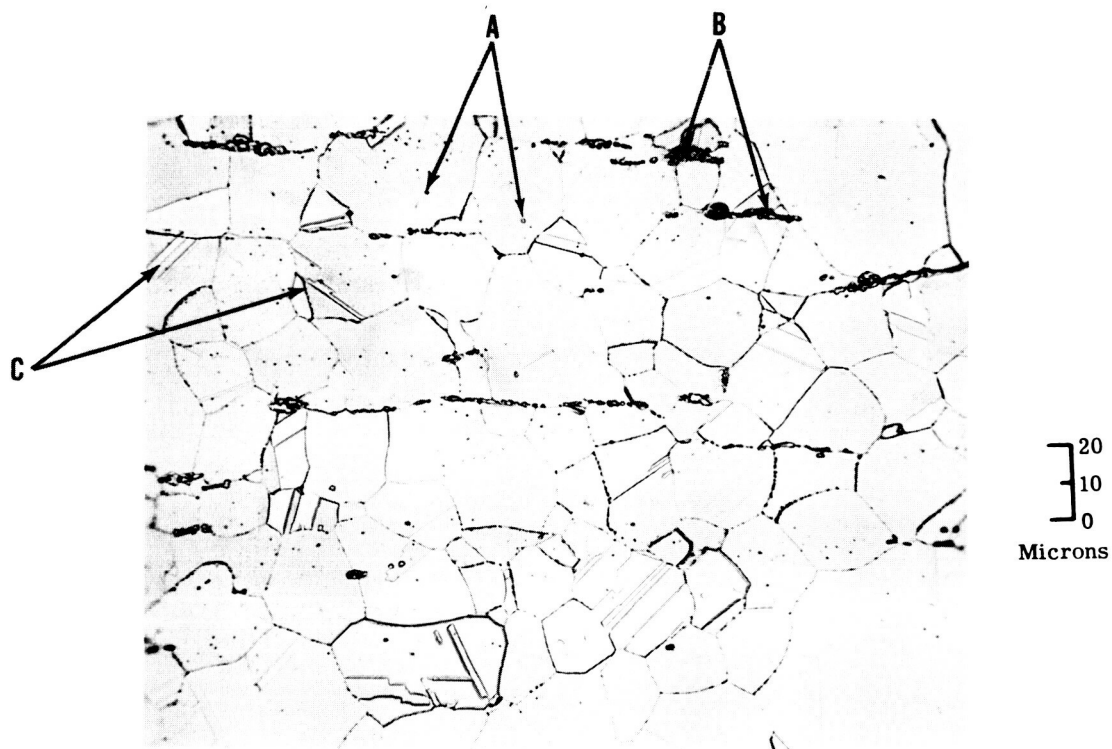


- A - Second phase particles
- B - Discontinuous precipitate (cellular precipitate at grain boundaries)
- C - Twin boundaries

Note the beginning of discontinuous precipitation.

Etchant: 20 ml HCl, 40 ml HNO₃, 60 ml glycerin

FIGURE II-13. Microstructure of Alloy 1-B-V-1 (71.7Co-5Fe-15Ni-1.5Ti-1.5Al-0.3Zr-5Ta) After 100 Hours Aging at 1292°F (700°C)
500 X

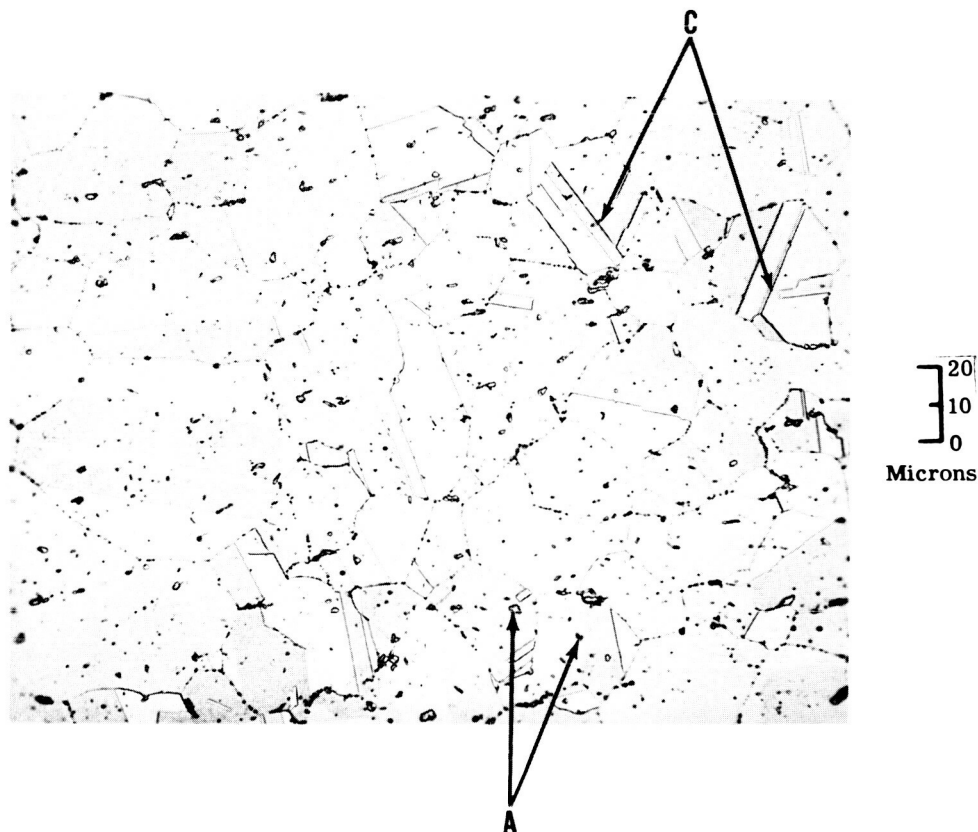


- A - Second phase particles
- B - Discontinuous precipitate (cellular precipitate at grain boundaries)
- C - Twin boundaries

Note the beginning of discontinuous precipitation.

Etchant: 20 ml HCl, 40 ml HNO₃, 60 ml glycerin

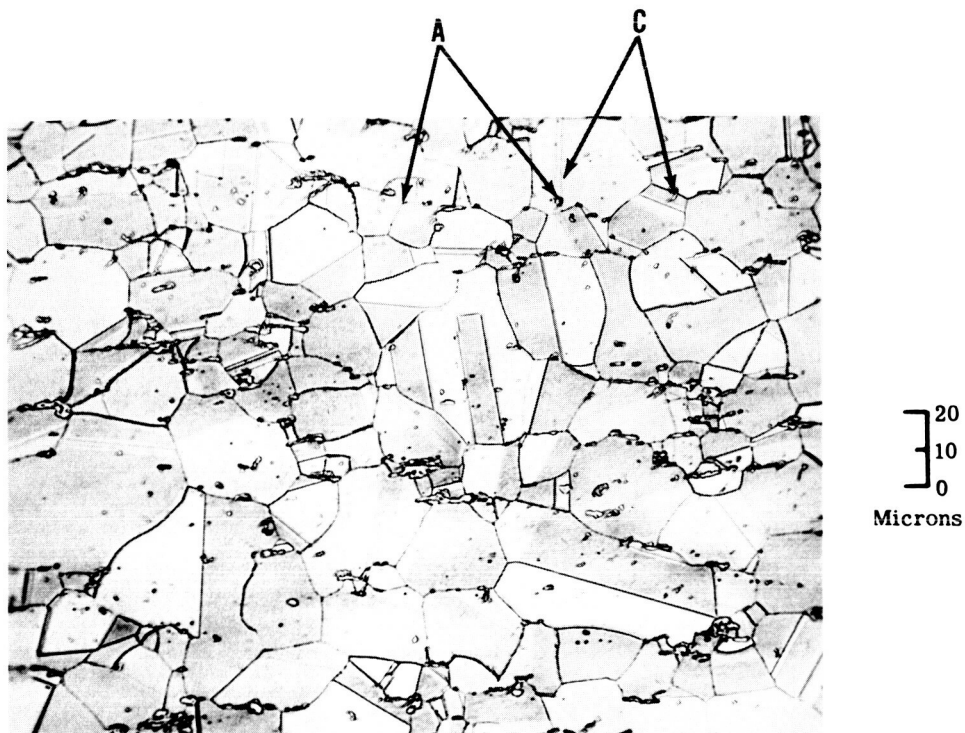
FIGURE II-14. Microstructure of Alloy 1-B-V-2 (80.5Co-5Fe-10Ni-1.2Al-0.3Zr-3Ta) After 100 Hours Aging at 1292°F (700°C) 500 X



A - Second phase particles
C - Twin boundaries

Etchant: 20 ml HCl, 40 ml HNO₃, 60 ml glycerin

FIGURE II-15. Microstructure of Alloy 1-B-V-3 (76.3Co-5Fe-12Ni-1.0Ti-1.4Al-0.3Zr-4Ta) After 100 Hours Aging at 1292°F (700°C)
500X



A - Second phase particles
C - Twin boundaries

Etchant: 20 ml HCl, 40 ml HNO₃, 60 ml glycerin

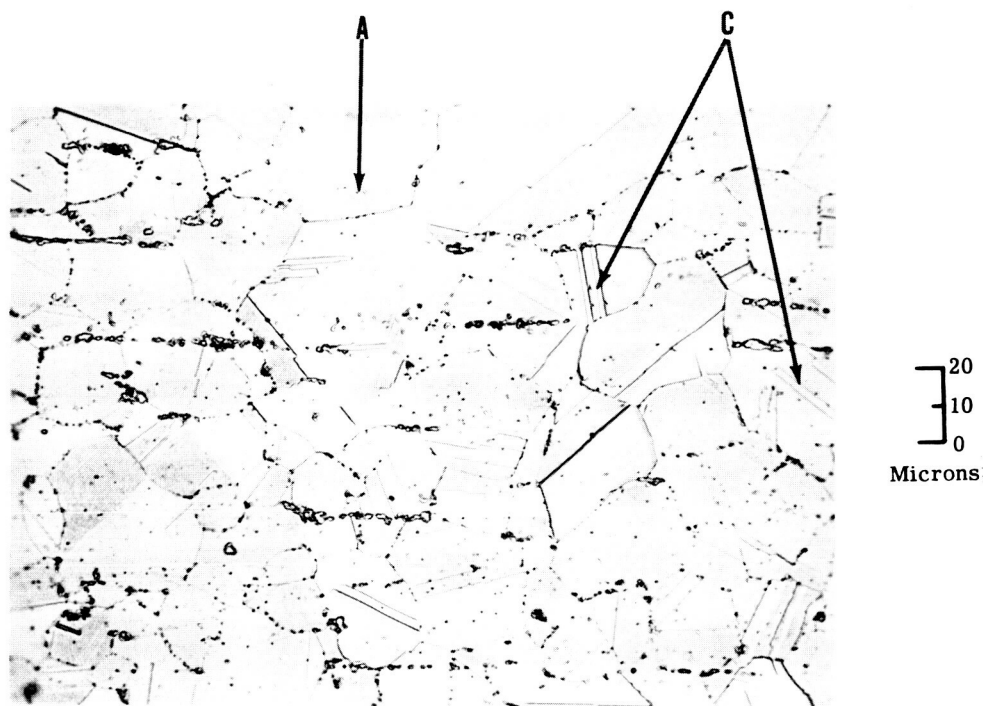
FIGURE II-16. Microstructure of Alloy 1-B-V-4 (73.5Co-5Fe-15Ni-1.2Al-0.3Zr-5Ta) After 100 Hours Aging at 1292°F (700°C) 500 X



A - Second phase particles

Etchant: 20 ml HCl, 40 ml HNO₃, 60 ml glycerin

FIGURE II-17. Microstructure of Alloy 1-B-V-5 (78.2Co-5Fe-10Ni-1.5Al-0.3Zr-5Ta) After 100 Hours Aging at 1292°F (700°C) 500 X



A - Second phase particles
C - Twin boundaries

Etchant: 20 ml HCl, 40 ml HNO₃, 60 ml glycerin

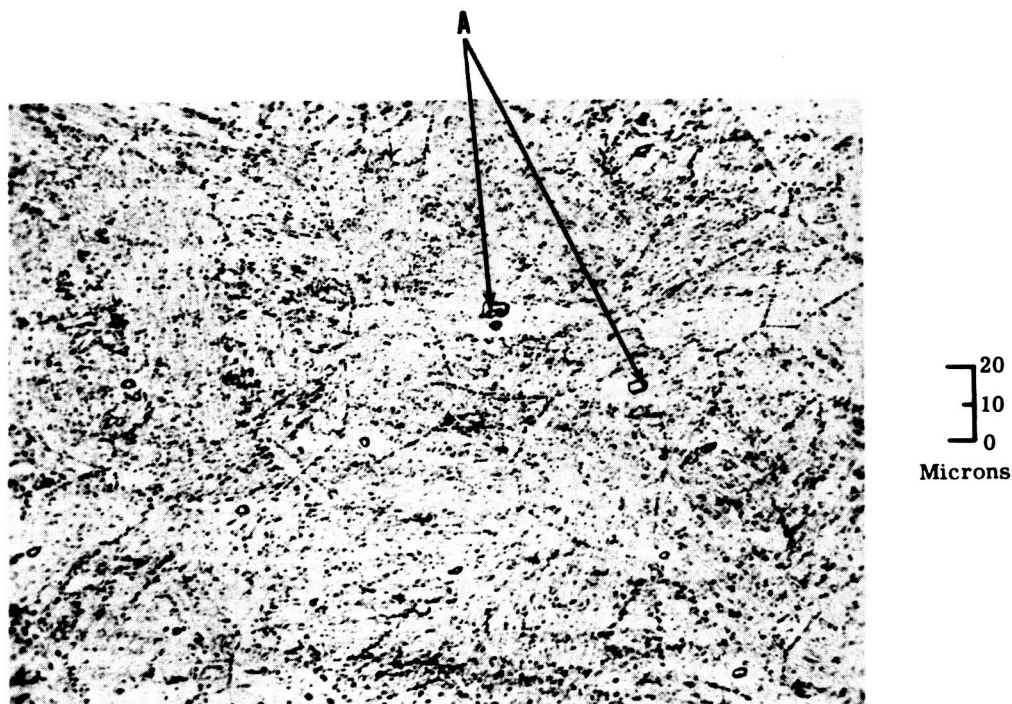
FIGURE II-18. Microstructure of Alloy 1-B-V-6 (74Co-5Fe-15Ni-1.5Ti-1.2Al-0.3Zr-3Ta) After 100 Hours Aging at 1292°F (700°C)
500X



A - Second phase particles

Electrolytically etched in 10 percent chromic acid.

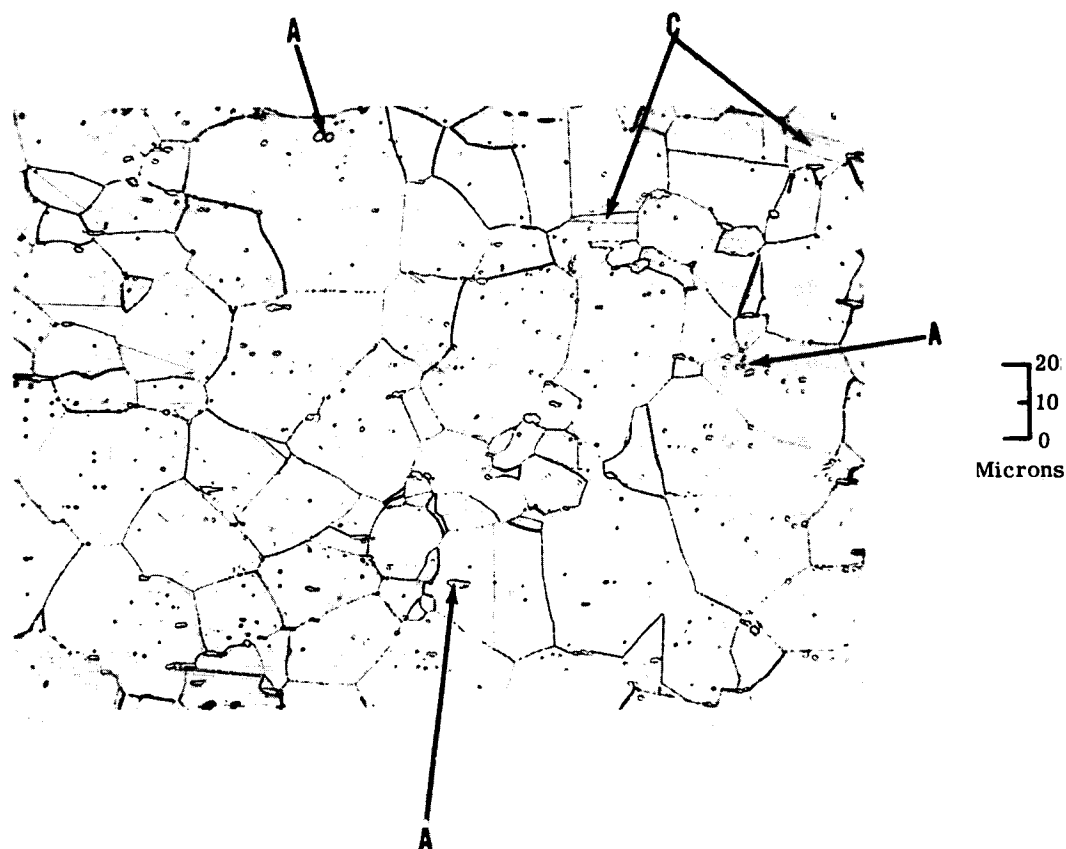
FIGURE II-19. Microstructure of Alloy 1-A-S-1 (50.3Fe-15Ni-30Co-1W-3Ta-0.3Al-0.4Ti+0.001B+0.003Zr) After 100 Hours Aging at 1022°F (550°C) 500 X



A - Second phase particles

Electrolytically etched in 10 percent chromic acid.

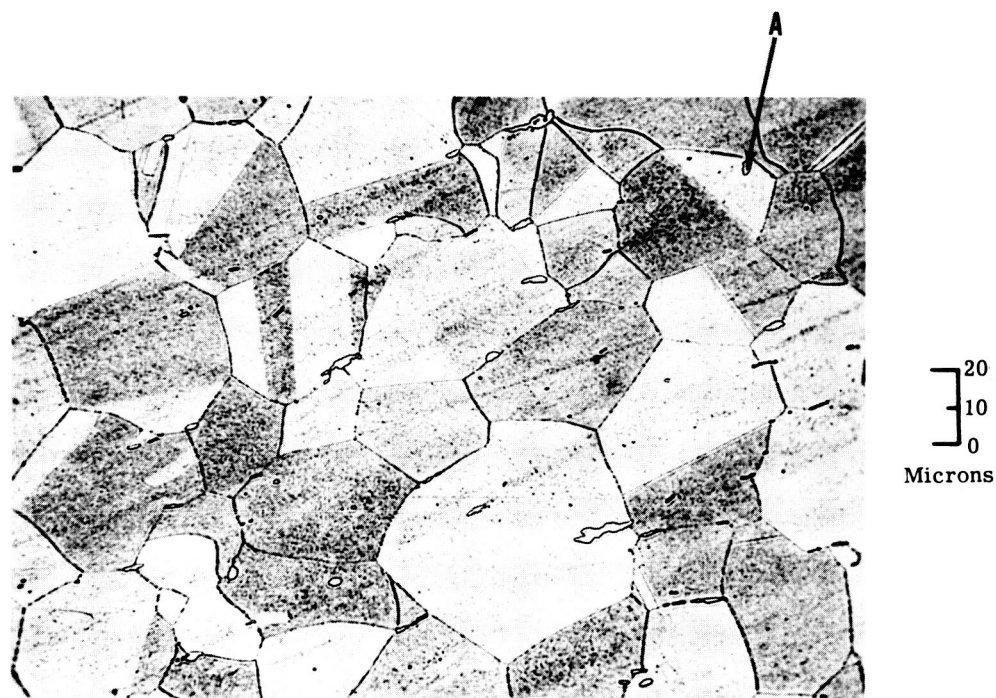
FIGURE II-20. Microstructure of Alloy 1-A-S-2 (53.2Fe-12Ni-30Co-1W-3Ta-0.4Al-0.4Ti+0.001B+0.003Zr) After 100 Hours Aging at 1022°F (550°C) 500 X



A - Second phase particles
C - Twin boundaries

Etchant: 20 ml HCl, 40 ml HNO₃, 60 ml glycerin

FIGURE II-21. Microstructure of Alloy 1-B-S-1 (73.55Co-5Fe-15Ni-1.25Al-5.0Ta-0.2Zr-0.001B) After 100 Hours Aging at 1292°F (700°C)
500 X



A - Second phase particles

Etchant: 20 ml HCl, 40 ml HNO₃, 60 ml glycerin

FIGURE II-22. Microstructure of Alloy 1-B-S-2 (73.55Co-5Fe-15Ni-1.25Al-5.0Ta-0.1Zr-0.1Be-0.001B) After 100 Hours Aging at 1292°F (700°C) 500X

boundary precipitate may be seen in alloys 1-B-V-1, 1-B-V-2, 1-B-V-3, and 1-B-V-6, Figures II-13, II-14, II-15, and II-18 respectively. However, no discontinuous precipitate is present.

The microstructure of the final ferritic alloys melted as 15-pound ingots shown in Figures II-19 and II-20 indicate that the amount of second phase inclusions is rather small. There is a trace of fine precipitate delineating the substructure of a martensitic matrix. In the microstructure of the final cobalt-base alloys (Figures II-21 and II-22), no discontinuous precipitate is evident; however, small inclusions of a second phase are present. The darkening of the grain faces during etching of 1-B-S-2 indicates the presence of a submicroscopic continuous precipitate.

The micrographs obtained by electron microscopy are shown in Figures II-23 through II-27. The microstructure of 1-A-V-4 after annealing shows a martensitic structure with a high dislocation density. Small precipitate particles of 0.1μ are present in some areas. After aging for 100 hours at 1022°F (550°C), a dense precipitate phase may be observed (Figure II-24). Most of the needle-shape particles are 100 to 200 \AA in diameter and 0.1μ to 0.2μ in length. Large stringer-like particles 300 to 500 \AA in diameter and a few microns long which appear to delineate the boundaries of the martensite lathes, may also be seen in the transmission micrograph in Figure II-24. The replica of Figure II-25 shows only the small needles and a few larger particles along grain boundaries. Table II-16 lists the tentative identification of these phases according to electron diffraction studies. The fine needle-like phase resembles the hexagonal Ni_3Ti phase of the DO_{24} type. The electron diffraction studies of the replica, resulted in a pattern which could fit a hexagonal lattice with a parameter 10 percent smaller than the Ni_3Ta phase with the DO_{24} lattice. The stringer-like phase was identified as a fcc phase with a lattice constant of $a = 3.6\text{ \AA}$ which is most likely austenite.

The structure of the aged cobalt-base alloys (Figures II-26 and II-27) shows a rather fine continuous precipitate. The majority of the particles are 100 to 200 \AA in diameter and

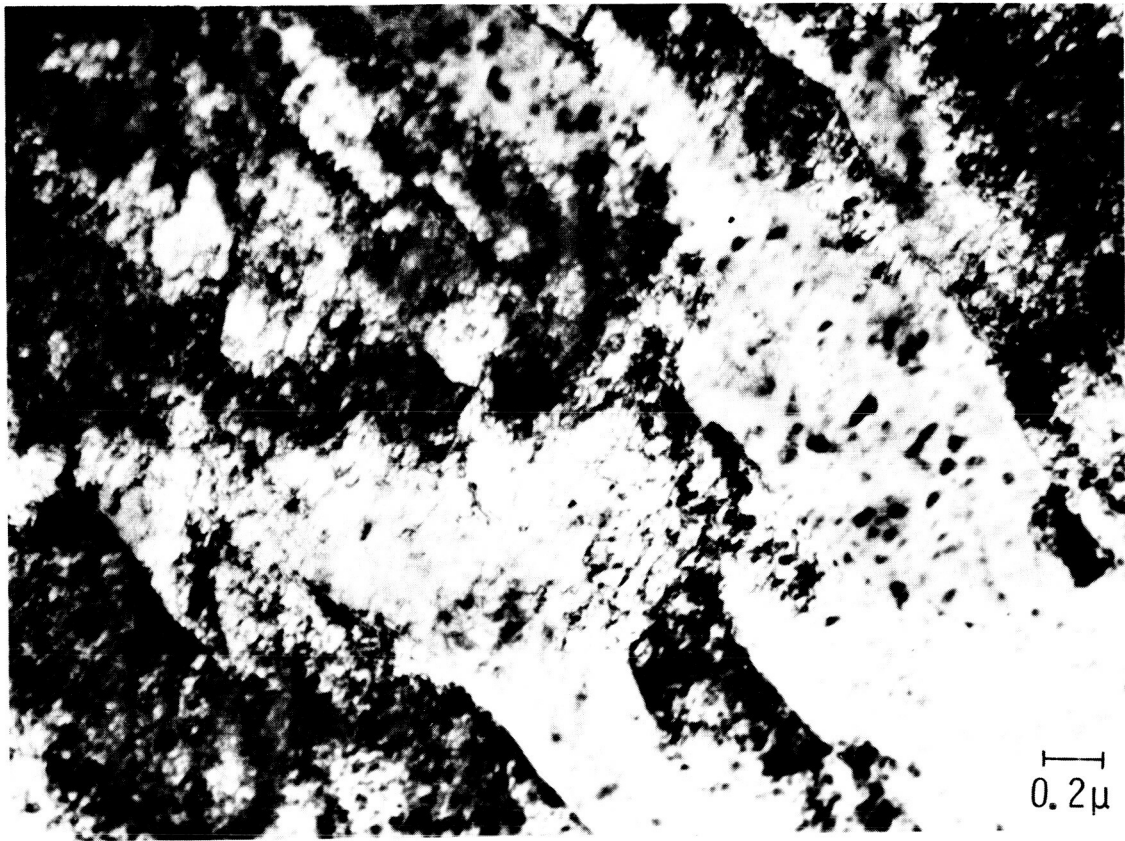


FIGURE II-23. Electron Transmission Micrograph of Alloy 1-A-V-4 (51Fe-15Ni-30Co-3Ta-0.5Al-0.5Ti) After Annealing One Hour at 1832° F (1000° C) 42,000 X

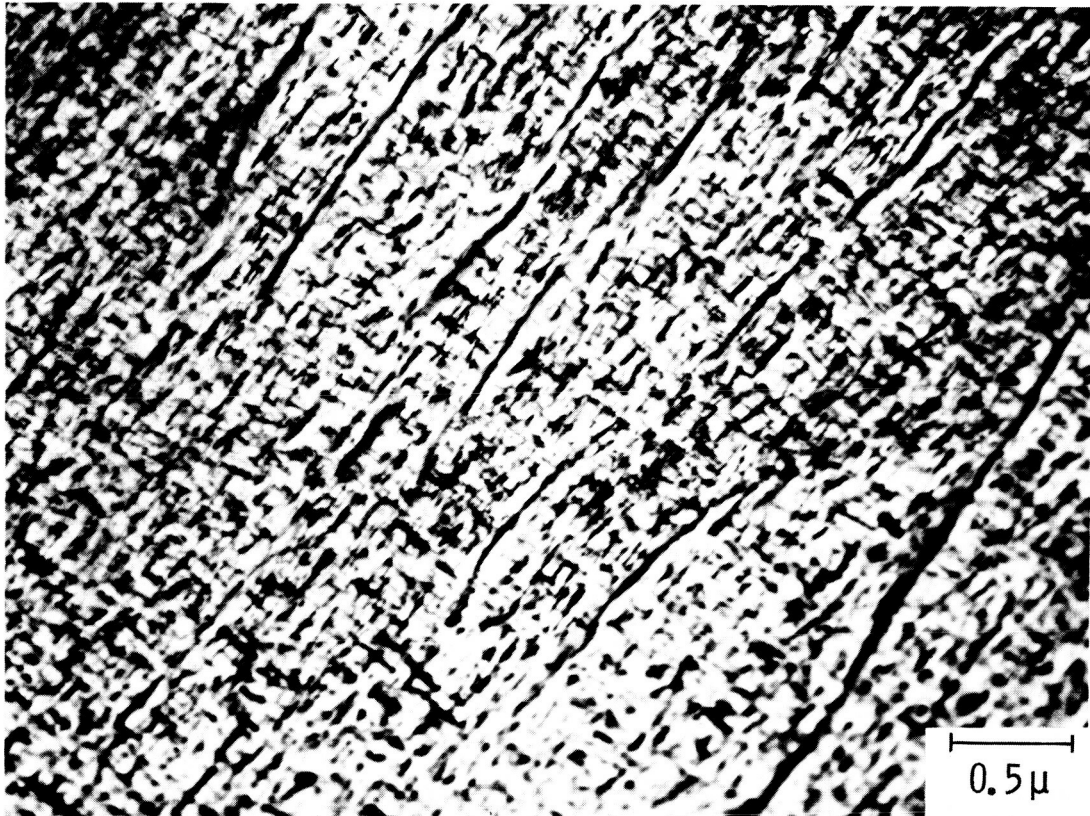


FIGURE II-24. Electron Transmission Micrograph of Alloy 1-A-V-4 (51Fe-15Ni-30Co-3Ta-0.5Al-0.5Ti) After Annealing One Hour at 1832°F (1000°C) and 100 Hours Aging at 1022°F (550°C)
31,000 X

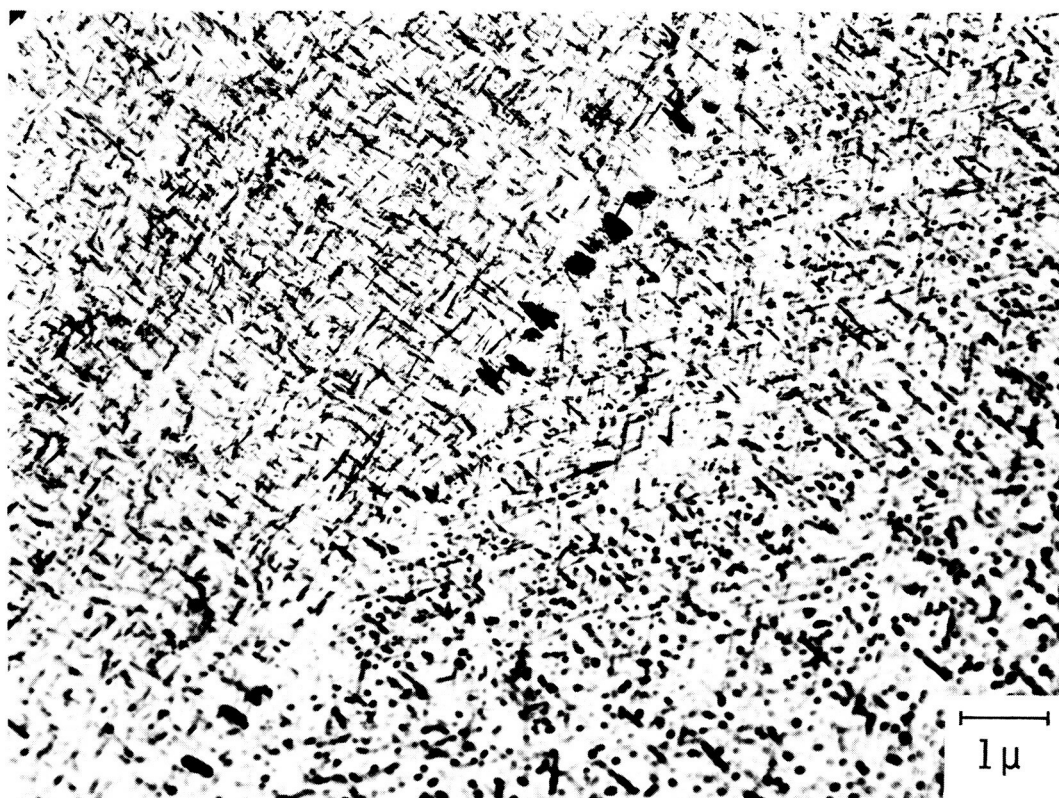


FIGURE II-25. Electron Microscope Replica of Alloy 1-A-V-4 (51Fe-15Ni-30Co-3Ta-0.5Al-0.5Ti) After Annealing One Hour at 1832°F (1000°C) and 100 Hours Aging at 1022°F (550°C) 10,500 X

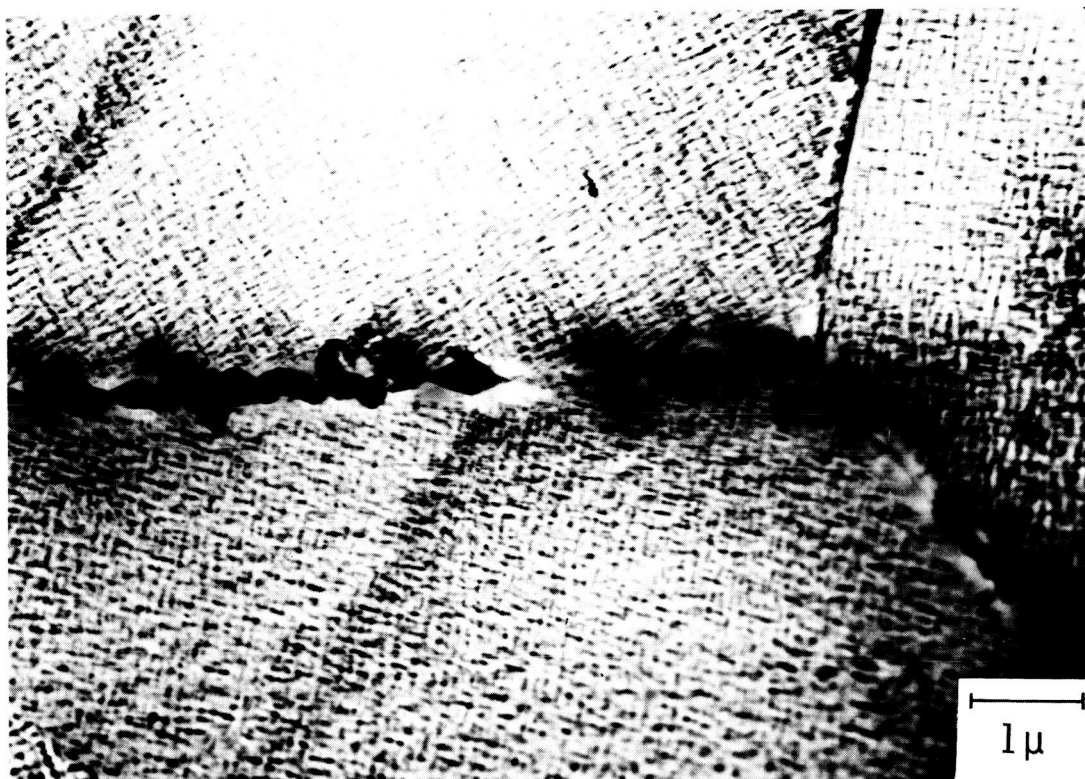


FIGURE II-26. Electron Transmission Micrograph of Alloy 1-B-V-4 (73.5Co-5Fe-15Ni-1.2Al-0.3Zr-5Ta) After Annealing One Hour at 1832°F (1000°C) and Aging 100 Hours at 1292°F (700°C) 14,000 X



FIGURE II-27. Electron Microscope Replica of Alloy 1-B-V-4 (73.5Co-5Fe-15Ni-1.2Al-0.3Zr-5Ta) After Annealing One Hour at 1832°F (1000°C) and 100 Hours Aging at 1292°F (700°C) 17,500 X

TABLE II-16. Phases Detected in Alloy 1-A-V-4, After Aging 100 Hours at 1022°F (550°C) and in Alloy 1-B-V-4, After Aging 100 Hours at 1292°F (700°C) With and Without a Previous Deformation by 50 Percent Cold Rolling

Shape of Phases	Lattice	Probable Identification
<p><u>1-A-V-4</u> (Fe-14.8Ni-29.4Co-0.64Al-0.52Ti-3.48Ta) (electron diffraction analysis)</p> <p>Needles 100 Å diameter 1000 Å long</p> <p>Black small stringer 300 to 500 Å diameter 1 to 3 μ long</p> <p>A few larger globular precipitate at grain boundaries</p>	<p>hexagonal a ~ 4.5 Å c ~ 4.0 Å</p> <p>face centered cubic a ~ 3.6 Å</p> <p>cubic</p>	<p>Similar to Ni₃Ta but 10% smaller containing Ta + Ti and Ni</p> <p>Austenite</p> <p>Ta or Ti carbonitrides</p>
<p><u>1-B-V-4</u> (Co-5.1Fe-0.26Zr-14.8Ni-1.25Al-5.19Ta) aged without deformation (electron diffraction analysis)</p> <p>Small particles cubic shape 100 to 200 Å width arranged in chains</p> <p>Coarser grain boundary precipitate particles</p>	<p>face centered cubic</p> <p>face centered cubic</p>	<p>Gamma Prime</p> <p>Gamma Prime</p>
<p><u>1-B-V-4</u> (Co-5.1Fe-0.26Zr-14.8Ni-1.25Al-5.19Ta) aged with previous deformation (X-ray diffraction)</p> <p>Heterogenized matrix</p>	<p>face centered cubic a₀ = 3.552 Å</p> <p>face centered cubic L1₂ a₀ = 3.612 Å</p>	<p>Matrix</p> <p>Gamma Prime</p>

are associated in chains.

Only the larger particles could be extracted in the replica. They have a quadratic form and are aligned toward the orientation of the parent matrix.

Cold rolling the alloy 50 percent before aging, as an aid in phase identification, resulted in a heterogenized two-phase structure containing particles with an approximate diameter of several microns. The X-ray diffraction analysis (Table II-16) confirmed that the precipitate is the γ' phase with a lattice constant somewhat larger than the Ni_3Al phase. This indicated that the γ' phase in the alloy 1-B-V-4 may contain a substantial amount of tantalum which substitutes for aluminum positions in the Ll_2 lattice.

(6) Selection of Ferritic Alloys

The composition of the ferritic alloys melted in the form of 300 gram buttons, covers the range of alloying content which is regarded as the most suitable to provide high yield strength, good magnetic properties, and good stability. The analyzed composition of the alloys made as 300 gram buttons was very near the nominal composition. The only noticeable difference was that the tantalum content was generally 0.5 weight percent higher and the aluminum content 0.1 weight percent higher than expected. The data obtained from the test results on these ferritic alloys are listed in Table II-17.

The following requirements were set previously for selecting suitable alloys from the screening program and apply in the selection of the final alloys for investigation:

- a) Magnetic saturation at 1112°F (600°C) equal to or greater than 150 emu/g (15,000 gauss).
- b) Maximum hardness during isochronal aging equal to or greater than 550 VHN.
- c) Temperature at which maximum hardness was obtained equal to or greater than 1022°F (550°C).

TABLE II-17. Properties of Martensitic Alloys 1-A-V-1 to 1-A-V-6 and 1-A-S-1 and 1-A-S-2

Alloy Number	Analyzed Composition (weight percent)	Aged One Hour at 1112° F(600° C) Measured at 1112° F(600° C) Saturation Magnetic Moment(a) (emu/g)	Aged One Hour at 1022° F(550° C)				Aged 100 Hours at 1022° F(550° C)		Change in Hardness After 100 Hours Aging (percent)
			Temperature at Which Maximum Room Temperature Hardness Was Obtained (° F)	Room Temperature Hardness (° C)	Maximum Room Temperature Hardness (VHN)	Room Temperature Coercivity At Maximum Hardness (oersteds)	Room Temperature Hardness (VHN)	Room Temperature Coercivity (oersteds)	
1-A-V-1	Fe-14.6Ni-29.2Co-0.56Al-0.49Ti-2.15W-4.5Ta	160	1112	600	732	35	746	62.5	-0.5
1-A-V-2	Fe-9.57Ni-20.1Co-0.63Al-0.53Ti-3.56Ta	172	1022	550	570	22	512	30	-13.5
1-A-V-3	Fe-11.4Ni-25.0Co-0.61Al-0.52Ti-1.00W-4.06Ta	166	1022	550	641	30.5	630	42.5	-4.1
1-A-V-4	Fe-14.8Ni-29.4Co-0.64Al-0.52Ti-3.48Ta	168	1112	600	670	35	683	48.5	-2.3
1-A-V-5	Fe-14.5Ni-29.8Co-0.62Al-0.54Ti-2.10W-3.48Ta	161	1112	600	704	37	721	62.5	-0.4
1-A-V-6	Fe-4.66Ni-5.19Cr-25.7Co-0.64Al-0.49Ti-1.18W-3.56Ta	150	1022	550	553	33	540	37	-7.0
1-A-S-1	Fe-15.3Ni-29.1Co-2.90Ta-0.92W-0.42Ti-0.27Al	162	1112	600	664	32	625	46	-7.5
1-A-S-2	Fe-12.2Ni-29.5Co-2.95Ta-0.96W-0.41Ti-0.38Al	171	1112	600	643	31	630	44	-5.5

(a) To convert saturation magnetic moment per gram to the approximate saturation induction in gauss, multiply the listed value by 100.

(a) To convert saturation magnetic moment per gram to the approximate saturation induction in gauss, multiply the listed value by 100.

- d) Room temperature coercive force even after 100 hours aging at 1022°F (550°C) equal to or less than 50 oersteds.
- e) The drop in hardness during isothermal aging at 1022°F (550°C) from the maximum value should be less than 10 percent.

The requirements listed in a, b, and c were fulfilled by all selected alloys. Alloys 1-A-V-1 and 1-A-V-5 did not fulfill requirement d. This may be due to the higher amount of tantalum and aluminum additions than expected. Alloy 1-A-V-2 does not meet requirement e. The results very clearly show the influence of cobalt on stability and coercive force. The higher cobalt content produces better thermal stability, but the coercive force increases. The chromium content keeps the coercive force lower.

However, stability of hardness and saturation of alloy 1-A-V-6 is less than alloys 1-A-V-3 and 1-A-V-4. The latter two alloys were selected for the final alloy compositions with some minor adjustments (1-A-S-1 and 1-A-S-2). Cobalt was chosen at 30 percent to give better stability. Ta, Al, and Ti were reduced to give lower coercive force.

The results of the final martensitic alloys are included in Table II-17. The analyzed composition was very close to the nominal composition. The results were similar to that obtained on alloys 1-A-V-3 and 1-A-V-4. However, alloy 1-A-V-3 and 1-A-V-4 showed better stability than the final alloys. The lower aluminum content in the final alloys can be regarded as responsible for this behavior. The coercive force of 1-A-V-3 was lower than the final alloys which is due to the lower cobalt content. Therefore, the 15-pound alloys can not be regarded as fully optimized alloys. However, they give a good combination of properties well within the established range of requirements. The alloy 1-A-S-2 is superior to alloy 1-A-S-1 as far as high magnetic saturation, low coercive force, and stability are concerned. Alloy 1-A-S-2 will therefore be selected for the final evaluation.

The coercive force measurements at elevated temperature show that in the case of the iron-base alloys nominally containing 30 percent cobalt (1-A-V-1, 1-A-V-4, 1-A-V-5), the reduction of coercive force from room temperature to 1112°F

(600°C) is between 15 and 20 percent; while in alloy 1-A-V-6 which contains chromium, the reduction is more than 30 percent. One may conclude that a further refinement in alloy development would be a suitable balance between tolerable coercive force and stability in strength. This balance may be obtained by adjusting the cobalt content versus aluminum and chromium content. An additional measure to keep the coercive force down would be the application for ~5 percent plastic strain prior to aging.

The exploratory study on this program has defined the final alloy composition in the following manner:

Ni: 11 to 13 weight percent, Co: 25 to 35 weight percent, Cr: up to 2 weight percent by replacing 2 weight percent Ni with 1 weight percent Cr, Ta: 2 to 3 weight percent, W: up to 1 weight percent, Ti: 0.3 to 0.4 weight percent, Al: 0.3 to 0.5 weight percent, Fe: balance.

An adjustment of the alloying content is necessary to provide an optimum balance between stability and coercive force. An adjustment which may include minor changes in chemistry by additions of about 0.1 weight percent will also be necessary to develop the optimum creep properties. The upper limit for anticipated service temperature can be expected in the range of 1022°F to 1112°F (550°C to 600°C).

(7) Selection of Cobalt-Base Alloys

The cobalt-base alloys which were melted in the form of 300 gram buttons were chosen from the range of compositions as outlined previously. The analyzed compositions of the melts were quite close to the nominal compositions. A summary of test results is shown in Table II-18.

The following requirements were set previously for selecting suitable alloys from the screening program and apply in the selection of the final alloys:

- a) No discontinuous precipitate should occur during isothermal aging of 100 hours at 1292°F (700°C).

TABLE II-18. Properties of Cobalt-Base Alloys 1-B-V-1 to 1-B-V-6 and 1-B-S-1 and 1-B-S-2

Alloy Number	Analyzed Composition (weight percent)	Aged One Hour at 1382°F (750°C) Measured at 1112°F (600°C) Saturation Magnetic Moment (a) (emu/g)	Aged One Hour at 1292°F (700°C)				Aged 100 Hours at 1292°F (700°C)		
			Temperature at Which Maximum Room Temperature Hardness Was Obtained (°F)	Maximum Room Temperature Hardness (VHN)	Room Temperature Coercivity At Maximum Hardness (oersteds)	Room Temperature Coercivity (oersteds)	Room Temperature Hardness (VHN)	Room Temperature Coercivity (oersteds)	Discontinuous Precipitate
1-B-V-1	Co-5.0Fe-0.27Zr-14.6Ni-1.44Al-1.66Ti-5.20Ta	91	1382	750	354	4.7	388	26	None
1-B-V-2	Co-4.8Fe-0.27Zr-10.3Ni-1.19Al-3.07Ta	114	1292	700	248	3.1	255	6.7	None
1-B-V-3	Co-4.9Fe-0.26Zr-11.9Ni-1.40Al-1.07Ti-4.05Ta	102	1382	750	307	3.6	333	12.4	None
1-B-V-4	Co-5.1Fe-0.26Zr-14.8Ni-1.25Al-5.19Ta	106	1382	750	323	3.6	343	10.6	None
1-B-V-5	Co-5.0Fe-0.27Zr-9.85Ni-1.60Al-5.3Ta	105	1382	750	303	3.9	320	9.3	None
1-B-V-6	Co-4.8Fe-0.24Zr-15.0Ni-1.19Al-1.66Ti-3.17Ta	100	1382	750	313	3.4	338	14.2	None
1-B-S-1	Co-5.8Fe-15.3Ni-4.98Ta-1.28Al-0.21Zr	104	1382	750	311	3.3	331	14.7	None
1-B-S-2	Co-5.2Fe-15.2Ni-4.98Ta-1.36Al-0.12Zr-0.065Be	102	1382	750	313	3.1	336	14.8	None

(a) To convert saturation magnetic moment per gram to the approximate saturation induction in gauss, multiply the listed value by 110.

- b) The temperature at which maximum hardness is obtained during isochronal aging should be 1382°F (750°C) or higher.

The listed requirements were fulfilled in all the 300 gram cobalt-base alloys except 1-B-V-2 which did not meet requirement b. Apparently, the alloying content was too low in that alloy. Within the given range of additions; Ta: 3 to 5 weight percent, Al: 1.2 to 1.5 weight percent, Ti: 0 to 1.7 weight percent, the most suitable combination that produces the best balance of magnetic saturation, hardness, and coercive force must be found. Alloy 1-B-V-4 exhibits a good combination of properties. Among the 300 gram experimental alloys, the hardness data from alloy 1-B-V-4 were second best; the magnetic properties were also second best.

The results confirm the previous results from the 25 gram ingots that showed the addition of Al + Ta give a better balance of hardness, yield strength, and magnetic properties than the inclusion of Ti in the alloying content.

The influence of alloying elements may be expressed analytically in the following equation:

$$\begin{aligned} \text{Magnetic saturation } (\sigma) \text{ expressed as emu/g} &= 102 - 0.5 (\% \text{ Ni}) + 3.6 (\% \text{ Al}) - 7.0 (\% \text{ Ti}) - 3.0 (\% \text{ Ta}) \\ \text{Hardness expressed in VHN} &= 120 + 6 (\% \text{ Ni}) + 80 (\% \text{ Al}) \\ &+ 16 (\% \text{ Ti}) + 9 (\% \text{ Ta}) \end{aligned}$$

However, these expressions must be considered with some caution. The number of alloys tested before deriving the equation was not large enough to provide adequate significance to the results. In addition, the variation of aluminum content in the test alloys is too small to place any significance to the coefficients obtained for aluminum content. The standard error for this coefficient is greater than 100 percent. The computer analysis would indicate that an alloy with no Ti, but containing Ni, Al, and Ta at the upper limit would produce the best balance of hardness and saturation. However, for a candidate final alloy, composition 1-B-V-4 was chosen. Alloy 1-B-S-1 was melted to duplicate the former alloy. The test results obtained were comparable. There

are differences in chemical composition. Although very small, they may account for the observed differences in properties. The alloy 1-B-S-2 was slightly modified by minor additions of beryllium. The stability and saturation of this alloy were not as good as alloy 1-B-S-1. Therefore, the latter was selected for further evaluation of properties. It is felt that the composition Co-5 Fe-15 Ni-5 Ta-(1.2-1.5) Al-0.25 Zr, provides a very good balance of magnetic and mechanical properties. An optimum composition can only be defined if one knows the desired balance of both properties required in the generator design. On the other hand, some adjustment of the composition and some minor additions up to 1.1 weight percent, may become necessary during a development program for creep properties. The upper service temperature limit for this alloy is expected to be in the 1292 to 1382°F (700 to 750°C) range.

3. Program for the Next Quarter

- a) The kinetic studies on the final test alloys will be completed.
- b) Magnetic testing of the final alloys, including d-c magnetization curves and core loss data will be completed.
- c) Samples for creep testing will be machined.

B. TASK 2 - INVESTIGATION FOR RAISING THE ALPHA TO GAMMA
TRANSFORMATION TEMPERATURE IN COBALT-IRON ALLOYS

Work on this task is complete and will be reported in the Final Topical
Report.

C. TASK 3 - DISPERSION-STRENGTHENED MAGNETIC MATERIALS FOR APPLICATION IN THE 1200° TO 1600°F RANGE

1. Summary of Technical Progress

- a) One cobalt-base and two iron + 27 w/o cobalt-base compositions dispersion-strengthened with zirconia and/or boride particles were extruded in a Dynapak Machine using 1600°F maximum processing temperatures. These extrusions showed significantly higher tensile properties at 1200°F, but no significant improvement in strength at 1600°F in comparison with conventional hydraulic extruded material made with a 2000°F maximum processing temperature.
- b) X-ray diffraction studies were conducted on the dispersoids in extrusions of cobalt-base and iron + 27 w/o cobalt-base pre-alloyed atomized powders containing aluminum and beryllium which had been given internal oxidation treatments. The dispersed particles were identified as either alpha-alumina or beryllium oxide exclusively.
- c) In the cobalt-base and iron + 27 w/o cobalt-base dispersion-strengthened extrusions investigated to date, there has been a generally inverse relationship between yield strength and saturation magnetization at 1200° and 1600°F. The achievement of high strength combined with high saturation has been identified as a problem area. High strength was promoted by small interparticle spacings (small dispersed particles and large volume percents of dispersoid). On the other hand, saturation magnetization was lowered in proportion to the volume percent of nonmagnetic dispersoid. For this reason, the smaller dispersed particles are favored for achieving small interparticle spacing. Acceptably low values of coercive force at 1200° to 1600°F have been achieved in all materials, although those with the coarser particles tended to have the lower values of coercive force.
- d) The secondary working conditions (working temperature, percent reduction per cycle, number of cycles, and intermediate annealing temperature) to further increase the strength of hot-worked dispersion-strengthened materials for high-speed, solid rotors will have to be designed so that they are applicable to the eventual fabrication of a

large size produce (12 to 28 inches diameter and 12 to 28 inches long). The secondary working and thermomechanical treatments reported in the literature were applied mainly to dispersion-strengthened products having small cross-sections.

- e) The obtaining of additional powders in certain compositional systems, which have been identified to date as having the best combination of magnetic and mechanical properties, has been initiated for the intermediate evaluation phase (second phase) of this project.

2. Discussion

The purpose of the project is to develop a dispersion-strengthened, magnetically-soft material for use in the 1200° to 1600°F temperature range for rotor applications. As an initial and tentative goal, the material should have the following properties at some temperature between 1200° and 1600°F, preferably at 1600°F.

Saturation magnetization, B_s - 12,000 gauss minimum

Coercive force, H_c - 25 oersteds maximum

Creep strain in 10,000 hours at 10,000 psi - 0.4 percent maximum

In pursuit of this goal, dispersion-strengthened cobalt-base and iron + 27 percent cobalt-base extrusions were made from (a) prealloyed atomized powders containing boride compound particles, (b) internally oxidized powders containing alumina or beryllia, and (c) composite powders containing both a metal phase and a refractory oxide phase (alumina or thoria) within each powder particle. Also, dispersion-strengthened cobalt-base extrusions containing thoria were purchased from two suppliers. The work reported so far is part of the initial evaluation phase of the project which includes determination of saturation magnetization, coercive force, and tensile properties at room temperature and in the 1200° to 1600°F range. Later on, the intermediate and final evaluation phases of this project will be conducted on the best candidate compositional systems developed in the first phase. Changes in powder processing conditions and application of secondary working treatments to extruded material will be made on a selective basis.

a. PROCESSING OF POWDERS INTO EXTRUSIONS

The extrusion of compositions of atomized powder (minus 325 mesh or less than 44 microns) to rod in a Dynapak 1220C Machine using an extrusion ratio of 6 to 1 was described in the fifth quarterly report. The powders for these extrusions were processed in the normal manner except that the temperature was held to 1600°F maximum. By contrast, the normal billet pre-heat for conventional hydraulic extrusion was one hour at 2000°F. The purpose of this work was to investigate the effect of lower processing temperatures (1600°F maximum) on magnetic and tensile properties. The resultant properties will be presented later in this report.

b. TESTING OF EXTRUSIONS

(1) Microstructure

The Dynapak extrusions contained a finer dispersion of constituent particles (smaller size and smaller interparticle spacing) and finer grain size than extrusions of the same prealloyed atomized powders made with a conventional hydraulic press, Figures II-28 and II-29. Holding the processing temperatures to 1600°F maximum in the former, compared with 2000°F maximum in the latter, minimized coarsening of the constituent.

All of the iron + 27 weight percent cobalt-base extrusions made on this program, including Dynapak extrusions, were in the recrystallized condition. The Dynapak extrusions (1600°F billet) were made below the transformation temperature of the iron-cobalt matrix (approximately 1771°F from face centered cubic to body centered cubic on cooling) whereas the hydraulic extrusions (2000°F billet) were made above the transformation temperature and underwent a phase change on cooling.

X-ray diffraction studies were performed on hydraulic extrusions of additional compositions listed in Table II-19, since the last quarterly report in order to identify and confirm the dispersed phases present. In the case of the Co + 1.3 w/o B + 3.4 w/o Zr powder extrusion (atomized powder No. 4), a relatively small amount of ZrO₂ was found in

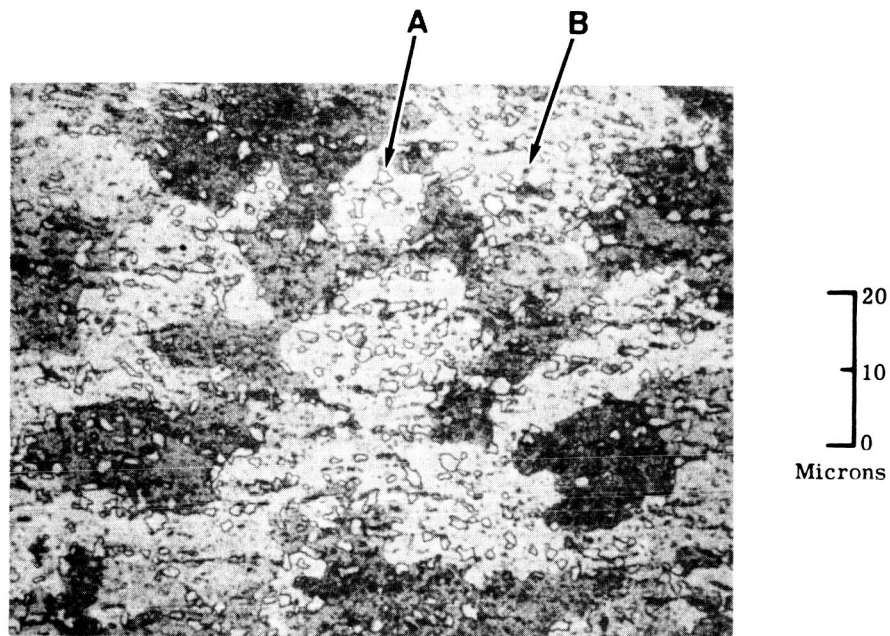


FIGURE II-28. Dynapak As-Extruded Rod of Atomized Powder No. 13, Fe + 24.8% Co + 1.1% B + 3.2% Zr, Showing $(\text{Fe, Co})_2\text{B}$ Particles (A-light) and ZrO_2 Particles (B-dark) Dispersed in Fe-Co Recrystallized Matrix, Longitudinal Section, 1000X, Etched in Carapella's Reagent

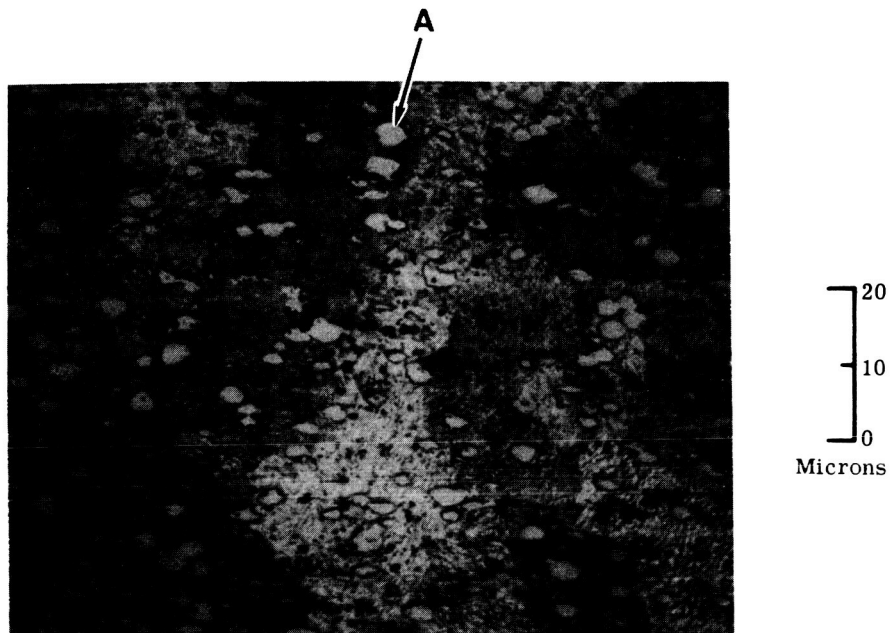


FIGURE II-29. Hydraulic As-Extruded Rod of Atomized Powder No. 13, Showing Coarser $(\text{Fe,Co})_2\text{B}$ Particles (A-light) than in Figure II-28 in Fe-Co Recrystallized Matrix, Longitudinal Section, 1000X, Etched in Carapella's Reagent

TABLE II-19. X-ray Diffraction Identification of Dispersed Constituent Particles in Extrusions

Powder Type	Powder Supplier	Nominal Composition (weight percent)	Dispersed Phases Identified
Atomized No. 4	Hoeganaes	Co+1.3B+3.4Zr	Tau Ternary Boride and ZrO ₂
Internally Oxidized No. 8 ^(a)	Hoeganaes	Co+4.7Al ₂ O ₃	Alpha-Al ₂ O ₃
Internally Oxidized No. 9 ^(b)	Domtar	Co+3.6BeO	BeO
Internally Oxidized No. 17 ^(a)	Hoeganaes	Fe+25.6Co+5.1Al ₂ O ₃	Alpha-Al ₂ O ₃
Internally Oxidized No. 18 ^(b)	Domtar	Fe+26.0Co+3.9BeO	BeO
Composite No. 11	Chas. Pfizer	Fe+23.7Co+12.1ThO ₂	ThO ₂
<p>Notes:</p> <p>(a) Prealloyed atomized powder obtained from Hoeganaes and internally oxidized by Westinghouse.</p> <p>(b) Prealloyed atomized powder obtained from Domtar Chemicals Ltd. and internally oxidized by Westinghouse.</p>			

addition to the expected tau ternary boride phase. The previous quarterly report mentioned that ZrO_2 and $(\text{Fe}, \text{Co})_2\text{B}$ were the dispersed phases in the extrusion of prealloyed atomized powder No. 13, Fe + 24.8 w/o Co + 1.1 w/o B + 3.2 w/o Zr. The original atomized powder No. 13 contained ZrO_2 and the tau boride. The zirconium in the latter boride either continued to react with oxygen during the processing into an extrusion until it was completely tied up as ZrO_2 or the tau boride appeared as a non-equilibrium phase in the powder, which underwent very rapid cooling from the liquid state during manufacture.

Zirconium has been found to be the most reactive element with oxygen during powder making and processing in this program - more reactive than cerium, aluminum, or beryllium. This is contrary to expectations based on the thermodynamic free energy of formation (ref. 1). The presence of 500 to 1500 ppm oxygen in the original powder (minus 325 mesh) might be anticipated from oxygen analyses reported for nickel-base and iron-base prealloyed atomized powders (ref. 2 to 5). Thus, rather substantial amounts of oxygen must be removed during hydrogen reduction of the powders before extrusion in order to avoid internal oxidation of the more reactive alloying elements. The substitution of completely welded Inconel 600 retorts for the previously used mechanical-seal arrangement is being investigated as a method of achieving still lower dew points during hydrogen reduction of the powder and hydrogen sintering of the powder compact.

The dispersed phases in the other extrusions listed in Table II-19 were those expected.

(2) Magnetic Properties

The coercive force values determined at room temperature on the Dynapak extrusions are presented in Table II-20 and may be compared with those for the hydraulic extrusions. The Co + 1.3 w/o B + 3.4 w/o Zr Dynapak extrusion had a much lower coercive force than the hydraulic extrusion, probably because the Dynapak extrusion contained a much higher ratio of cubic cobalt to hexagonal cobalt than did the

TABLE II-20. Comparison of Room Temperature Coercive Force Values of Extrusions Made with a Conventional Hydraulic Press and Dynapak

Nominal Composition (weight percent)	Extrusion		Amount of Dispersed Phase (percent by volume)	Average Size of Dispersed Particles (microns)	Average Interparticle Spacing (microns)	Coercive Force at Room Temperature, H_c (oersteds)
	Method	Billet Preheat (°F)				
Co + 1.3B + 3.4Zr	Hydraulic	1 hr. at 2000	26	1.0	2.7	48.0
Co + 1.3B + 3.4Zr	Dynapak	15 min. at 1600	26	0.7	2.0	25.7
Fe + 24.8Co + 1.1B + 3.2Zr	Hydraulic	1 hr. at 2000	20	0.9	3.6	18.8
Fe + 24.8Co + 1.1B + 3.2Zr	Dynapak	15 min. at 1600	20	0.5	2.0	24.5
Fe + 24.8Co + 1.1B + 3.2Zr	C. W. 65%(a)	--	20	0.5	2.0	57.3
Fe + 25.8Co + 0.9B + 4.1Cb	Hydraulic	1 hr. at 2000	20	0.8	3.1	19.6
Fe + 25.8Co + 0.9B + 4.1Cb	Dynapak	15 min. at 1600	20	0.6	2.4	23.3

NOTE: (a) Dynapak extrusion was given a 65 percent reduction in area by swaging at room temperature after extrusion.

hydraulic extrusion. This resulted from the fact that in the Dynapak process the extrusion was cooled through the transformation temperature (783°F from face centered cubic to hexagonal on cooling) to room temperature more rapidly than in the hydraulic process. Also, the finer dispersoid in the Dynapak extrusion would tend to retard the transformation. The two iron + cobalt-base Dynapak extrusions had slightly higher values of coercive force than their hydraulic extrusion counterparts. The dispersoid and recrystallized grain size was finer in the Dynapak extrusions, accounting for their higher coercive force. The one iron + cobalt-base Dynapak extrusion given a 65 percent cold reduction by swaging exhibited a large increase in coercive force due to internal stress.

Coercive force values of the Dynapak extrusions were not determined at 1200° to 1600°F. It would be expected that the coercive force in the 1200° to 1600°F range would be substantially lower than at room temperature in accordance with the trend reported previously for the hydraulic extrusions.

(3) Tensile Properties

A comparison of tensile properties of extrusions made with a hydraulic press and Dynapak, Table II-21, showed that the one cobalt-base and the two iron + 27 w/o cobalt-base compositions of prealloyed atomized powders had significantly higher strengths at 1200°F when extruded by Dynapak. On the other hand, there was no significant improvement in strength at 1600°F.

As mentioned earlier, the purpose of employing the Dynapak was to enable extrusions to be made at a lower temperature (1600°F billet) by a high energy rate process than used for conventional hydraulic extrusion (2000°F). The boride dispersed particles were smaller in the Dynapak extrusions, as shown earlier in Table II-20, and led to higher strengths in the specimens tensile tested at 1200°F (after aging 100 hours at 1200°F). The lack of improvement in strength at 1600°F (after aging the specimens 100 hours at 1600°F) was attributed to the coarsening of the boride particles at that temperature. This latter feature suggested a limitation on strength stability by dispersed boride phases of these particular chemical compositions.

TABLE II-21. Comparison of Elevated Temperature Tensile Properties of Extrusions Made With a Conventional Hydraulic Press and Dynapak

Nominal Composition (weight percent)	Extrusion Method	Test Temp. (°F)	Tensile Properties (a)		
			Ultimate Tensile Strength (1000 psi)	Yield Strength, 0.2% Offset (1000 psi)	Elongation in 4D (percent)
Co+1.3B+3.4Zr	Hydraulic	1200	75.7	38.9	20.0
" " "	Hydraulic	1600	30.3	10.1	52.0
" " "	Dynapak	1200	82.9	48.4	30.0
" " "	Dynapak	1600	24.6	6.1	114.0
Fe+24.8Co+1.1B+3.2Zr	Hydraulic	1200	62.1	31.5	40.0
" " "	Hydraulic	1600	18.5	10.0	82.0
" " "	Dynapak	1200	70.7	42.3	44.0
" " "	Dynapak	1600	18.1	10.2	62.0
" " "	C. W. 65% (b)	1200	80.2	38.5	2.0(c)
Fe+25.8Co+0.9B+4.1Cb	Hydraulic	1200	67.2	31.5	34.0
" " "	Hydraulic	1600	17.7	7.3	48.0
" " "	Dynapak	1200	71.0	36.7	52.0
" " "	Dynapak	1600	19.8	9.8	118.0

Notes:

- (a) All tensile specimens aged 100 hours in vacuum (pressure of 1 x 10⁻⁵ torr or less) at the elevated test temperature before testing in vacuum of 1 x 10⁻⁵ torr in order to stabilize structure.
- (b) Dynapak extrusion was given a 65 percent cold reduction in area by swaging.
- (c) Low elongation probably resulted from longitudinal crack present at one end of tensile specimen.

A short length of the Fe + 24.8 w/o Co + 1.1 w/o B + 3.2 w/o Zr Dynapak extruded rod was cold reduced 65 percent by swaging. Cold working did not greatly affect the tensile and yield strengths at 1200°F. The low elongation, 2.0 percent, at 1200°F probably was related to a longitudinal crack present near one end of the tensile specimen which became apparent after final machining. The cracked condition may have originated from the extrusion defect located near the back of the extrusion, although precautions were taken to try to avoid this.

All of the Fe + 27 w/o Co-base extrusions in Table II-21 had a recrystallized structure, both hydraulic and Dynapak. The higher strengths of the Dynapak extrusions at 1200°F were related to the smaller size of dispersed particles and, hence, smaller interparticle spacing in the matrix achieved by keeping the material processing temperatures at 1600°F maximum. However, aging for 100 hours at 1600°F before tensile testing at 1600°F resulted in some coarsening of the dispersoid, so that the 1600°F strengths of the Dynapak extrusions were approximately the same as those of the hydraulic extrusions.

As mentioned in previous reports, the achievement of relatively low values of coercive force in the 1200° to 1600°F range has not been a problem with any of the dispersion-strengthened compositions investigated to date. A more difficult problem has been the achievement of high values of saturation magnetization combined with high values of yield strength at 1200° to 1600°F. Figures II-30 and II-31 present graphically the relative combinations of yield strength and saturation achieved with materials evaluated in the hot-extruded condition during the initial evaluation phase (one of three phases) of this task at 1200°F and 1600°F, respectively. Nivco alloy is included for comparison and appears to be a strong contender at 1200°F (on the basis of short-time tensile tests rather than creep tests), but is not competitive at 1600°F.

The boundary lines, or envelopes, on either side of the data in Figures II-30 and II-31 indicate a generally inverse relationship between yield strength and saturation in the experimental compositions made and tested to date. The short-term

Figure II-30. Yield Strength and Magnetic Saturation of Nivco and Dispersion Strengthened Extrusions

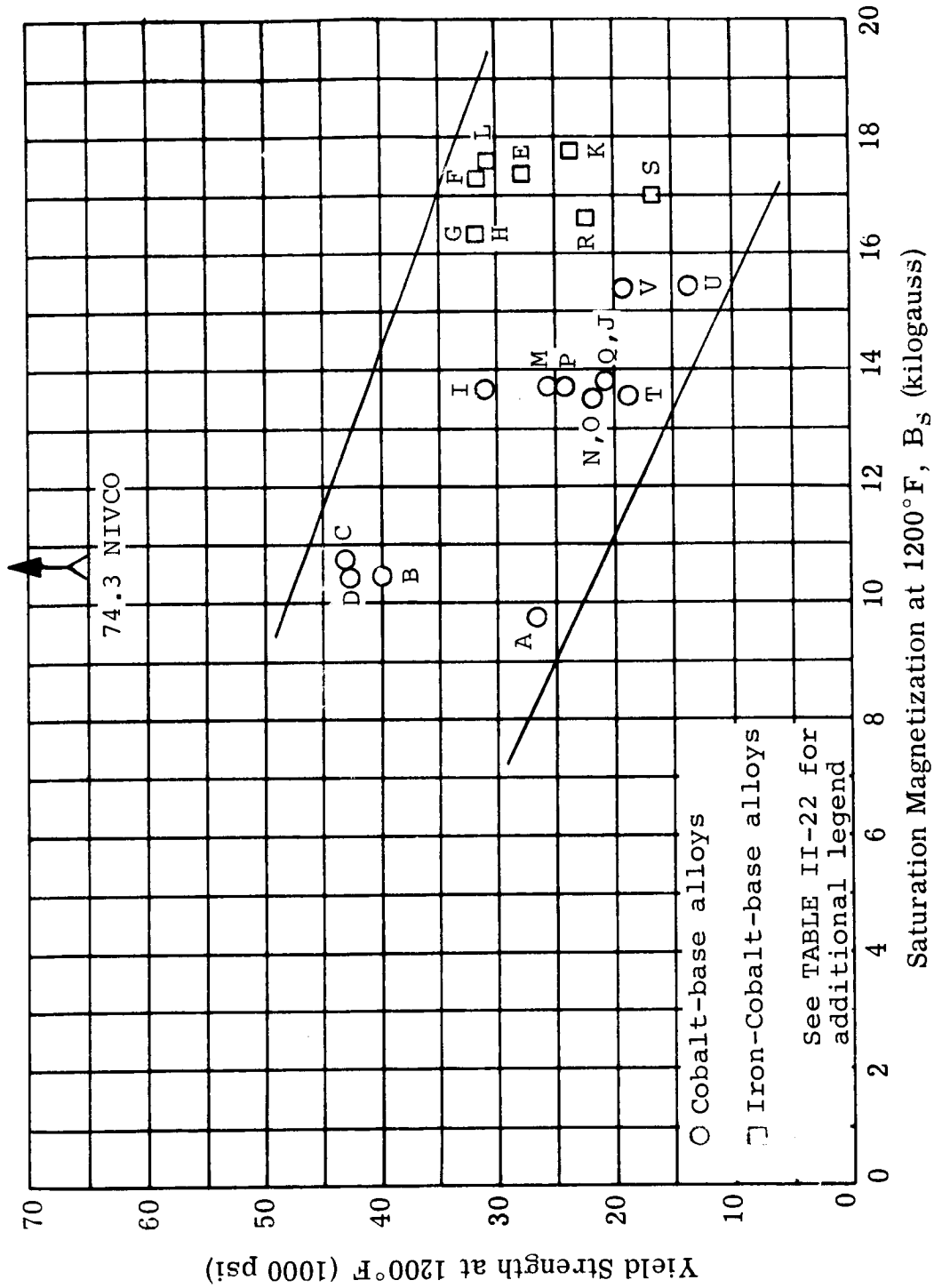


FIGURE II-30. Yield Strength and Saturation Magnetization at 1200°F of Dispersion-Strengthened Extrusions and Nivco

Figure II-31. Yield Strength and Magnetic Saturation of Nivco and Dispersion Strengthened Extrusions

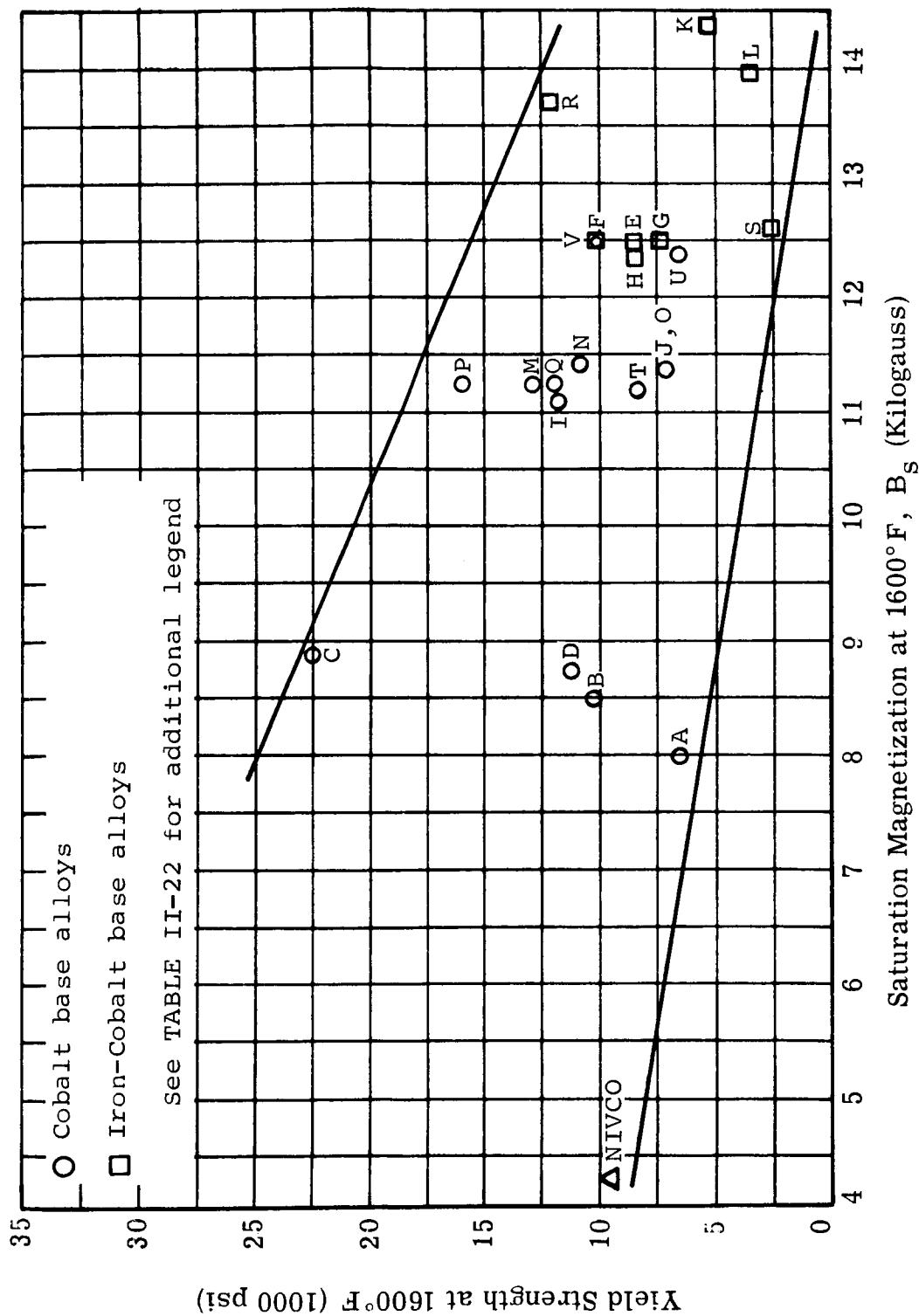


FIGURE II-31. Yield Strength and Saturation Magnetization at 1600°F of Dispersion-Strengthened Extrusions and Nivco

TABLE II-22. Legend for Figures II-30 and II-31

Symbol	Prealloyed Atomized Powders	Symbol	Composite Powders
A	Co+1.3B+1.6Ti	M	Co+11.2ThO ₂ (0.01-0.06 _μ) Sherritt Gordon
B	Co+1.3B+3.4Zr	N	Co+4.75Al ₂ O ₃ (0.01-0.06 _μ) Chas. Pfizer
C	Co+1.1B+4.4Cb	O	Co+4.75Al ₂ O ₃ (0.01-0.06 _μ) Chas. Pfizer
D	Co+1.2B+7.7Ta	P	Co+11.2ThO ₂ (0.01-0.06 _μ) Chas. Pfizer
E	Fe+26.5Co+0.9B+1.8Ti	Q	Co+11.2ThO ₂ (0.1-0.6 _μ) Chas. Pfizer
F	Fe+24.8Co+1.1B+3.2Zr	R	Fe+23.7Co+12.1ThO ₂ (0.01-0.06 _μ) Chas. Pfizer
G	Fe+25.8Co+0.9B+4.1Cb	S	Fe+23.7Co+12.1ThO ₂ (0.01-0.06 _μ) Vitro Labs
H	Fe+24.1Co+1.0B+7.0Ta		
Symbol	Internally Oxidized Powders	Symbol	Supplier Extrusions
I	Co+4.7Al ₂ O ₃	T	Co+10.4ThO ₂ (0.01-0.06 _μ), Nem - Lab
J	Co+3.6BeO	U	Co+2.0ThO ₂ (0.01-0.06 _μ), Curtiss Wright
K	Fe+25.6Co+5.1Al ₂ O ₃	V	Co+2.0ThO ₂ (0.01-0.06 _μ), Curtiss Wright 85% Cold Reduction
L	Fe+26.0Co+3.9BeO		

creep tests now being initiated will give some indication as to whether or not creep resistance and saturation magnetization are similarly related in hot-extruded material.

(4) Selected Compositions

The elevated temperature tensile and magnetic properties of eight extrusions (out of the 19 made by Westinghouse) which tended to have the best combination of tensile and magnetic properties are listed in Table II-23. The extruded rods were made with a conventional hydraulic press using an extrusion ratio of 11 to 1 and a billet preheat of one hour at 2000°F. These extrusions represent different types of dispersion-strengthened materials: (a) prealloyed atomized powders, (b) internally oxidized powders, and (c) composite powders. None of the supplier extrusions of dispersion-strengthened cobalt are listed because their tensile properties were generally not as high as those in Table II-23.

For comparison the corresponding properties of precipitation-hardened Nivco alloy and secondary-worked TD Nickel (Du Pont data, ref. 6) are listed at the bottom of the table.

At 1200°F it may be seen that some of the experimental extrusions processed in the initial evaluation phase of the program have a yield strength approximately the same as TD Nickel. One of the experimental compositions, Co + 1.1 w/o B + 4.4 w/o Cb has a higher yield strength than TD Nickel at both 1200°F and 1600°F. At 1600°F, some of the experimental compositions have a higher yield strength than Nivco, but all have saturation magnetization values at least two to three times greater than Nivco alloy. These data suggest that a number of promising alloy systems have been identified. The intermediate evaluation (phase 2), and the final evaluation (phase 3), which includes creep testing, will identify those compositions having the greatest mechanical strength and stability. The present mechanical property data have verified that a suitable soft magnetic material can be made by the dispersion-strengthening mechanism.

TABLE II-23. Tensile and Magnetic Properties of Dispersion-Strengthened Rod (as-extruded) at 1200°F and 1600°F

Nominal Composition (weight percent)	Amount of Dispersed Phase (percent by volume)	Test Temp. (°F)	Tensile Properties ^(a)			Magnetic Properties	
			Ultimate Tensile Strength (1000 psi)	Yield Strength 0.2% Offset (1000 psi)	Elongation in 4D (percent)	Coercive Force, H _c (oersteds)	Saturation Magnetization, B _s (kilogauss)
a. Prealloyed Atomized Powders:							
Co+1.1B+4.4Cb	27	1200	80	42	23	10.3	10.9
Co+1.1B+4.4Cb	27	1600	41	23	66	4.6	8.6
Fe+24.8Co+1.1B+3.2Zr	20	1200	62	32	40	8.4	17.2
Fe+24.8Co+1.1B+3.2Zr	20	1600	19	10	82	3.6	12.5
b. Internally Oxidized Powders:							
Co+4.7Al ₂ O ₃	9.8	1200	38	30	17	9.7	13.7
Co+4.7Al ₂ O ₃	9.8	1600	21	12	15	6.1	11.1
Co+3.6BeO	8.3	1200	33	21	78	9.0	13.9
Co+3.6BeO	8.3	1600	13	7	28	4.4	11.4
Fe+26.0Co+3.9BeO	9.6	1200	48	31	24	9.3	17.5
Fe+26.0Co+3.9BeO	9.6	1600	12	4	36	2.7	14.0
c. Composite Powders:							
Co+11.2ThO ₂ (0.01-0.06μ), Sherritt Gordon	10	1200	26	26	4(c)	21.5	13.7
Co+11.2ThO ₂ (0.01-0.06μ), Sherritt Gordon	10	1600	13	(b)	0	13.0	11.2
Co+11.2ThO ₂ (0.01-0.6μ), Chas. Pfizer	10	1200	30	24	8	12.4	13.9
Co+11.2ThO ₂ (0.01-0.6μ), Chas. Pfizer	10	1600	20	16	3	8.2	11.2
Fe+23.7Co+12.1ThO ₂ (0.01-0.06μ), Chas. Pfizer	10	1200	35	22	4	9.0	17.3
Fe+23.7Co+12.1ThO ₂ (0.01-0.06μ), Chas. Pfizer	10	1600	20	12	38	4.4	13.7
d. Comparison Materials:							
Nivco 5 8 in. Dia. Forged Bar		1200	97	74	30	6.8	10.8
Nivco 5 8 in. Dia. Forged Bar		1600	25	9.5	124	2.3	4.3
TD Nickel 1-1 4 in. Dia Bar (Secondary Worked)		1200	38	33	14	Nonmagnetic(d)	
TD Nickel 1-1 4 in. Dia Bar (Secondary Worked)		1600	26	22	10	Nonmagnetic(d)	
Notes:							
(a) All tensile specimens except TD Nickel aged 100 hours in vacuum (pressure of 1 x 10 ⁻⁵ torr or less) at the elevated test temperature before testing in vacuum of 1 x 10 ⁻⁵ torr in order to stabilize structure.							
(b) Failed before reaching 0.2 percent offset.							
(c) Failed outside gage length.							
(d) Nickel has a Curie Temperature of 680 F.							

c. SECONDARY WORKING

Secondary working and thermomechanical treatments have been reported to have a substantial effect on the strength of dispersion-strengthened copper (ref. 7), nickel (refs. 6, 8, 9, and 12 to 15), cobalt (ref. 10), and iron (ref. 11) having oxide contents in the range from 0.4 to 3 percent by volume. The mechanical properties of TD Nickel are reported to depend on the cold work-stress relief cycle (ref. 6). The best high-temperature strength of nickel-thoria strip was obtained by working with a maximum number (21) of cold reduction-annealing cycles with a minimum reduction in thickness (less than 10 percent) in each working cycle (ref. 9).

Previous quarterly reports on this program have listed the tensile properties at 1200°F and 1600°F of dispersion-strengthened Co + 2 w/o ThO₂ rod in the hot-extruded and 85 percent cold-swaged conditions. The latter condition provided significantly higher tensile and yield strengths. On the other hand, the Fe + 24.8 w/o Co + 1.1 w/o B + 3.2 w/o Zr Dynapak extrusion, which was recrystallized and contained 20 volume percent of a relatively coarse dispersion (listed in Table II-21 of this report), received a cold reduction of 65 percent by swaging. In comparison to the tensile properties at 1200°F of the original hot-extruded Dynapak rod, the cold-worked material had only a slightly higher tensile strength and a slightly lower yield strength at 1200°F.

The literature on the effect of secondary working and thermomechanical treatments of dispersion-strengthened metals revealed that these methods of improving elevated temperature strength have been applied successfully to wire, small diameter bar, sheet, and tubing where the product size is small or at least the thickness of the material is small in one direction (sheet and tubing). Small cross-sections permit dispersion-strengthened products to be worked thoroughly and uniformly. However, the eventual application for the material being developed on this program will be a solid, high-speed rotor whose size may be 12 to 28 inches diameter by 12 to 28 inches long. One method of fabrication would be to make the rotor as one piece. Another method would be to fabricate it from laminated and bonded sections with a minimum of reluctance added to the magnetic circuit. Therefore, secondary working treatments which are selected and applied to small diameter (3/4 inch) extrusions in this program must have been designed with consideration for methods which could be applied

later on to the fabrication of much larger products. To date the emphasis has been placed on determining the properties at 1200° to 1600°F of cobalt-base and iron + 27 w/o cobalt-base compositions containing various amounts of dispersoid in the primary hot-worked (hot-extruded) condition. Next, the properties of the most promising compositional systems must be determined after secondary working.

d. PLANS FOR INTERMEDIATE EVALUATION

The work reported to date was performed on the initial evaluation or screening phase of this program where extrusions of dispersion-strengthened compositions representing different methods of powder manufacture, powder compositions, dispersoid types, volume percentages and particle sizes were fabricated and tested. The next phase of the program, an intermediate evaluation, involves investigation of the best types of dispersoids revealed in the initial evaluation in order to improve magnetic properties and strength. Also, some changes in powder production, processing, and fabricating conditions will be made.

For the intermediate evaluation, the following new powder compositions are being obtained.

- (1) Prealloyed Atomized Powder No. 19: Fe + 24.8 w/o Co + 8.3 w/o Zr

The zirconium will be oxidized to form a maximum of 15 volume percent ZrO_2 dispersoid. It was mentioned in the fifth quarterly report that a similar composition, but of lower zirconium content and containing boron, was dispersion-strengthened by ZrO_2 particles and coarser boride particles. The new composition is of higher zirconium content, but without boron. The increased amount of ZrO_2 will provide a greater dispersion-strengthening effect.

- (2) Composite Powder No. 13: Co + 4.52 w/o ThO_2 (0.01 - 0.06 micron thoria)

Composite Powder No. 14: Co + 8.41 w/o ThO_2 (0.01 - 0.06 micron thoria)

The two composite powder compositions contain 4 and 7.5 volume percent thoria, respectively. Both of these powders will be obtained from two suppliers, Sherritt Gordon Mines and Chas. Pfizer. Previous evaluation of the Co + 10 v/o ThO₂ powder composition obtained from both these suppliers showed a promising combination of magnetic and tensile properties at 1200° to 1600°F. The lower thoria contents of the new powders will provide higher values of saturation magnetization (less dilution by the non-magnetic phase), higher tensile elongations, and lower notch sensitivity.

3. Program for the Next Quarter

- a) Obtain 100 hour (maximum) creep test data at 1400°F on seven dispersion-strengthened compositions previously shown to have a good combination of tensile and magnetic properties at 1200° to 1600°F.
- b) Complete chemical analyses of six extrusions, and compare with Westinghouse compositional target limits and analyses of powders.
- c) Process five dispersion-strengthened compositions into extrusions using improved processing methods based on recommendations developed in the preliminary evaluation phase of the program. Mechanical property data will be obtained in the 1200° to 1600°F range.
- d) Proceed with the processing of powders into extrusions as powders for the intermediate evaluation phase of the program are received.

D. TASK 4 - CREEP TESTING

1. Summary of Technical Progress

- a) Specimen No. 2 from Nivco heat 10-NO2V-1099 has accumulated 6210 hours on test at 37,500 psi and 1100°F. Creep strain amounts to 0.66 percent. Capsule pressure is 1.7×10^{-9} torr.
- b) After 3184 hours at 1150°F and 30,000 psi, specimen No. 3 shows 2.05 percent creep strain. Capsule pressure is 3.5×10^{-9} torr.
- c) The fourth specimen from heat 10-NO2V-1099 is on test at 1150°F and 25,000 psi. Test pressure is 8.4×10^{-9} torr after 2752 hours. Creep strain is 1.25 percent.
- d) Specimen No. 5 has accumulated 2680 hours on test at 1050°F and 50,000 psi. Creep strain is 0.59 percent and capsule pressure is 4.3×10^{-9} torr.

2. Discussion

Long-time creep data are needed on high-strength materials suitable for use as rotors in high-temperature electrical alternators. Nivco alloy is presently the highest-temperature rotor material available. Ten thousand-hour tests are now planned for specimens two, four, and five. Specimen No. 3 will be terminated at 5000 hours since it may have started transition to third stage creep. All creep data are plotted on Figures II-32, II-33, and II-34. One last specimen from heat 10-NO2V-1099 will be started on test at 20,000 psi at 1150°F.

3. Program for the Next Quarter

The four specimens presently on test will be continued. The sixth 10,000-hour test will be started upon termination of the test on specimen No. 3.

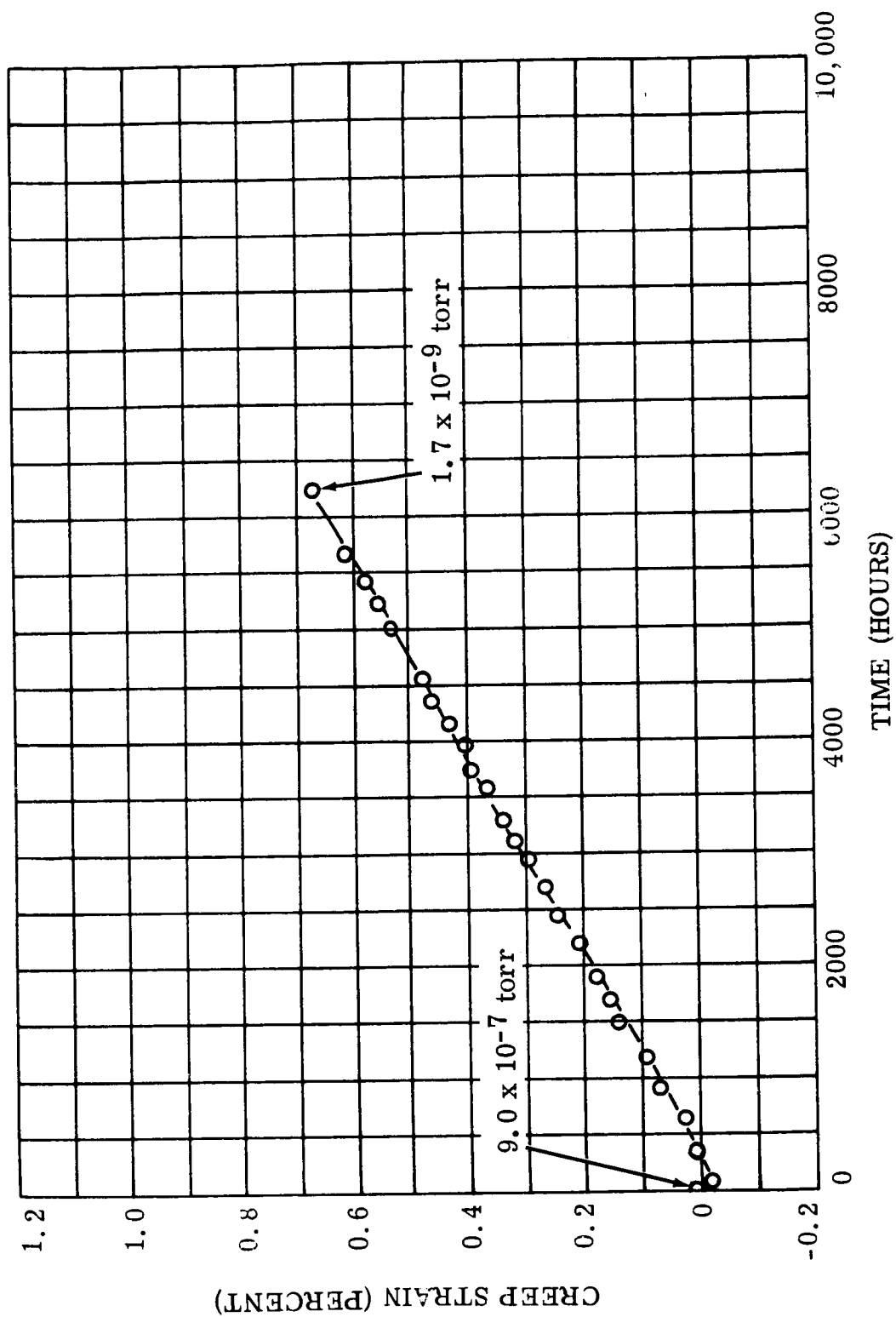


Figure II-32. Creep Nivco Bar 1100°F

FIGURE II-32. Creep, Nivco Heat 10-NO2V-1099, Tested in Vacuum at 1100°F and 37,500 psi (Specimen #2)

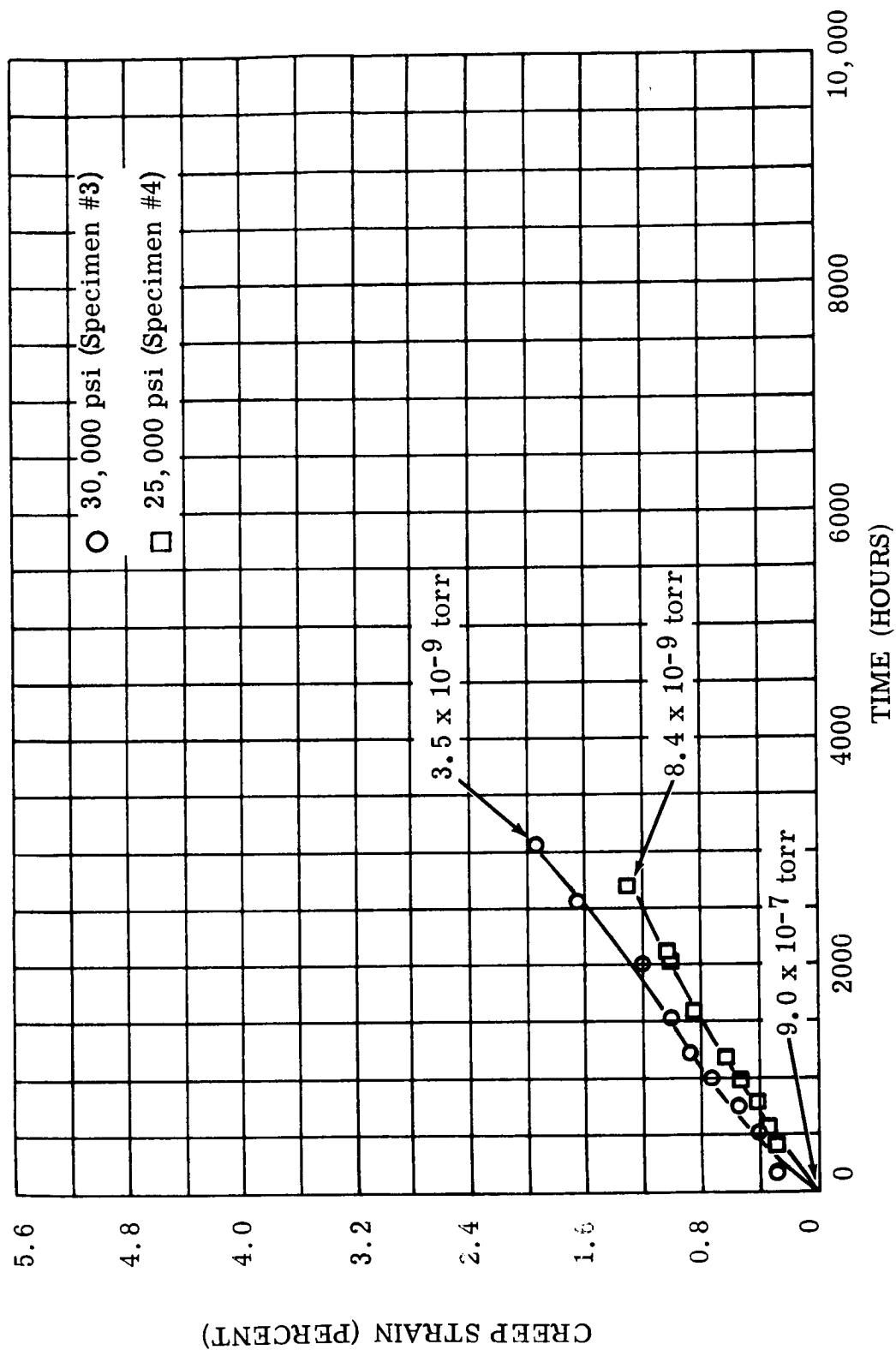


FIGURE II-33. Creep, Nivco Heat 10-NO2V-1099, Tested in Vacuum at 1150°F and 25,000 psi and 30,000 psi

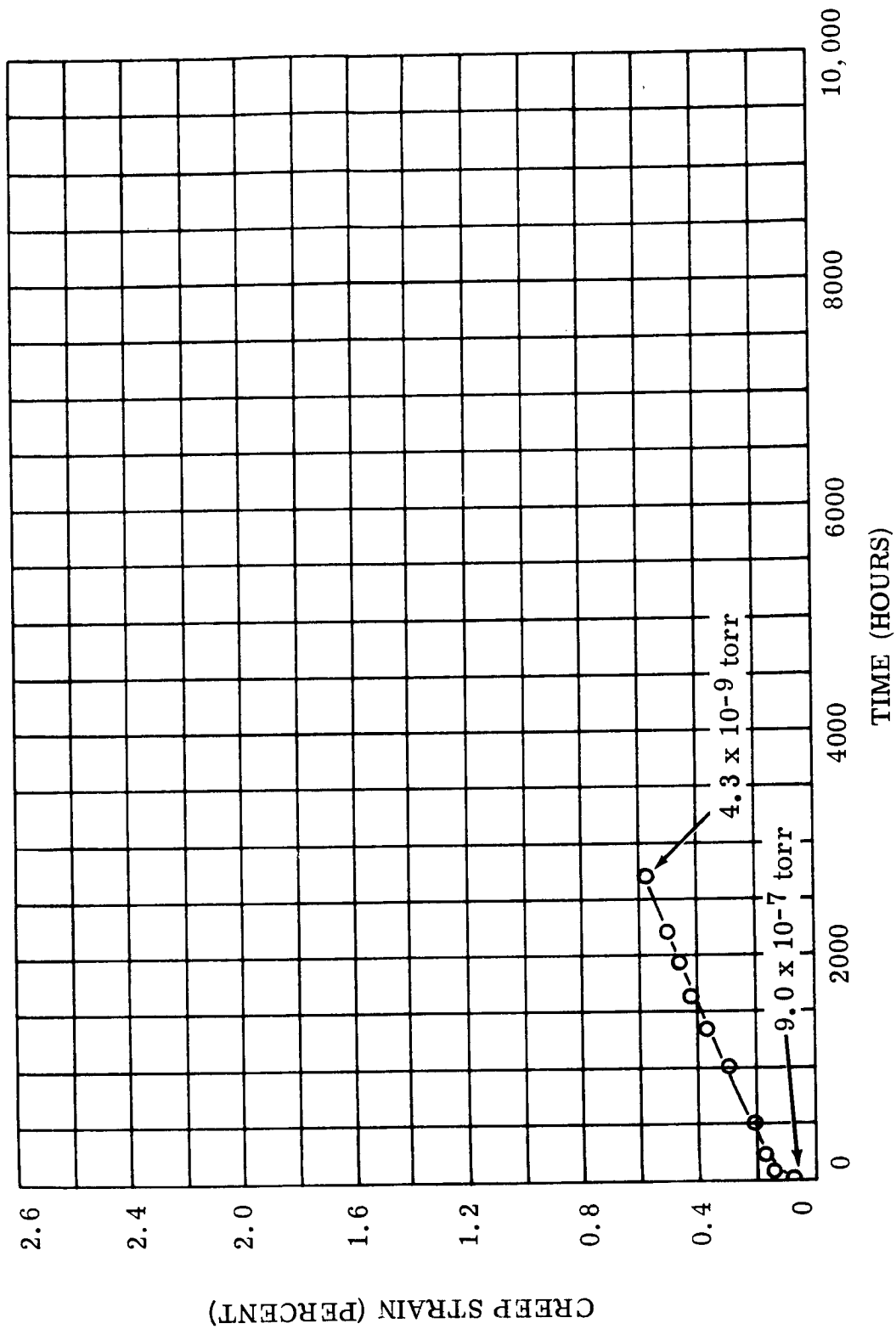


Figure II-34. Creep Nivco Bar 1050°F

FIGURE II-34. Creep, Nivco Heat 10-NO2V-1099, Tested in Vacuum at 1050°F and 50,000 psi (Specimen #5)

SECTION III

PROGRAM II - HIGH TEMPERATURE CAPACITOR FEASIBILITY

This program will study the feasibility of building a lightweight capacitor suitable for operation up to 1100°F. It will utilize high-purity dielectric materials and specialized fabrication methods. The ultimate application is in lightweight, high-temperature, power conditioning-equipment suitable for space application.

A. SUMMARY OF TECHNICAL PROGRESS

- 1) Two pyrolytic boron nitride multi-layer capacitors (nine wafers, average wafer thickness 0.76 mils and five wafers average wafer thickness 0.98 mils) were life tested at 1100°F in vacuum (10^{-7} to 10^{-9} torr). The five wafer unit has successfully completed 250 hours at 500 V d-c (in excess of 500 volts/mil electrical stress) with a capacitance change of less than 1.5 percent.
- 2) The initial nine wafer capacitor was electrically stressed at a maximum of 1000 volts/mil for the 0.5 mil wafers. Normal electrical properties were initially measured at 1100°F but after several hours on test a short developed. Voltage (500 V d-c) was re-established but with a substantial decrease in capacitance (approx. 1/4). The test was continued for 162 hours with no further degradation. Inspection of the capacitor showed that interelectrode diffusion and sintering (sputtered rhodium 1500 to 2000Å thick on polished wafers) was one of the major sources of difficulty.
- 3) Another multi-layer capacitor consisting of five wafers was fabricated with (1) slightly thicker wafers (all wafers approximately one mil thick), (2) as lapped or matte wafer surfaces, and (3) sputtered platinum electrodes which have a lower modulus and yield strength. These modifications were made to decrease the probability of shorts, improve electrode adherence and minimize interelectrode diffusion. The successful completion of the 250 hour endurance test indicates these changes made a significant

improvement.

- 4) It was decided to delete further testing of rectangular wafer capacitors since there appears to be no important experimental advantages for this geometry versus tabbed wafers.

B. DISCUSSION

The overall objective of this program is to determine the feasibility of fabricating high-temperature capacitors which are compact, lightweight and suitable for operation in static power conditioning apparatus for space applications. A group of specific capacitor capabilities has been established as program objectives. These include:

- 1) Volume Parameter ($\text{mF} \cdot \text{volts/in}^3$): 50 to 150
- 2) Dissipation Factor ($\text{Tan } \delta$) at 1100°F : 0.005 to 0.03 maximum (60 cps to 50 kc/sec).
- 3) Capacitance change: $\pm 5\%$ (Room Temperature to 1100°F).

Feasibility will be demonstrated if these goals are achieved and the capacitor will be capable of operating in the 800 to 1100°F temperature range without supplemental cooling. Furthermore, a high-temperature capacitor meeting these requirements will be competitive in terms of size, weight, and electrical properties with more conventional capacitors designed for much lower operating temperatures.

Five quarterly reports have been issued on this program with detailed discussions of the results. The following summarizes these results:

- 1) Fixturing and methods have been developed for slicing, lapping, and polishing thin wafers of pyrolytic boron nitride (Boralloy), polycrystalline Al_2O_3 (Lucalox and hot pressed Linde A), single-crystal sapphire, and hot-pressed polycrystalline BeO. Pyrolytic boron nitride has been successfully made into wafers one-inch square with thicknesses as thin as 0.5 mils (12 microns). The minimum thickness that can be reliably achieved with the other materials is in the range from 3 to 5 mils (75 to 125 microns).
- 2) Electrical data (capacitance, $\text{Tan } \delta$, d-c resistance), obtained over the temperature range from room temperature to 1100°F in vacuum for each of these thin wafer materials and the d-c breakdown strength, were measured at room temperature and 1100°F for several different materials. Test capacitors were prepared with sputtered high-purity platinum alloy electrodes using a CVC Plasma-Vac sputtering system.

- 3) The electrical data has been analyzed and compared for each candidate material. The results show that pyrolytic boron nitride is the most promising high-temperature capacitor material. Measured values obtained for a pyrolytic boron nitride capacitor with 1 mil thick dielectric are:
- a) $\tan \delta$ at 1100°F: 0.0009 (1 kc/sec)
 - b) Capacitance change from room temperature to 1100°F:
-1.5%
 - c) DC electric strength: Room temperature - 10,000 volts/mil
1100°F - 7,000 volts/mil

The above indicates that the program objectives can be exceeded by a substantial margin using this material. In addition, a "figure of merit" was determined for each candidate material in order to assign a quantitative number to relative fabricabilities combined with electrical properties. The selection of pyrolytic boron nitride for a high-temperature capacitor was clearly indicated by this type of comparison (see fourth quarterly report).

- 4) A prototype multi-layered capacitor was fabricated with 1-mil thick pyrolytic boron nitride and "wrap around" sputtered electrodes to achieve parallel electrical interconnection in a three-wafer stacked configuration. Design feasibility has been demonstrated based on 1100°F electrical data in vacuum.
- 5) Satisfactory pyrolytic boron nitride wafers as thin as 0.4 mils have been made and tested. Sputtered thin-film electrodes of platinum and rhodium have been evaluated together with process controls necessary to achieve thickness reproducibility. An evaluation of rectangular vs. tabbed wafer geometries has been made and the results and analysis of the data obtained for a five (5) wafer multi-layer capacitor has been presented.

This report includes the results of life tests performed at 1100°F in vacuum for two multi-layer pyrolytic boron nitride capacitors.

1. Pyrolytic Boron Nitride Multi-Layer Capacitors

a. RECTANGULAR WAFER CAPACITORS

The fifth quarterly report shows room temperature data measured

in vacuum (capacitance and $\tan \delta$, 50 cps to 50 kc/sec) for a five wafer stack of rectangular capacitor wafers. These results were satisfactory and it was decided to test the five wafer stack at higher temperatures. Prior to heating, a resistance measurement was started using a 500 V d-c test voltage. After the voltage was applied for about one minute, an arcing condition was indicated and then an open circuit appeared.

The fixture and stacked wafers were disassembled. Each capacitor wafer was tested individually at 1000 V d-c and was found to be satisfactory. However, the electrode overlap on several of the wafers showed a loss of continuity from one side of the wafer to the other. Careful inspection of the wafers in a clamped position in the fixture indicated that the edges of the wafers (in the electrode overlap area) were not being tightly compressed because of a rounded edge and slight warpage in the top pressure plate. This condition apparently resulted in intermittent contact on application of voltage causing arcing between wafers and vaporization of the electrode material in the overlap area. It will be necessary to re-deposit electrodes on the edges of these wafers and to modify the fixture to insure that satisfactory contact between stacked wafers is made before further electrical tests can be performed.

In view of these difficulties it has been decided to abandon rectangular wafer geometry in favor of the tabbed wafers. In addition, the comparative electrical data for the two wafer geometries (fifth quarterly report) shows no significant differences.

b. TABBED WAFER CAPACITORS

(1) Nine Wafer Capacitor

A total of 12 pyrolytic boron nitride tabbed wafer capacitors with polished surfaces and rhodium electrodes (1500-2000Å thickness) were completed for life testing. Wafer thicknesses ranged from 0.5 to 1.0 mils. Nine of these wafers were selected for a multi-layer capacitor after screening at 1000 V d-c. Evaluation data for each of the nine wafers in this unit is shown in Table III-1.

The capacitor was placed on life test in a sputter-ion pumped, cold-wall vacuum furnace (R.D. Brew & Co., Inc.). The test

TABLE III-1. Evaluation Data For Individual Wafers In the Nine (9) Wafer Pyrolytic Boron Nitride Capacitor

Tabbed Wafer No.	Electrode ^(a) Thickness (rhodium)	Wafer Surface Finish	Calculated Wafer Thickness ^(b) (mils)	Capacitance (pF) & Tan δ at Room Temperature				1000 V DC Test Applied For One Minute	Voltage Stress at 500 V DC (volts/mil)
				1 kc/sec		10 kc/sec			
				pF	Tan δ	pF	Tan δ		
1	1500-2000Å	Polished	0.94	296.76	0.00067	296.51	0.00049	Pass	532
2	1500-2000Å	Polished	0.91	305.95	0.00095	305.61	0.00068	Pass	550
3	1500-2000Å	Polished	1.0	277.98	0.00059	277.79	0.00041	Pass	500
4	1500-2000Å	Polished	0.71	389.89	0.00028	389.75	0.00024	Pass	704
5	1500-2000Å	Polished	0.50	556.01	0.00082	555.49	0.00079	Pass	1000
6	1500-2000Å	Polished	0.71	390.22	0.00068	389.89	0.00058	Pass	704
7	1500-2000Å	Polished	0.73	381.04	0.00048	380.81	0.00043	Pass	685
8	1500-2000Å	Polished	0.82	340.52	0.00071	340.21	0.00054	Pass	610
9	1500-2000Å	Polished	0.55	504.25	0.00057	503.87	0.00097	Pass	910

(a) Estimated from sputtering data using the relationship (derived):

$$T \approx \frac{j}{k}; \quad T = \text{electrode thickness (angstroms)}$$

$$j = \text{average measured target current density (ma/cm}^2\text{)}$$

$$k = \text{experimentally determined constant for different target materials:}$$

$$\text{Platinum} - 2.39 \times 10^4 \text{ ma/cm}^2/\text{\AA}$$

$$\text{Rhodium} - 3.38 \times 10^{-4} \text{ ma/cm}^2/\text{\AA}$$

(b) From the relationship:

$$T = \frac{KA}{4.45C}; \quad T = \text{thickness (inches)}$$

$$K = \text{dielectric constant (3.4) - Source: "Boralloy" Data Sheet, "C" direction at } 4 \times 10^9 \text{ cps}$$

$$A = \text{electrode area (0.364 in}^2\text{)}$$

$$C = \text{measured capacitance (pF at 1 kc/sec)}$$

fixture and test equipment used was the same as that described in previous quarterly reports. The vacuum furnace was evacuated to the 10^{-8} torr range and capacitance, $\tan \delta$ and d-c resistance (at 500 V d-c) was measured at room temperature. Furnace power was applied, the temperature stabilized at about 1100°F and another set of electrical measurements were made. These data and the data subsequently recorded at various time intervals is shown in Table III-2.

These data show that after the initial short and vaporization of electrode material a higher $\tan \delta$ value and lower d-c resistance was obtained (compared to values before the short). It is also estimated that six of the wafers became electrically isolated leaving three wafers interconnected. After 66 hours at 500 V d-c the measured $\tan \delta$ values show a decrease but the d-c resistance also decreased. However, just before terminating the test at 162 hours, measurements showed a further decrease in $\tan \delta$ and an increase in the d-c resistance.

It is indicated from these results that 500 volts per mil is probably a satisfactory stress level for wafers in the one mil thickness range. Two of the wafers in this unit had thicknesses of about 0.5 mils (refer to Table III-1) and were therefore stressed at about 1000 volts per mil. (Apparently an excessive stress level for wafers in this thickness range.) When the capacitor stack was examined after the test, it was not possible to determine which wafers or wafer caused the initial short because several of the wafers were stuck together via their electrodes. The rhodium electrodes could be peeled from some of the wafers indicating the initial electrode-wafer interfacial bond was destroyed by the electrode-electrode diffusion bond that developed under heat, pressure and vacuum. The two outer electrodes on the top and bottom wafers in the stack did not show a loss of adherence presumably because they were not in contact with an electrode of another wafer but with the surfaces of the boron nitride fixture.

(2) Five Wafer Capacitor

Another group of tabbed wafers were prepared and the

TABLE III-2. Life Test Data - Nine (9) Wafer Pyrolytic Boron Nitride Capacitor

Elapsed Time at 500 V DC	Furnace Temp. (°F)	Pressure (torr)	Capacitance & Tan δ										DC Resistance [ohms at 500 V DC]	RC Product [megohms x microfarads]
			100 cps		1 kc/sec		10 kc/sec		50 kc/sec					
			pF	Tan δ	pF	Tan δ	pF	Tan δ	pF	Tan δ				
Room Temp.	75	1x10 ⁻⁸	3451.3	0.0005	3448.7	0.00046	3447.2	0.00058	3448.8	0.00155			5x10 ¹³	1.72x10 ⁵
Start	1112	2x10 ⁻⁸	3423.0	0.005	3402.9	0.0035	3389.2	0.0026	3384.5	0.0034			2.38x10 ⁹	8.1
19 Hours (Approx.)	1113				897.66	0.0236	890.11	0.0062					3.13x10 ⁹	2.3
25 Hours	1112	2.0x10 ⁻⁸			898.03	0.0162	890.32	0.0055					1.25x10 ⁸	0.112
66 Hours	1115	7.5x10 ⁻⁹	911.3	0.058	897.03	0.0161	890.04	0.0050					1.47x10 ⁷	0.013
162 Hours	1114	4x10 ⁻⁹	906.8	0.029	896.67	0.0095	889.70	0.0042					2.0x10 ⁷	0.018

following modifications were made based on the results of the nine (9) wafer unit:

- a) Wafer thickness was maintained in the one mil range to decrease the probability of a defect induced short.
- b) Wafer surfaces were not polished. Electrodes were sputtered on "as lapped" or matte surfaces. This should increase the effective electrode adherence and minimize the contact area between two electrodes on different wafers.
- c) A double thickness of electrode material (platinum) was sputtered on the tab extensions only to decrease the contact resistance between inter-connecting electrodes.
- d) Platinum was selected for the electrodes because of its greater ductility and lower modules (vs. rhodium).

Table III-3 shows the thickness of each wafer in the five (5) wafer unit, capacitance and $\tan \delta$ at 1 kc/sec and 10 kc/sec and the voltage stress on each capacitor wafer when connected in parallel with 500 V d-c applied. Table III-4 shows $\tan \delta$ values at several frequencies for the five (5) wafer stacked unit. The slight increase in $\tan \delta$ at 10 kc/sec (Table III-2) indicates that the double thickness of platinum on the tabs was effective in reducing the contact resistance (effective series resistance) to a value comparable to that obtained with polished wafers and rhodium electrodes (lower resistivity).

The five (5) wafer unit was placed on life test 1100°F using the same conditions, procedures and equipment previously described for the nine (9) wafer capacitor. Figure III-1 shows the change in capacitance as a function of time. The total change was only 1.39% for the 259 hour period. The greatest part of this change (1.1%) occurred during the first 65 hours. Table III-4 shows the values recorded for $\tan \delta$ and d-c resistance (shown as an RC product) at indicated furnace temperatures ranging from 1100 to 1117°F.

TABLE III-3. Evaluation Data For Individual Wafers Used in the Five (5)
Wafer Pyrolytic Boron Nitride Capacitor

Tabbed Wafer No.	Electrode ^(a) Thickness (platinum)	Wafer Surface Finish	Calculated Wafer Thickness ^(b) (inches)	Capacitance (pF) & Tan δ at Room Temperature				1000 V DC Test Applied For One Minute	Voltage Stress at 500 V DC (volts/mil)
				1 kc/sec		10 kc/sec			
				pF	Tan δ	pF	Tan δ		
1	3500-4000Å	Matte or as lapped	0.00085 (0.85 mils)	326.17	0.00094	325.75	0.00085	Pass	587
2	3500-4000Å	Matte or as lapped	0.0010 (1 mil)	277.86	0.00127	277.39	0.00108	Pass	500
3	3500-4000Å	Matte or as lapped	0.0011 (1.1 mils)	253.54	0.00115	253.14	0.00104	Pass	454
4	3500-4000Å	Matte or as lapped	0.00103 (1.03 mils)	269.19	0.00071	268.93	0.00071	Pass	486
5	3500-4000Å	Matte or as lapped	0.00094 (0.94 mils)	295.01	0.00098	294.61	0.00093	Pass	532

(a) Estimated from sputtering data using the relationship (derived):
 $T \approx \frac{j}{k}$; T = electrode thickness (angstroms)
j = average measured target current density (ma/cm²)
k = experimentally determined constant for different target materials:
Platinum - 2.39 x 10⁴ ma/cm²/Å
Rhodium - 3.38 x 10⁻⁴ ma/cm²/Å

(b) From the relationship:
 $T = \frac{KA}{4.45C}$; T = thickness (inches)
K = dielectric constant (3.4) - Source: "Boralloy" Data Sheet, "C"
direction at 4 x 10⁹ cps
A = electrode area (0.364 in²)
C = measured capacitance (pF at 1 kc/sec)

TABLE III-4. Two Hundred Fifty Hour Life Test Data - Five (5) Wafer Pyrolytic Boron Nitride Capacitor

Elapsed Time at 500 V DC	Furnace Temp. (°F)	Pressure (torr)	Capacitance (pF) & Tanδ										DC Resistance [ohms at 500 V DC]	RC Product [megohms x microfarads]
			200 cps		500 cps		1 kc/sec		10 kc/sec		50 kc/sec			
			pF	Tanδ	pF	Tanδ	pF	Tanδ	pF	Tanδ	pF	Tanδ		
Room Temp.	75	2.6x10 ⁻⁷	1423.66	0.00058	1423.2	0.00055	1422.85	0.00058	1421.75	0.00064			1.66x10 ¹⁴	2.36x10 ⁵
Start	1111	4x10 ⁻⁷	(a)	(a)	1382.50	0.0030	1381.39	0.00231	1378.77	0.0012	1377.9	0.0015	1.06x10 ¹⁰	14.7
71 Hours	1104	1.6x10 ⁻⁸											1.25x10 ¹⁰	17.3
89 Hours	1109	1.4x10 ⁻⁸											1.09x10 ¹⁰	15.0
111 Hours	1110	1.4x10 ⁻⁸											1.47x10 ¹⁰	20.3
139 Hours	1114	1.2x10 ⁻⁸	(a)	(a)	1367.1	0.0036	1365.6	0.0028	1362.27	0.0014			0.8x10 ¹⁰	10.6
159 Hours	1117	1.2x10 ⁻⁸											0.7x10 ¹⁰	9.5
189 Hours	1100	1.2x10 ⁻⁸											1.43x10 ¹⁰	19.5
219 Hours	1099	1.2x10 ⁻⁸											1.82x10 ¹⁰	24.8
259 Hours	1100	1.1x10 ⁻⁸	(a)	(a)	1365.2	0.0031	1363.3	0.0024	1360.4	0.0013	1359.6	0.0016	1.77x10 ¹⁰	24.4

(a) A satisfactory null could not be obtained at a test frequency of 200 cps or less at 1100°F

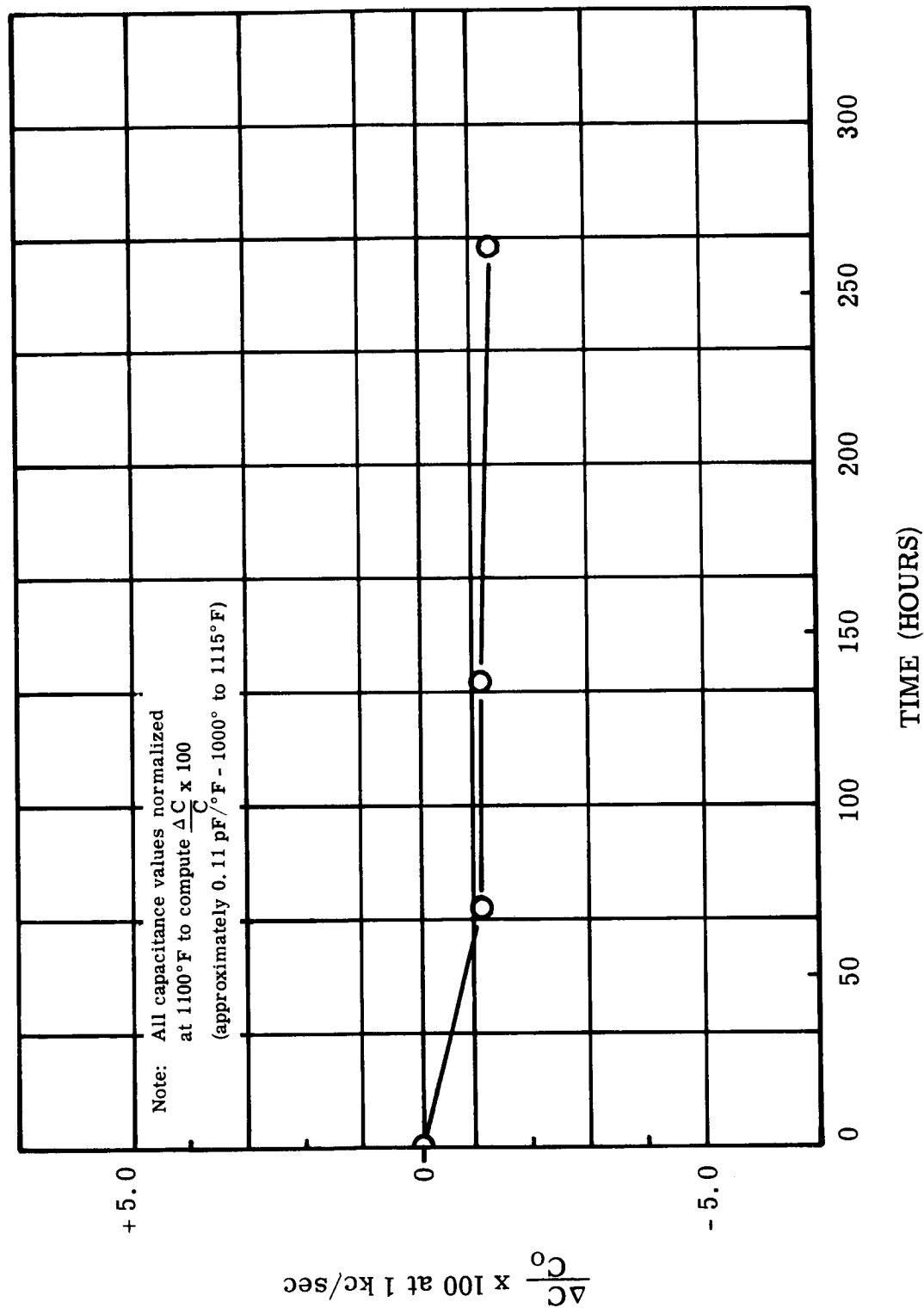


Figure III-1. Capacitance Change vs. Time for Pyrolytic BN Five Wafer Capacitor at 1100°F

FIGURE III-1. Change in Capacitance vs. Time at 500 Volts/mil in Vacuum (4×10^{-7} to 1.1×10^{-8} torr) at 1100°F for a Five (5) Wafer Pyrolytic Boron Nitride Capacitor

The variation in furnace temperature was apparently due to changes in line voltage for a pre-set voltage input. This method of control was necessary because of a malfunction in the automatic furnace controller thermocouple that developed during the early part of the test.

Table III-4 shows that $\tan \delta$ increased and the RC product also increased over the 259 hour period. Thus, the a-c losses increased but the d-c losses decreased. The magnitude of these changes, however, is not considered to be significant and much of the change might be attributed to experimental error. In general, therefore, it appears that the capacitor survived the test with relatively minor changes in electrical characteristics.

C. PROGRAM FOR THE NEXT QUARTER

- 1) Continue life test on the five (5) wafer capacitor at higher voltage stress levels (750 to 1000 V d-c/mil).
- 2) Visually inspect five (5) wafer capacitor and analyze life test data.
- 3) Start preparation of the topical report.

SECTION IV

PROGRAM III - BORE SEAL DEVELOPMENT AND COMBINED MATERIAL INVESTIGATIONS UNDER A SPACE-SIMULATED ENVIRONMENT

The bore seal effort under Task 1 will evaluate promising ceramic-metal sealing systems in potassium and lithium vapor at temperatures to 1600°F for 2000 hours. Elevated temperature seal strength and vacuum tightness will be determined. A four-inch diameter bore seal loaded with potassium will be incorporated in a stator design and evaluated in a 5000 hour endurance test at temperature and in a high-vacuum environment. This test will confirm data determined on smaller geometries.

Two 5000-hour tests will be run under Task 2 on a stator which typifies the construction of an inductor alternator or a motor. The first will be run between 800 and 1100°F temperature. The second test will be run with a bore seal at temperatures between 1100 to 1600°F. All will be tested at a high-vacuum (less than 10^{-8} torr) under electric and magnetic stresses.

A transformer and two solenoids under Tasks 3 and 4 will be similarly tested for two 5000 hour periods under high vacuum and at elevated temperature. The purpose will be to evaluate the combined effects of electric and magnetic stresses, and high vacuum on combinations of materials suitable for application to advanced space electric power systems. One solenoid test will be under d-c excitation and the other under intermittent excitation so the effects of a constant electric stress can be investigated.

The design features incorporated into the stator, transformer and bore seal were defined in detailed drawings in Appendixes A, B, and C of the first quarterly report.

A. TASK 1 - BORE SEAL DEVELOPMENT

1. Summary of Technical Progress

- a) A time-temperature brazing study of Alloy 9 (60Zr-25V-15Cb) was completed. Joints stronger than the ceramic were produced at brazing temperatures of 2320°F and 2520°F. A temperature of 2425°F was selected for brazing the four-inch model beryllia bore seal.
- b) Ceramics for two inch by two inch bore seal test assemblies were received. All were of rather poor quality, but those without cracks were vacuum leak-tight. The leak-tight tubes will be used for high temperature vacuum leak tests and brazed geometry evaluation.
- c) Conceptual design of the elevated temperature vacuum tightness and thermal cycle resistance tests, and creep tests were completed.
- d) The low-silica beryllia tubes, representing the best high-purity beryllia ceramics currently available for large bore seals, were received. Two of the six four-inch diameter tubes failed the vacuum leak test. Although excessive surface porosity was noted in the accepted ceramics, the probability of the ceramic leaking during potassium exposure is lessened because the walls are relatively thick (0.100 inch). Bore seal fabrication was started using the accepted ceramics.
- e) Two four inch by four inch model bore seals were successfully brazed using Alloy 9 and evaporated molybdenum metalizing. The first was made with a ceramic cylinder which did not pass the ceramic leak test as a trial and will not be filled with potassium. The electron-beam welder malfunctioned during closure after filling the second bore seal with potassium.

The ceramic portion of the first bore seal will be sectioned, exposed to potassium vapor for 500 hours at 1600°F, strength-tested, and evaluated. The second bore seal will be cleaned and held for possible use as a back-up bore seal.

2. Discussion

The program on ceramic-to-metal seals expands on the work initiated under NAS 3-4162. In this phase, alkali-metal loading of potassium and lithium will be conducted under vacuum ($< 1 \times 10^{-5}$ torr). The oxygen content in potassium will be less than 10 ppm. The nitrogen level goal in lithium will be less than 40 ppm.

Active-metal seals are being pursued since these offer less brittle structures than refractory-metal metallizings with thermodynamically stable second phases as observed in NAS 3-4162. Small samples used in evaluations include modulus-of-rupture specimens for flexural strength, tab-peel specimens for brittleness and notch sensitivity, and joined cylinders for leak tightness. Two-inch diameter ceramic-to-metal seals and a four-inch seal tested with saturated potassium vapor will complete the ceramic-to-metal seal investigations. Thermal cycling tests and mechanical strength and leak tightness at elevated temperature complement the other investigations.

a. PROPERTIES OF CERAMIC-TO-METAL SEAL COMPONENTS

(1) General

Delivery of beryllia ceramics for the two-inch diameter bore seals was delayed six months. Tests outlined in this section were consequently rescheduled for the next two quarters.

Twenty-four sets of Thermalox 998 beryllia ceramics for two-inch bore seal assemblies were received from the vendor. The vendor's analysis is shown in Table IV-1. All ceramics passed dimensional inspection, but excessive surface porosity and roughness were noted. Dye checking as reported in Appendix A of the second quarterly report revealed many sizeable pores, in all ceramics, and cracks in five cylinders and three back-up rings (Figure IV-1).

The developmental nature of fabricating low-silica, high-density beryllia cylinders is reflected in the quality of these ceramics. All of the two-inch diameter Thermalox 998 beryllia ceramics failed the standard EIMAC inspection

TABLE IV-1. Analysis^(a) of Beryllia Powder Used in Fabrication of Two Inch by Two Inch Bore Seal Test Assemblies^(b)

Constituent	Content (parts per million)
Al	60
Fe	50
Ca	60
Si	120
Mg	1050
Na	60
<p>(a) Spectrographic analysis provided by Brush Beryllium Company. Analysis of BeO powder made before pressing or fabrication of shapes Cr, Mn, Ni, Co, Li, Zn, Ti, Ag, Mo, Pb, and Cu all less than 30 ppm.</p> <p>(b) Density of the beryllia tubes ranged from 2.948 to 2.961 g/cc; average value 2.954 g/cc.</p>	

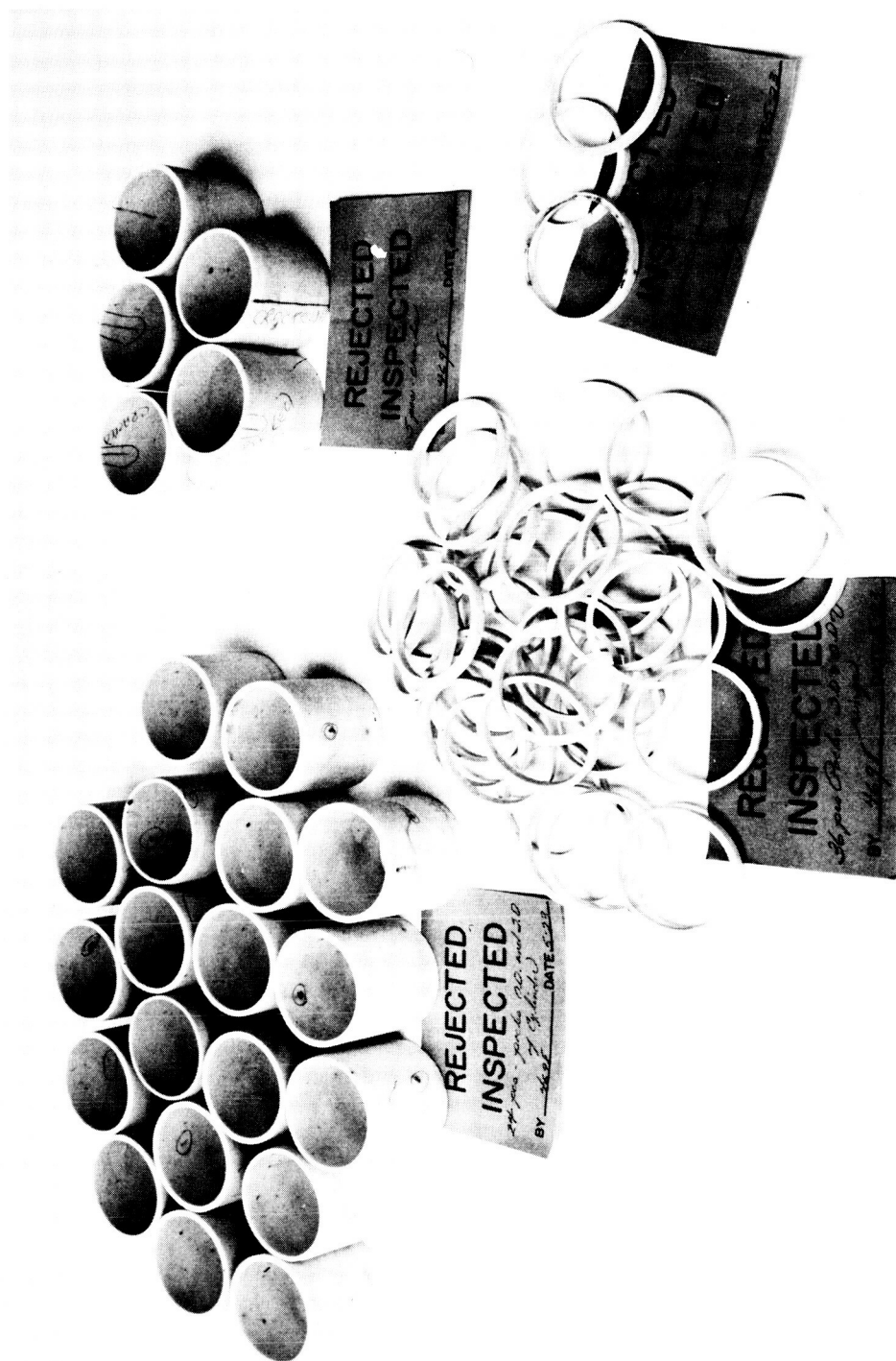


FIGURE IV-1. Photograph of the Beryllia Rings and Tubes Used In the Two Inch Ceramic-to-Metal Seal Test Assemblies

procedure used for 96 percent beryllia ceramics. The cracked cylinders were rejected. Nineteen cylinders were vacuum leak-tight. Of these, four have tapered ends for compression seals; the remainder have flared ends for butt seals. The use of these cylinders will be restricted to an evaluation of compression and butt seals and to elevated temperature vacuum integrity tests in conjunction with thermal cycling.

Alloys 3 (56Zr-28V-16Ti) and 9 (60Zr-25V-15Cb) were selected for all future tests requiring evaluation of two alloys. These two alloys were shown in the fifth quarterly report to be the best of the alloys tested with regard to potassium vapor compatibility. Alloy 9 appears to be the better of the two, although less brazing experience has been accumulated with it.

(2) Elevated Temperature Modulus-of-Rupture

All parts were received for the elevated temperature modulus-of-rupture (MoR) apparatus. Some of the MoR specimens have been brazed during brazing runs for other purposes.

(3) Elevated Temperature Vacuum Tightness and Thermal Cycle Resistance of Two-Inch Bore Seal Assemblies

Conceptual design of the test rig was completed. The two-inch bore seal configuration was substituted for the 1/2-inch cylinders for the elevated temperature vacuum tightness test after a method was devised to combine the test with the thermal cycling test. The general plan is as follows:

- a) Fabricate two-inch bore seal test assemblies (Figure IV-2).
- b) Test assembly in the cold vacuum/pressure test apparatus (Section IV. A. 2. c. (5)).
- c) Mount leak-tight assembly in the hot-vacuum test apparatus (Figure IV-3).

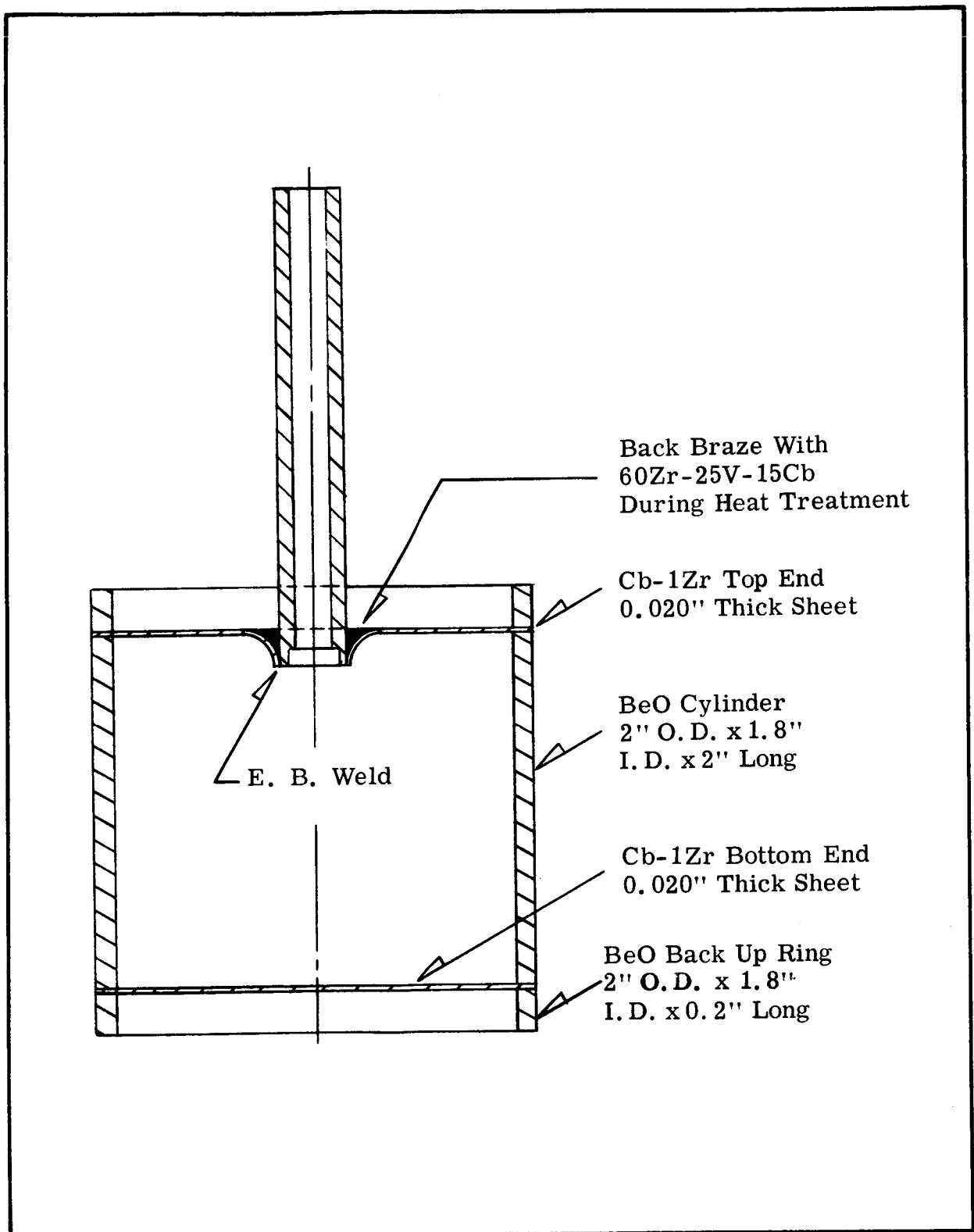


FIGURE IV-2. Schematic of Two Inch Ceramic-to-Metal Seal Used In the High Temperature Mechanical and Vacuum Tests.

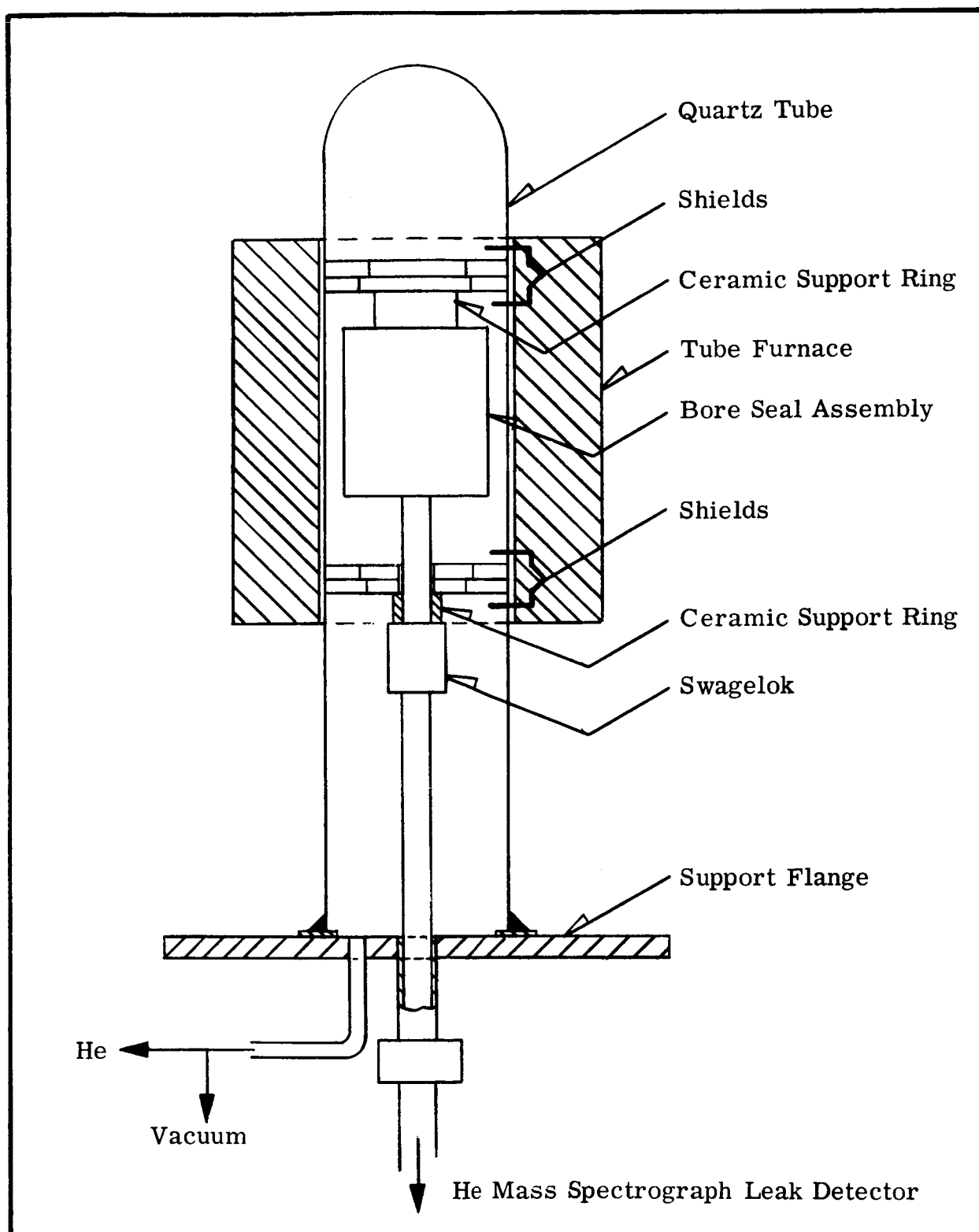


FIGURE IV-3. Schematic of High Temperature Leak Detector Apparatus
Used On the Two Inch Ceramic-to-Metal Seals.

- d) Evacuate the assembly and chamber.
- e) Activate leak detector on the evacuated specimen.
- f) Refill chamber with helium.
- g) Heat assembly to 1400°F within one hour.
- h) Shut power off and cool to room temperature at the natural cooling rate.
- i) Repeat previous two steps for a maximum of 10 cycles or until leak occurs.

b. CERAMIC-TO-METAL JOINING

(1) Preparation of Modulus-of-Rupture Assemblies

Modulus-of-rupture bars (ref. 1) are made by pressing the powder into slabs and firing in an electric kiln. The fired slabs are then cut and diamond-ground to dimension. The steps in making the assemblies are:

- a) Ceramics are dye-checked (see appendix of the second quarterly report).
- b) Ceramics are cleaned (see appendix of the second quarterly report) and fired in 75N₂, 25H₂ atmosphere for 30 minutes at 2597°F, and the metal members are cleaned.
- c) A one to three micron thick layer of molybdenum is evaporated on one end of each ceramic piece. A jig holding four bars is mounted on the turntable of the apparatus so that parts for two assemblies can be made at one time (see Figures IV-4 and IV-5).
- d) The parts are assembled in a brazing jig (ref. 1).
- e) The outgassing and brazing cycle is completed (ref. 1).
- f) After excess metal sheet is trimmed off, the specimens are ready for testing.

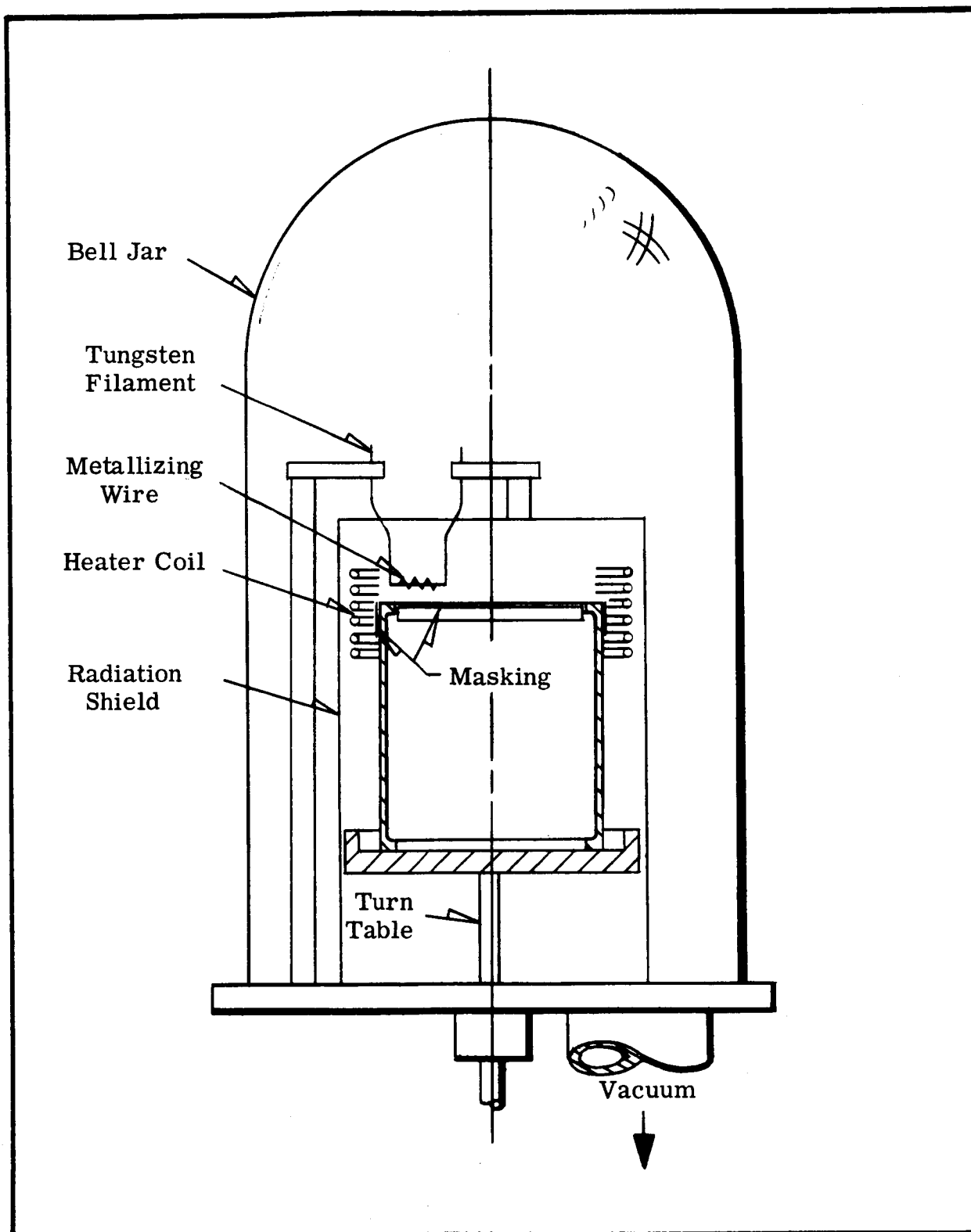


FIGURE IV-4. Schematic of Ceramic Metallizing Apparatus



FIGURE IV-5. Photograph of Ceramic Metalizing Apparatus

(2) Evaluation of Alloy 9 (60Zr-25V-15Cb)

A brazing study was conducted to evaluate the brazing characteristics of Alloy 9. Modulus-of-rupture bar assemblies were prepared and brazed at reference conditions (5 minutes at 2425°F), and at 90°F higher, 180°F higher, and 105°F lower. Brazes at all temperatures filleted well, although those held at the higher temperatures did not flow as well as desired.

Room temperature modulus-of-rupture data were obtained as shown in Table IV-2. Values for as-received ceramics from the same lot (lot EA) of Thermalox 998 beryllia are shown as well as previously reported values for another lot (lot E) of Thermalox 998. In addition, values for the most recently received lot (BeO-B) are shown. These data indicate that all joints brazed between 2320 and 2515°F are stronger than the ceramic. The trend of higher strength with higher temperature cannot be considered associated with the joint because the breaks were in the ceramic. Possibly a heat treatment effect on the ceramic is being manifested. The same trend is noted with lot BeO-E between the as-received and the vacuum exposed (at 1600°F for 500 hours) specimens. The joints brazed at 2605°F are weaker than the ceramic as shown both by the modulus-of-rupture values and the fact that the fractures were all in the ceramic/braze interface.

It was concluded from this work that the 2425°F reference brazing temperature is suitable for initial attempts to braze the larger seals and that a substantial range of temperatures is available within which good seals may be made.

(3) Evaluation of Other Alloys

Samples of seals made with other alloys previously investigated were mounted and modulus-of-rupture bar assemblies of other seal combinations were fabricated and brazed, but work to complete their evaluation was deferred due to the priority on the four inch by four inch model bore seals.

TABLE IV-2. Room Temperature Flexural Strength of Several Lots of Thermalox 998 Beryllia Ceramics and Ceramic-to-Metal Seal Assemblies

Ceramic Body	Metal Member	Braze Alloy (weight percent)	Brazing Temperature (a) (°F)	Key	Room Temperature Flexural Strength (b) (psi)	Remarks
Thermalox 998 Beryllia 99.8% BeO Lot E				\bar{x} s n	19,820 1,420 5	
Thermalox 998 Beryllia 99.8% BeO Lot B				\bar{x} s n	21,100 2,500 3	
Thermalox 998 Beryllia 99.8% BeO Lot EA				\bar{x} s n	20,900 2,160 5	
Thermalox 998 Beryllia 99.8% BeO Lot E (c)				\bar{x} s n	21,100 1,410 5	
Thermalox 998 Beryllia 99.8% BeO Lot E	Cb-1%Zr	60Zr-25V-15Cb (Alloy 9)	2425	\bar{x} s n	16,700 1,790 3	Specimens broke in the ceramic
Thermalox 998 Beryllia 99.8% BeO Lot EA	Cb-1%Zr	60Zr-25V-15Cb (Alloy 9)	2425	\bar{x} s n	23,300 490 4	Specimens broke in the ceramic
Thermalox 998 Beryllia 99.8% BeO Lot EA	Cb-1%Zr	60Zr-25V-15Cb (Alloy 9)	2515	\bar{x} s n	26,340 1,360 5	Specimens broke in the ceramic
Thermalox 998 Beryllia 99.8% BeO Lot EA	Cb-1%Zr	60Zr-25V-15Cb (Alloy 9)	2605	\bar{x} s n	13,700 2,840 5	Specimens broke in the braze joint
Thermalox 998 Beryllia 99.8% BeO Lot EA	Cb-1%Zr	60Zr-25V-15Cb (Alloy 9)	2320	\bar{x} s n	21,100 1,850 5	Specimens broke in the ceramic
<p><u>Key</u> \bar{x} - arithmetic mean s - standard deviation n - number of specimens tested</p> <p><u>Notes:</u></p> <p>(a) All brazed specimens were brazed in a vacuum furnace at 1×10^{-6} torr. Specimens were held at the indicated temperature for 5 minutes.</p> <p>(b) Strength determinations were made by four point loading on 0.1 inch x 0.1 inch x 1 inch modulus-of-rupture specimens or brazed assemblies. The load was applied at the rate of 0.1 inch per minute.</p> <p>(c) Tested after 500 hour exposure to vacuum of 1×10^{-6} torr at 1600°F.</p>						

c. MODEL BORE SEAL CONSTRUCTION

(1) Ceramic Inspection and Testing

Six sets of Thermalox 998 beryllia ceramics (tubes and back-up rings) for four inch by four inch bore seals (Figures IV-6 and IV-9) were received from the vendor. The vendor's spectrographic analysis is shown in Table IV-3. Silicon content of the starting BeO powder was 65 ppm. Other significant points are:

- a) Iron content of the fired ceramic is lower than that of the pre-fired powder. This is contrary to the vendor's normal experience (ref. 2).
- b) Silicon content in the fired beryllia is higher with respect to the starting powder (75 ppm vs. 65 ppm) than is usually found (ref. 2).
- c) No explanation was offered by vendor (ref. 2) on the change in magnesium content.
- d) The decrease in sodium content after firing is normal (ref. 2) because of volatilization during the sintering process.

The ceramics were inspected for dimensional tolerance and all were acceptable except for excessive surface porosity and roughness. Dye checking revealed many sizeable pores (Figure IV-7). Leak checking disclosed two leaking ceramic tubes. None of the tubes met the standard EIMAC ceramic specification. In view of the best effort basis on which the ceramics were produced, five of the cylinders were retained and one vacuum leaker was returned for replacement. Subsequently a leak-tight replacement cylinder was received. One rejected cylinder was retained for ceramic-to-metal process development. The ceramics were fired, then cleaned according to procedures reported in Appendix A of the second quarterly report.

(2) Preparation of Metal Members

End Bells (Figures IV-6 and IV-9) were cold pressed from

TABLE IV-3. Analyses^(a) of Beryllia Powder and Fired Ceramics for the Four Inch by Four Inch Beryllia Tubes

Constituent	Content (parts by million)		
	No. 1 Ready to Press Powder	No. 2 No. 1 Fired In Platinum Crucible (control sample)	No. 3 Fired Stock (from 4-in. diam. tube)
Al	60	70	70
Fe	65	50	45
Ca	65	75	75
Si	65	75	75
Mg	700	850	620
Cr	12	< 3	8
Mn	2	2	2
Ni	10	8	8
B	1	< 1	< 1
Co	< 1	< 1	< 1
Li	2	2	2
Cd	(b)	(b)	(b)
Cu	2	< 2	< 2
Mo	< 3	< 3	< 3
Na	50	30	30
Ag	< 1	< 1	< 1
Pb	2	< 2	< 2
Ti	3	3	3
Zn	< 20	< 20	< 20
<p>(a) Spectrographic analyses representing the average of three separate analyses from three samples. On all elements except Mg, the variation was ± 5 ppm from the values shown. Analyses by Brush Beryllium Company.</p> <p>(b) Not detected.</p>			

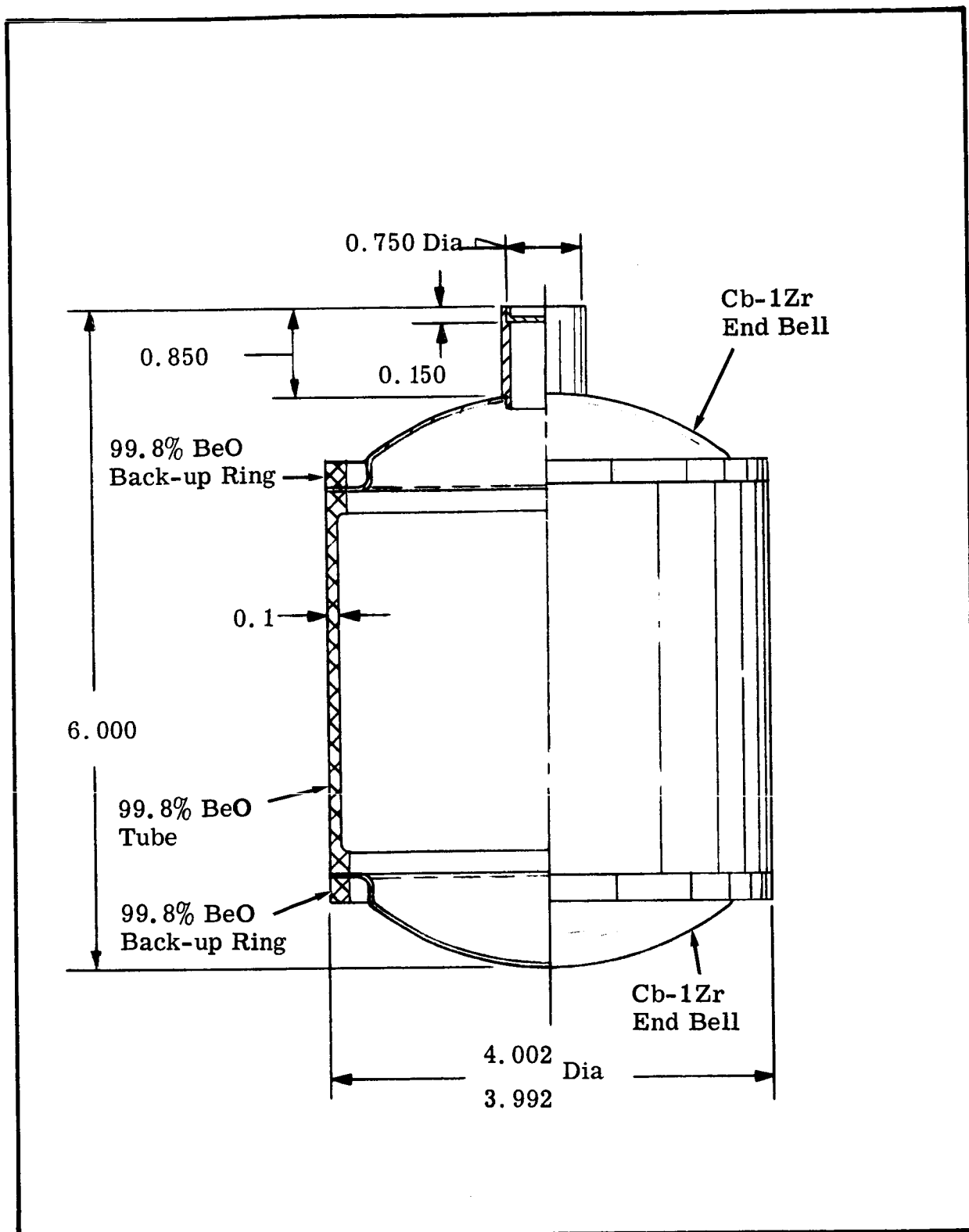


FIGURE IV-6. Schematic of Four Inch Model Bore Seal

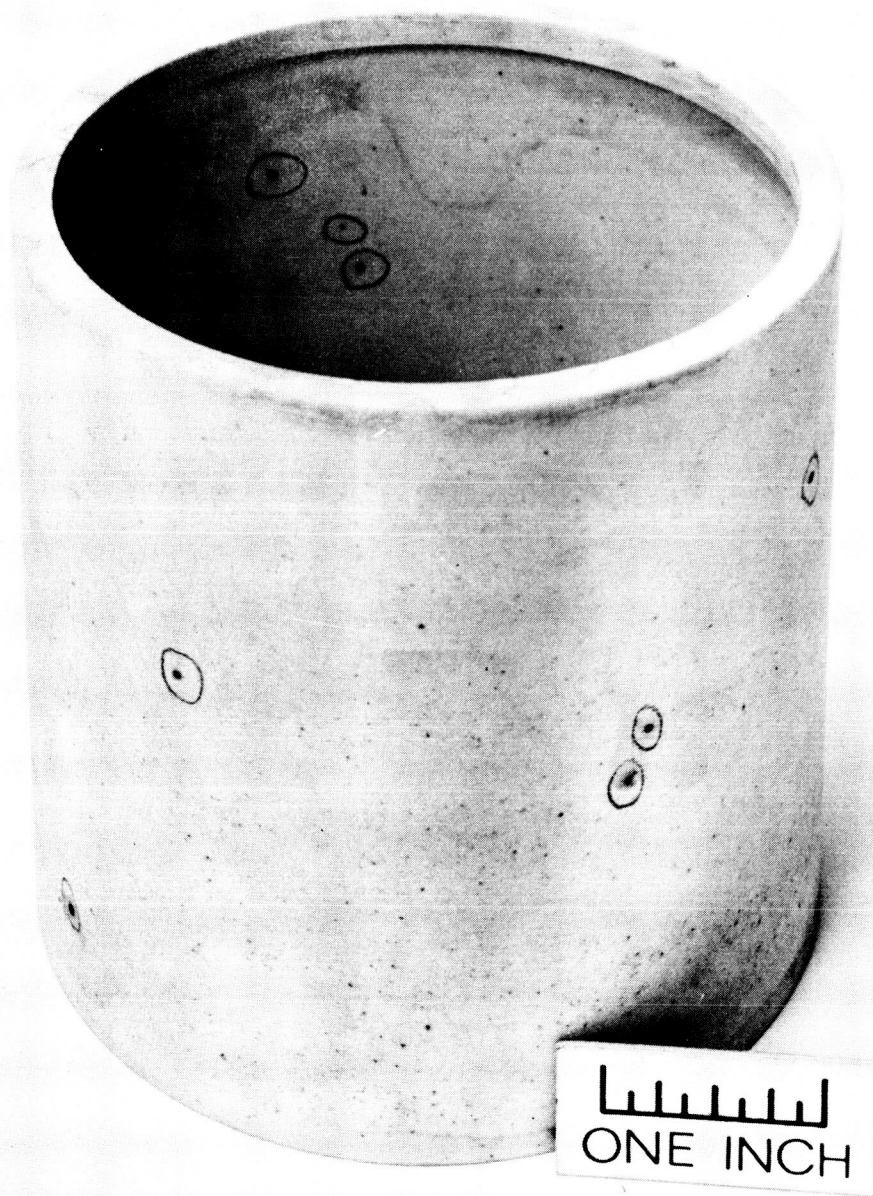


FIGURE IV-7. Photograph of Thermalox 998 Beryllia Tube After Dye Penetrant Check

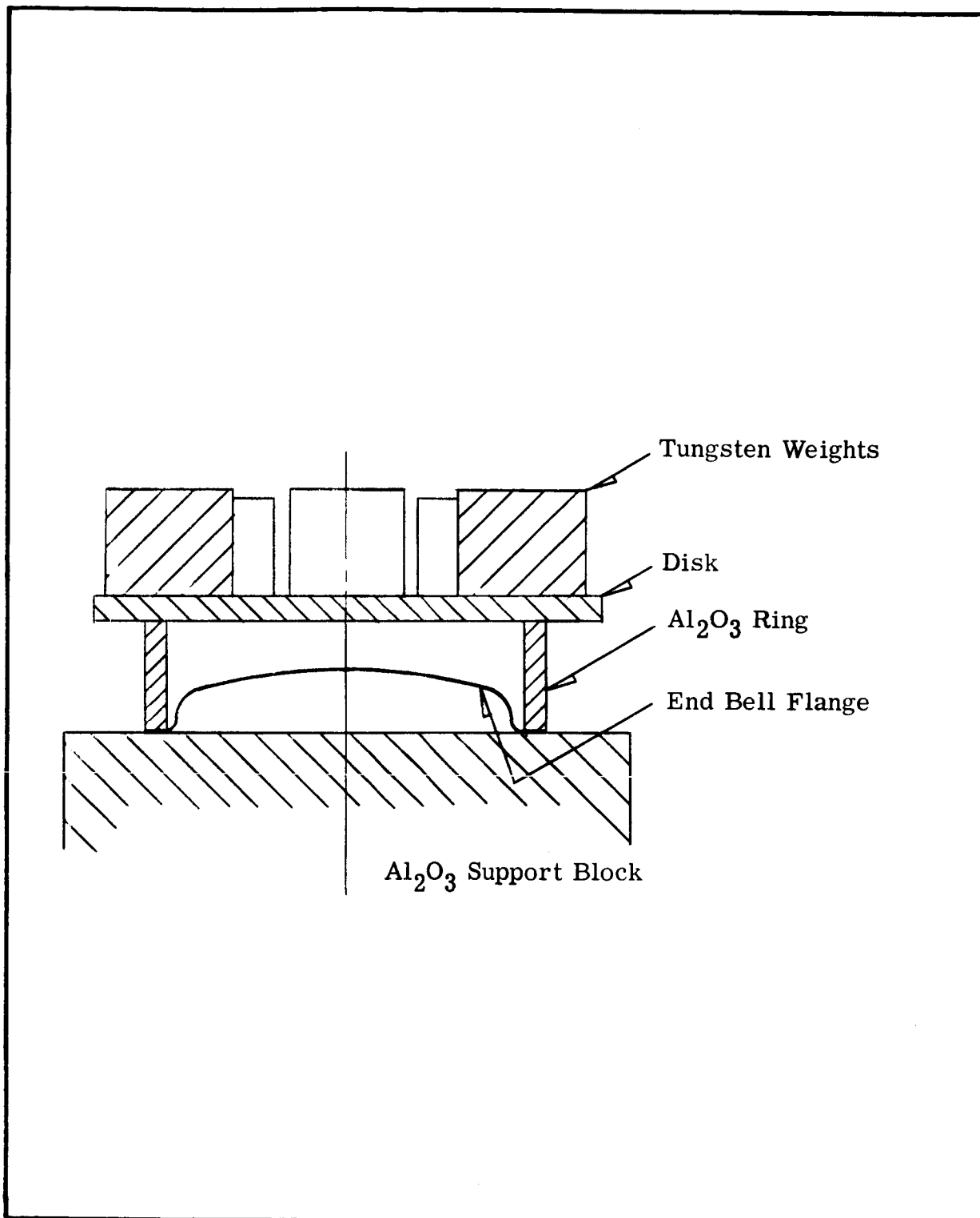


FIGURE IV-8. Schematic of Endbell Flange Leveling Fixture for the Four Inch Model Bore Seals

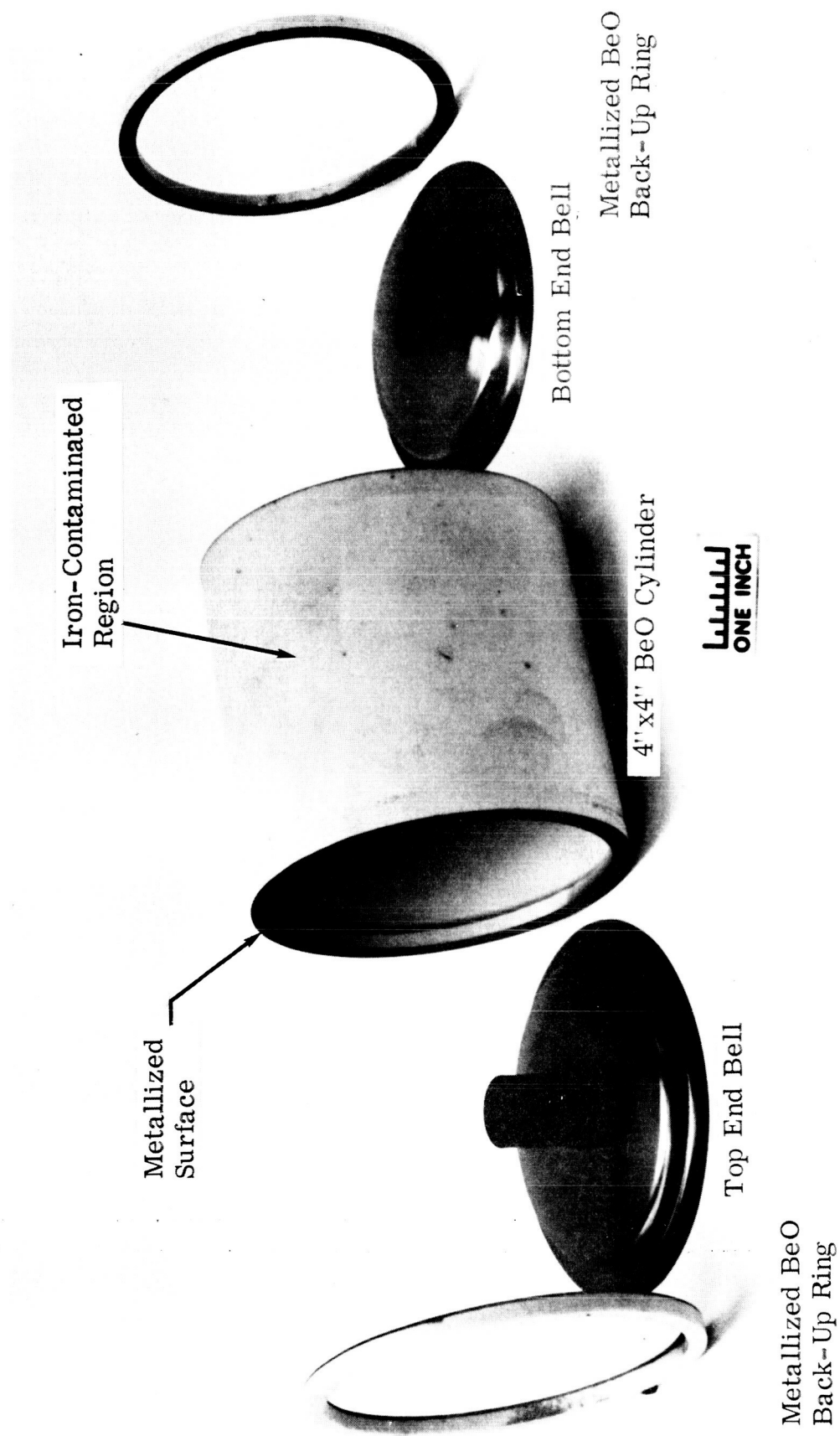


FIGURE IV-9. Sub-Assembly of a Model Four Inch Thermalox 998 BeO - (Cb-1Zr) Bore Seal

0.015 inch thick Cb-1Zr alloy sheet and cleaned. The tubulation was welded to the top end bell by electron-beam welding. Four sets of metal members were started but welding was successful on only one set. The end bell was found to warp easily due to the difference between tube wall-thickness and thickness of the end bell. A second set was made useable by brazing the joint with Alloy 9 (60Zr-25V-15Cb) during the heat treatment step. A modified design permitting easier welding was devised and will be used in subsequent metal members. The modified design was used for the two inch by two inch bore seal test assemblies, reported in Section IV.A.2.

The flanges on the end bells were flattened by the following procedure:

- a) The flange was mounted in the fixture (Figure IV-8) with the analysis specimen.
- b) The fixture was then mounted in the six-inch brazing furnace.
- c) The parts were heated to 2200°F, keeping the furnace pressure below 1×10^{-5} torr.
- d) The temperature was held at 2200°F for two hours and cooled to room temperature under vacuum.

The above procedure also acts as an annealing step. The analysis specimen is a one inch by one inch piece of sheet from the same lot of material as the end bell. It accompanies the bell through every handling step during bore seal manufacture so that an estimate of impurity pickup can be made if desired.

(3) Ceramic Metallizing

The four-inch beryllia tubes and back-up rings were metallized (ref. 3) as follows:

- a) The inside and outside of the cleaned ceramic were masked with five mil thick molybdenum foil.

- b) The ceramic was mounted on a turntable in the metallizing apparatus (Figure IV-4).
- c) Sufficient five mil molybdenum wire was wrapped on the tungsten filament to provide a metalized layer greater than one micron thick.
- d) The apparatus was evacuated to less than 5×10^{-6} torr and the ceramic was heated to above 932°F .
- e) The molybdenum was evaporated onto the ceramic as it rotated at six rpm.
- f) The apparatus was cooled to room temperature before breaking vacuum.

Three sets of ceramics were metallized by this method.

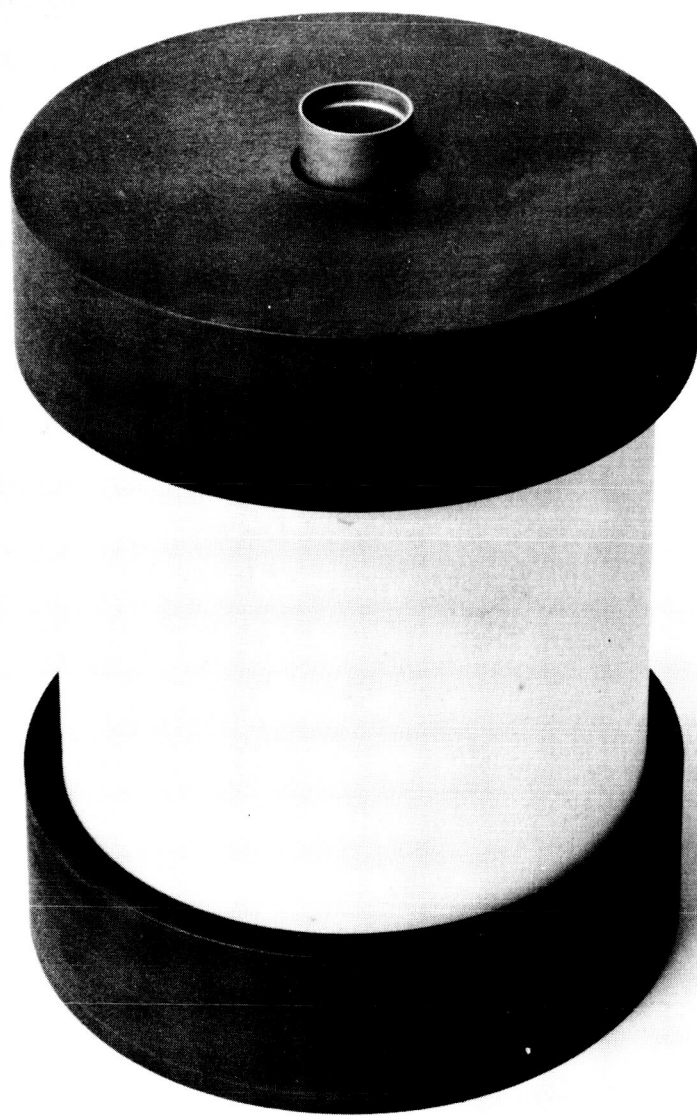
(4) Model Bore Seal Brazing

Parts for four-inch bore seal No. 1 ready for brazing are shown in Figure IV-9. The metallizing shows as the dark surface on the ends of the ceramic. The dark spots on the side of the ceramics are actually internal stained regions which have been attributed to minute iron oxide inclusions. During sintering, the iron reacts with and diffuses into the BeO (ref. 2).

(a) Four by Four Inch Bore Seal No. 1 (trial braze).

Alloy 9 (60Zr-25V-15Cb) was applied by the powder method described in Appendix A of the second quarterly report. Preparation of the alloy powder was described previously (ref. 1).

Parts were assembled into the brazing fixtures (Figure IV-10); the brazing run was conducted as previously described in the second quarterly report. Hold time was five minutes at 2426°F . The actual





ONE INCH

FIGURE IV-10. Photograph of Four Inch Model Bore Seal in Brazing Fixture

time-temperature/pressure history for the run is shown in Figure IV-11. The actual run was preceded by a trial run (with no braze alloy, but using the same parts) to insure that the desired time-temperature profile could be achieved.

Examination of the bore seal after brazing indicated that a good braze was made although a generous amount of alloy had been used. The alloy also appeared grainy in spots as if complete melting had not been achieved. Good, even filleting on the outside of the seal was achieved with a negligible amount of alloy running onto the sides of the ceramic (Figure IV-12).

Since a rejected ceramic cylinder was used for this trial run, the leak tightness of the seal was uncertain. The leak rate after brazing was the same as that of the ceramic alone. The brazed bore seal was filled with dye and placed in the vacuum-pressure test apparatus. Dye penetrated at two points (Figure IV-12) previously shown to be the approximate point of leakage on the bare ceramic.

(b) Four Inch Bore Seal No. 2

The welded and back-brazed top end bell was used in this assembly. Ceramic-to-metal brazing was performed as for bore seal No. 1 except that less brazing alloy was used. Also, brazing was done at 2462°F to obtain a more complete melt.

After brazing, joints were found to have exhibited even filleting, with no excess or deficiency of alloy evident. Melting appeared to be complete and no further changes in procedure appear to be necessary for subsequent bore seals.

(5) Inspection and Testing

The following post-brazing inspection and testing procedure was devised for four-inch model bore seals.

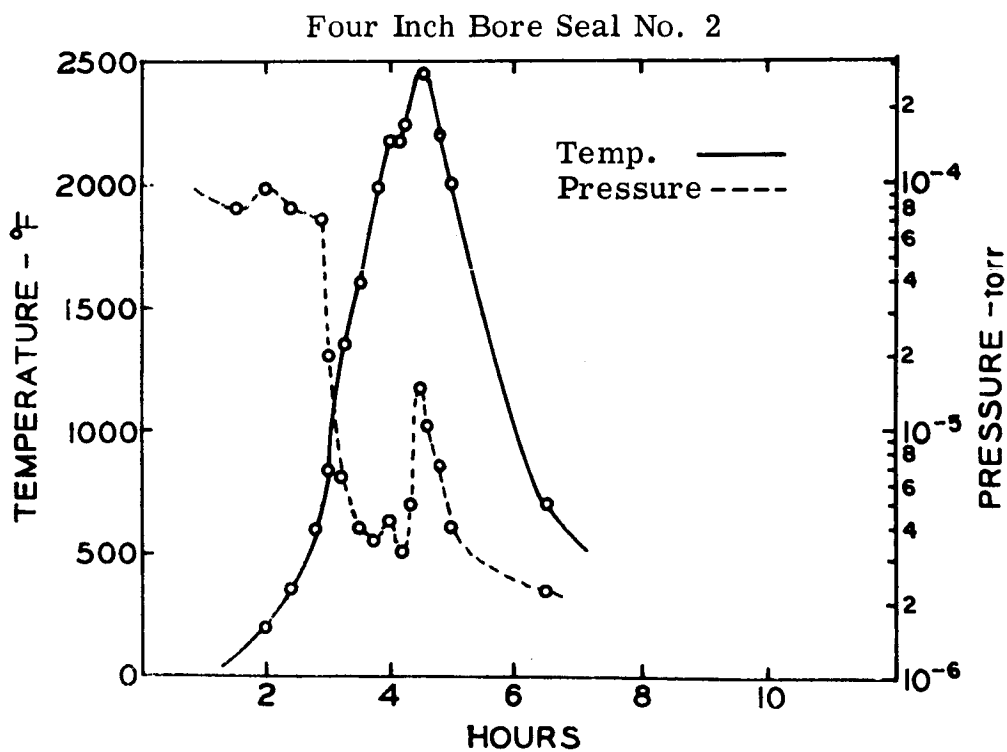
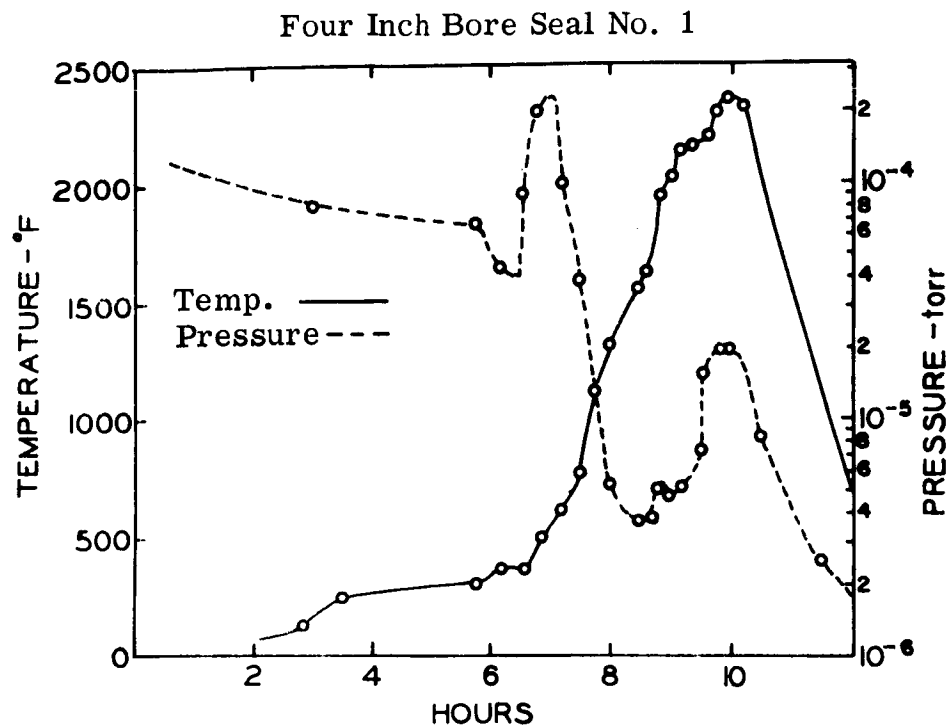


FIGURE IV-11. Time Temperature Brazing Curves of Thermalox 998 - (Cb-1Zr) Model Bore Seals No. 1 and 2

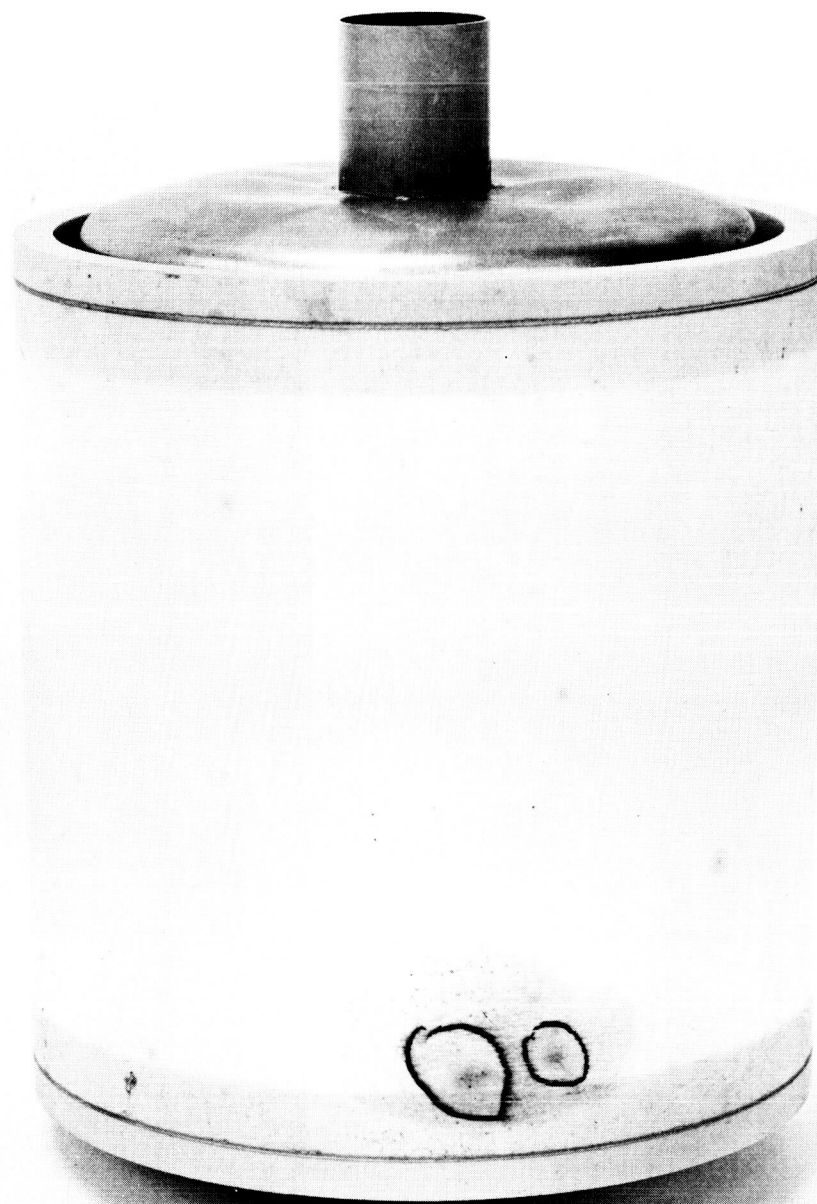


FIGURE IV-12. Photograph of Thermalox 998 - (Cb-1Zr) Brazed Bore Seal No. 1

Inspect brazed joints under the stereo-microscope for completeness of melting. Examine for proper amount of brazing alloy. Mount the brazed seal in the cold vacuum/pressure test apparatus (Figure IV-13). This apparatus consists of a vacuum chamber attached to and evacuated by the vacuum system of a Veeco helium mass spectrograph leak detector. The bore seal assembly is suspended from the top flange so that when the chamber is evacuated, a 15 psi differential pressure exists from the inside to the outside of the bore seal. This simulates the stress distribution that is expected in operation. Also, the pressure differential must be applied in this way because the Cb-1Zr end members are too thin to withstand the opposite differential without buckling. The tubing at the top may be attached to a high pressure gas source if a higher test differential pressure is desired. Evacuate the chamber slowly, being prepared for rupture of the bore seal assembly. If the chamber pumps down to its base pressure, inject helium into the bore seal through the top tube to check for small leaks.

Bore seal No. 2 passed the above test on the second try. A leak indication obtained on the first try was traced to the tubing clamped to the bore seal tubulation. The leak was found by filling the bore seal with the dye solution as for bore seal No. 1.

Bore seal No. 2 was made ready for filling with potassium by cleaning, as follows:

- a) The dye was washed out with acetone and the bore seal was air-dried.
- b) Stains were removed from the outside of the ceramic by liquid honing.
- c) Stains on the Cb-1Zr metal members were removed with brief exposure to 40 parts HNO_3 - 10 parts HF.
- d) The bore seal assembly was baked out at 1470°F for one hour at a pressure of $< 5 \times 10^{-6}$ torr.

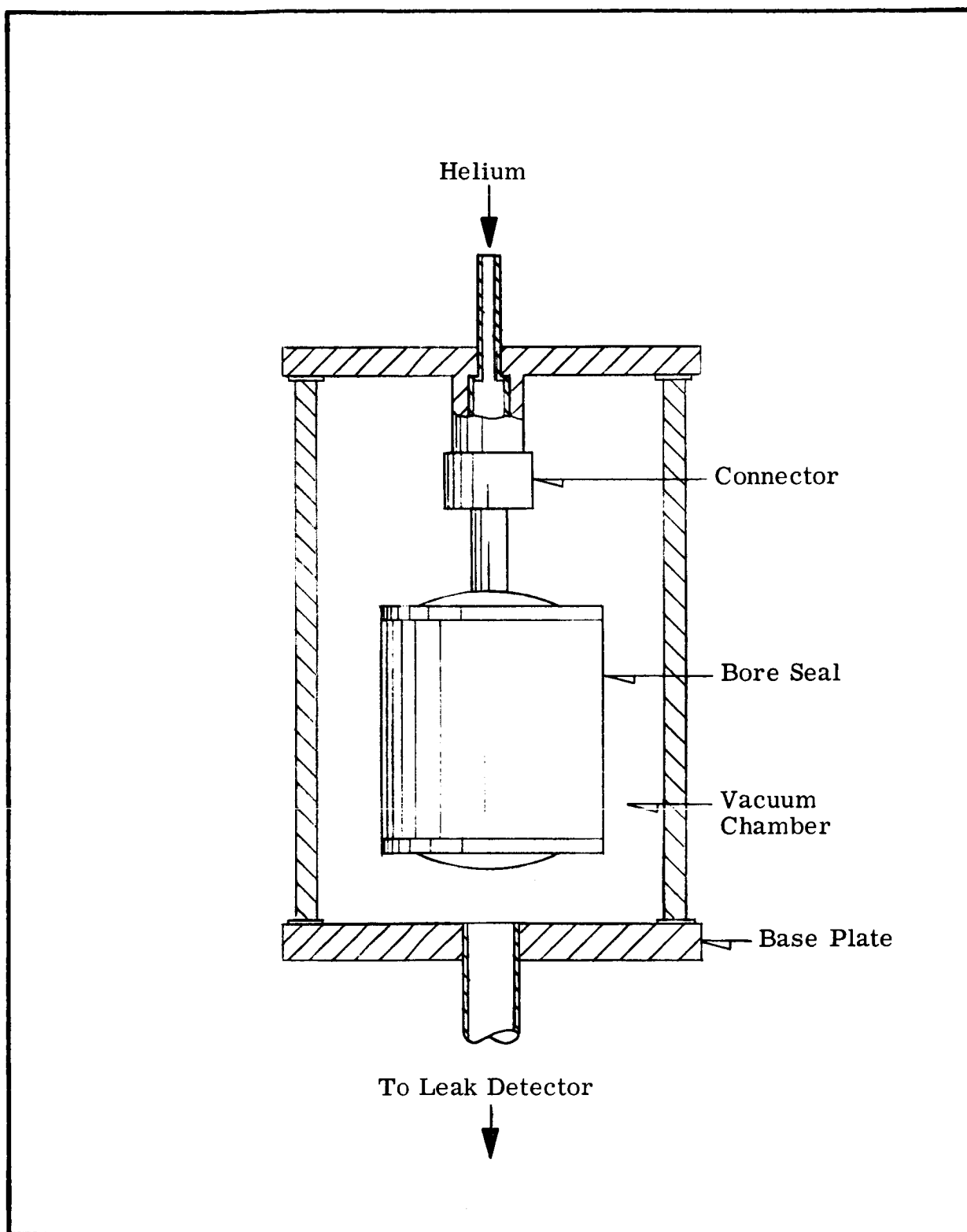


FIGURE IV-13. Schematic of Four Inch Model BeO - (Cb-1Zr) Bore Seal In Room Temperature Vacuum/Pressure Testing Apparatus

(6) Fill with Potassium and Seal by E. B. Welding

Bore seal No. 2 was ready to be filled with potassium at the end of the report period. The same procedure that was used for filling capsules is planned for the four-inch bore seals.

d. CONCLUSIONS

- 1) Despite earlier assurances to the contrary from the supplier, the process of fabricating large, high-purity beryllia cylinders requires further development to meet purity standards and to establish a meaningful quality inspection.
- 2) The brazing cycle and fixtures developed for the four inch by four inch model bore seal appear to be adequate to proceed with manufacture of two potassium-filled seals for long term testing.

3. Program for the Next Quarter

- a) Fabricate and deliver two four-inch diameter model bore seals filled with high-purity potassium.
- b) Complete the loading of high-purity potassium and lithium into exposure test capsules and start compatibility tests.
- c) Complete the brazed specimens for elevated temperature testing and start the tests.

B. TASK 2 - STATOR AND BORE SEAL

1. Summary of Technical Progress

- a) A total of 4091 endurance test hours was accumulated as of the end of the sixth program quarter.
- b) Thermal vacuum chamber pressure at the beginning of the period was 1.4×10^{-8} torr. Pressure had decreased to 4.2×10^{-9} torr at the end of the report period.
- c) A stator winding high-voltage lead was inadvertently disconnected from the vacuum chamber feedthrough with power on. The resulting arc burned through the metal portion of the ceramic-to-metal seal, causing a complete loss of vacuum and allowing air to enter the chamber. Automatic controls shut down the system satisfactorily. After the feedthrough was replaced, high-vacuum testing was resumed without difficulty.
- d) Manufacture of a 1300°F hot spot stator model was initiated.

2. Discussion

a. STATOR INSTALLATION, CONSTRUCTION AND OPERATION AT 1100°F

Figure IV-14 is a cutaway drawing of the thermal vacuum chamber which shows the stator installed in the furnace hot zone. The chamber is of double wall construction with baffles between the walls to channel cooling water flow. The chamber top cover is also double walled to provide a path for cooling water. Thermocouples were placed in position in the stator just prior to installation in the chamber. Stator winding leads were inserted into short lengths of hollow alumina tubing to insulate them as they passed through the top heat shields. Thermocouple and winding leads were then passed upward through perforations in the top heat shields as the shields were set in position. Winding leads were brazed to OFHC copper feedthrough bus bars inside the furnace, using a glass bell jar with supporting frame and foil curtains to maintain an argon atmosphere for the brazing operation. Thermocouples were passed through hollow Kovar tubes

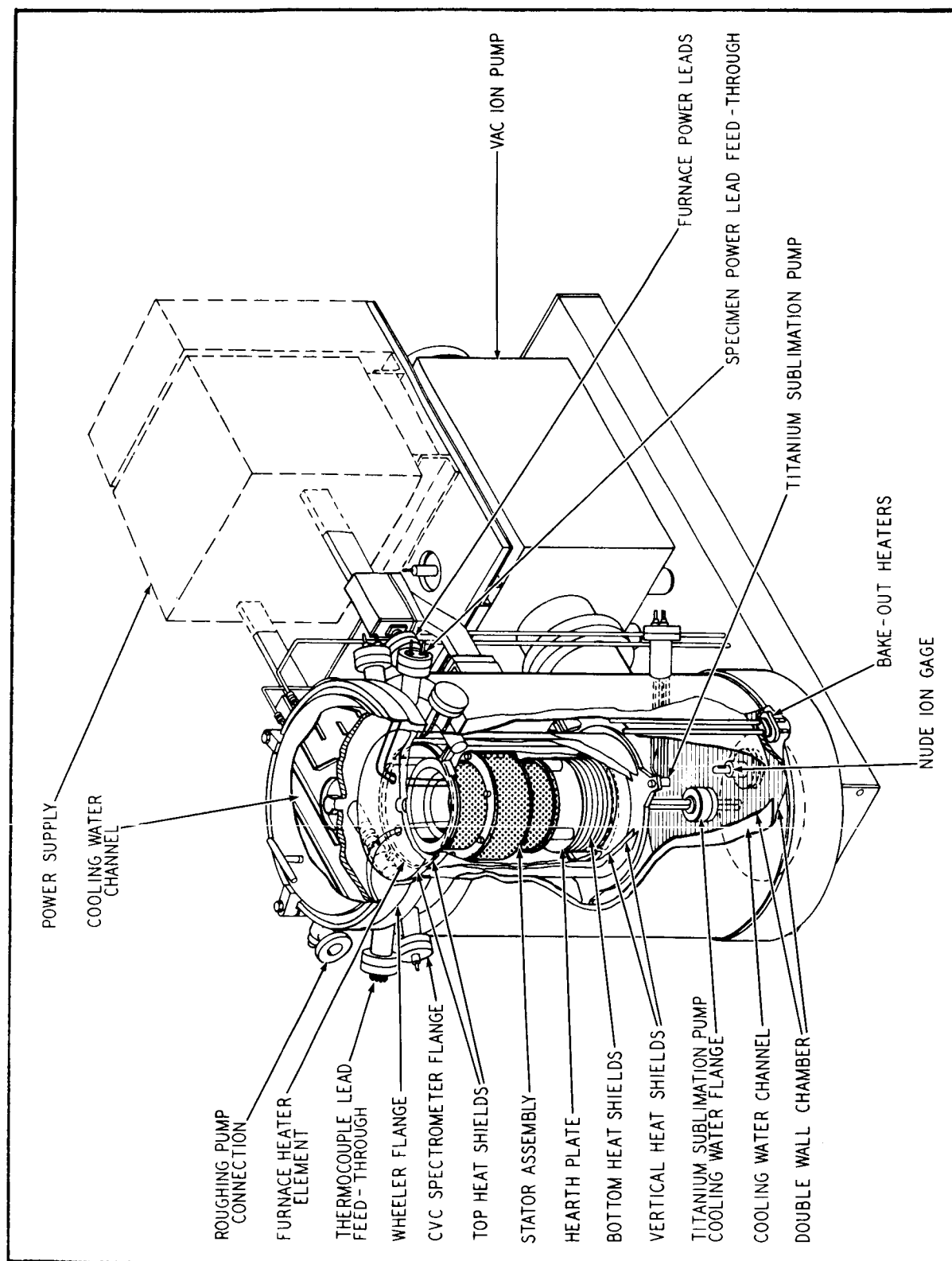


FIGURE IV-14. Cutaway View of Vacuum Furnace Showing the Stator Test Specimen Installed

and brazed externally by induction methods in special glass fixtures which provide an inert gas atmosphere.

The stator main frame was made from a Hiperco 27 (27% cobalt-iron) alloy forging, and the laminations were held in place in the frame by a retaining ring which was also made from a Hiperco 27 alloy forging. The magnetic stack consisted of 244 Hiperco 27 alloy laminations 0.008 inch thick, with a sapphire-like insulation coating of plasma-arc sprayed Linde A compound (Al_2O_3) on one side of each lamination. Conductor wire was rectangular nickel-clad silver (20% nickel cross-sectional area) coated with a 0.006 inch thick layer of Anadur, a refractory-oxide-filled glass fiber insulation. Coils were made in three segments and installed to be representative of a three phase winding. Slot insulation was provided by ceramic (99% Al_2O_3) U-shaped channels (slot liners), spacers and wedges. Westinghouse W-839 potting compound (aluminum-orthophosphate-bonded zircon) was used to fill small voids between the slot liners and slots, and extended about 3/8 inch beyond the slot liner ends to provide winding support. Hollow Al_2O_3 tubes were used as thermocouple insulators in the slot and stack areas. Thermocouples were installed in pairs in slots of each winding, in the stack, between the stack outside diameter and frame, on the frame outside diameter and on winding end turns. The stator physical size is representative of a three phase 15 KVA generator or 12 HP a-c induction motor operating at 12,000 RPM. The stator conductor and insulation system is being tested at a current-voltage level (292 volts & 41 amps/phase) equivalent to a 36 KVA machine. Winding test current density in each stator winding is 3330 amperes per square inch. Refer to the program fourth quarterly report for additional details on stator construction, preparations for installing the stator in the thermal vacuum chamber, and initiation of the test program.

Stator test operation was routine during the program quarter except for one incident. Vacuum-tight power leads into the test chamber are provided by copper rods which are sealed to a ceramic disk by a ceramic-to-metal brazed joint. The ceramic disk is then ceramic-to-metal brazed to a vacuum feedthrough flange. There are two isolated copper rods in each power feedthrough assembly (dual power lead feedthrough). A stator power lead connector was inadvertently disconnected from a test chamber copper feedthrough rod while power was being applied to the

stator windings. The resulting arc flashed across to the adjacent feedthrough rod, generating sufficient heat to melt the copper-to-ceramic brazed joint. The test chamber was at a pressure of 9.8×10^{-9} torr, and vacuum was lost immediately when the seal gave way. The test stator slot temperature was 1115°F.

The sputter-ion pump and heater element pressure interlocks functioned automatically to protect the chamber, and power to the test stator was shut off. The tantalum furnace heater element had been at approximately 870°F when the chamber returned to ambient room pressure, and there was some question as to whether or not it had been damaged. Varian Associates (the chamber manufacturer) was contacted for advice as to the best course of action. Varian suggested taking a resistance reading across the heater element, and replacing the failed feedthrough and trying to start the ion pump.

The heater element resistance was 1.6 milliohms, which indicated little if any damage to the element. New elements are in the 1 to 2 milliohm range. The feedthrough was replaced with a blank flange, the chamber was sorption pumped down to 2 to 3 microns, and the sputter-ion pump was turned on. The pump started in a normal manner.

After the sputter-ion pump operation had been verified as satisfactory, the chamber was backfilled with argon and opened up. Visual appearance of what could be seen inside the chamber was very good. A new dual power lead feedthrough was installed and the two stator leads involved were welded to the new copper bars in an inert atmosphere. The chamber was closed and after an initial period of sorption pumping the sputter-ion pump showed a normal start. The chamber was then put through two consecutive 24-hour bake-out cycles at 482°F (250°C). Heat-shrinkable plastic sleeves were installed on the stator power lead connectors to prevent repetition of such a failure.

Power was applied to the heater element in stages and chamber pressure was monitored for signs of severe outgassing. The highest pressure noted was 5.0×10^{-7} torr during the temperature stabilization period. Power was then applied to the stator windings, with a subsequent maximum chamber pressure of 1.3×10^{-6} torr resulting. By the time a stable stator slot liner

temperature of 1117°F was attained, chamber pressure had decreased to 4.0×10^{-8} torr, as compared to 9.8×10^{-9} torr when the accident occurred. The pressure subsequently decreased slowly into the 10^{-9} torr range. At no time was there any evidence that the sudden loss of vacuum had any detrimental effects on the test stator or the chamber itself.

Static electrical measurements were taken once each week, covering conductor resistance, d-c insulation resistance, and insulation leakage current when subjected to an a-c voltage potential.

Titanium sublimation pump (TSP) bursts of two minute duration were used at intervals to see if there would be any effect on the chamber base pressure. Early in the program quarter, the chamber pressure was reduced by approximately one decade after each TSP burst, but it would begin to return to the base level within minutes after reaching its lowest value. By the end of the program quarter a two minute TSP burst was drawing the chamber pressure down into the 10^{-10} torr range, where it would remain for several hours before beginning to rise.

b. STATOR DATA AND DISCUSSION

Figure IV-15 is a log-log plot of chamber pressure in torr versus endurance test time in days. The time scale does not necessarily show consecutive calendar days, as the logging of official endurance time occurred only when the stator had voltage and current applied and was at a stable hot-spot temperature. Thus, time was not logged when the power supply generator was off the line for a preventative maintenance bearing change. The curve as plotted shows pressure values for steady state conditions. Titanium sublimation pump burst pressure transients are shown as vertical lines in several places to indicate the magnitude of pressure reductions attained with titanium sublimation. Time was not logged during the period that loss of vacuum and subsequent repairs occurred, but the plot has been expanded slightly to show pressure before the failure and the pressure that was attained within a few days after test conditions were re-established.

Figure IV-16 is a dimensionless plot showing conductor resistance during the course of the endurance test. Base line ρ_0 was 0.0134 ohms at 78°F. The effect of temperature on resistance is noted

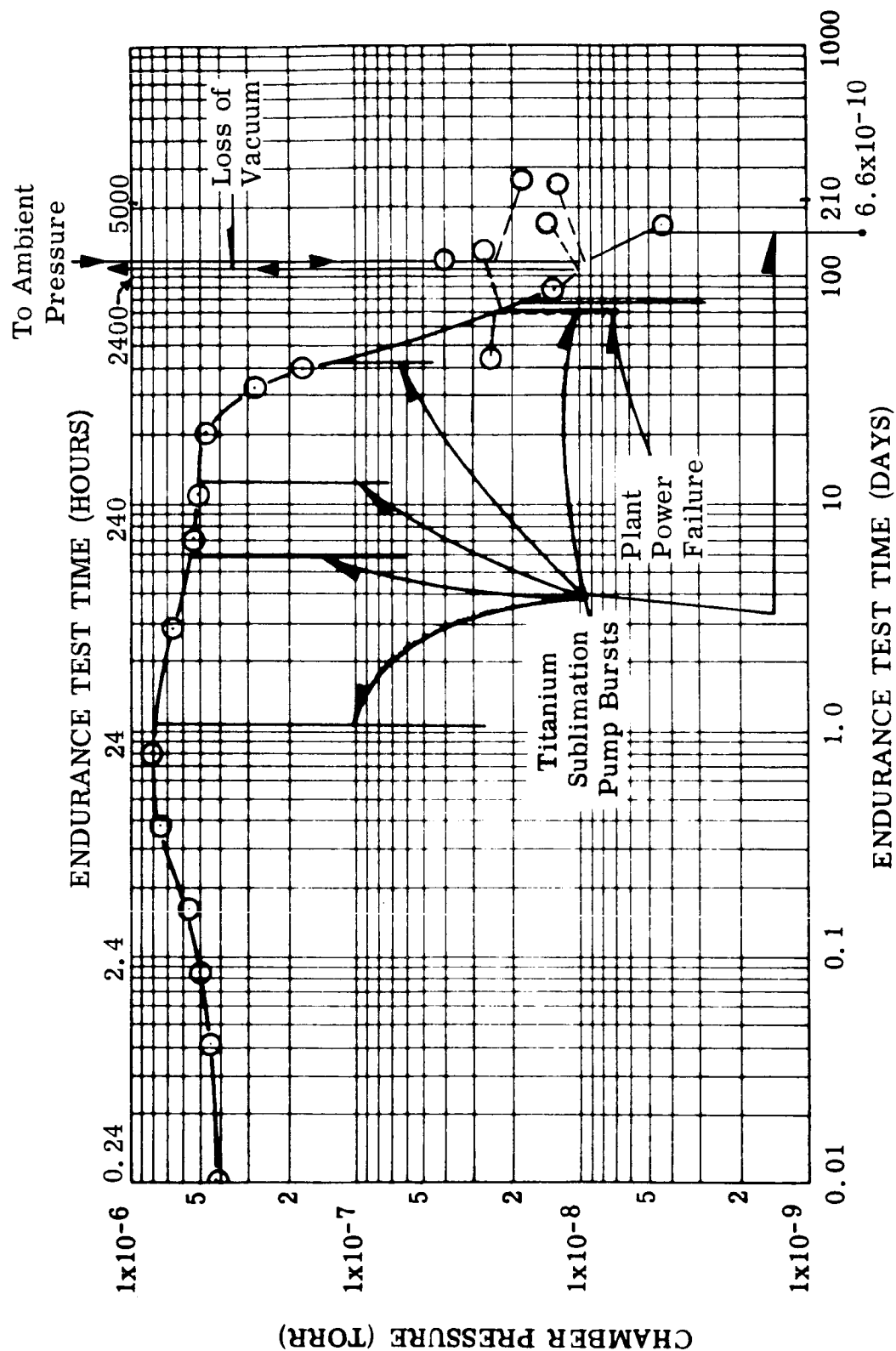


FIGURE IV-15. Stator Chamber Pressure vs. Endurance Test Time at 1100°F Stator Hot Spot

Figure IV-15. Stator Chamber Pressure vs. Endurance Test Time

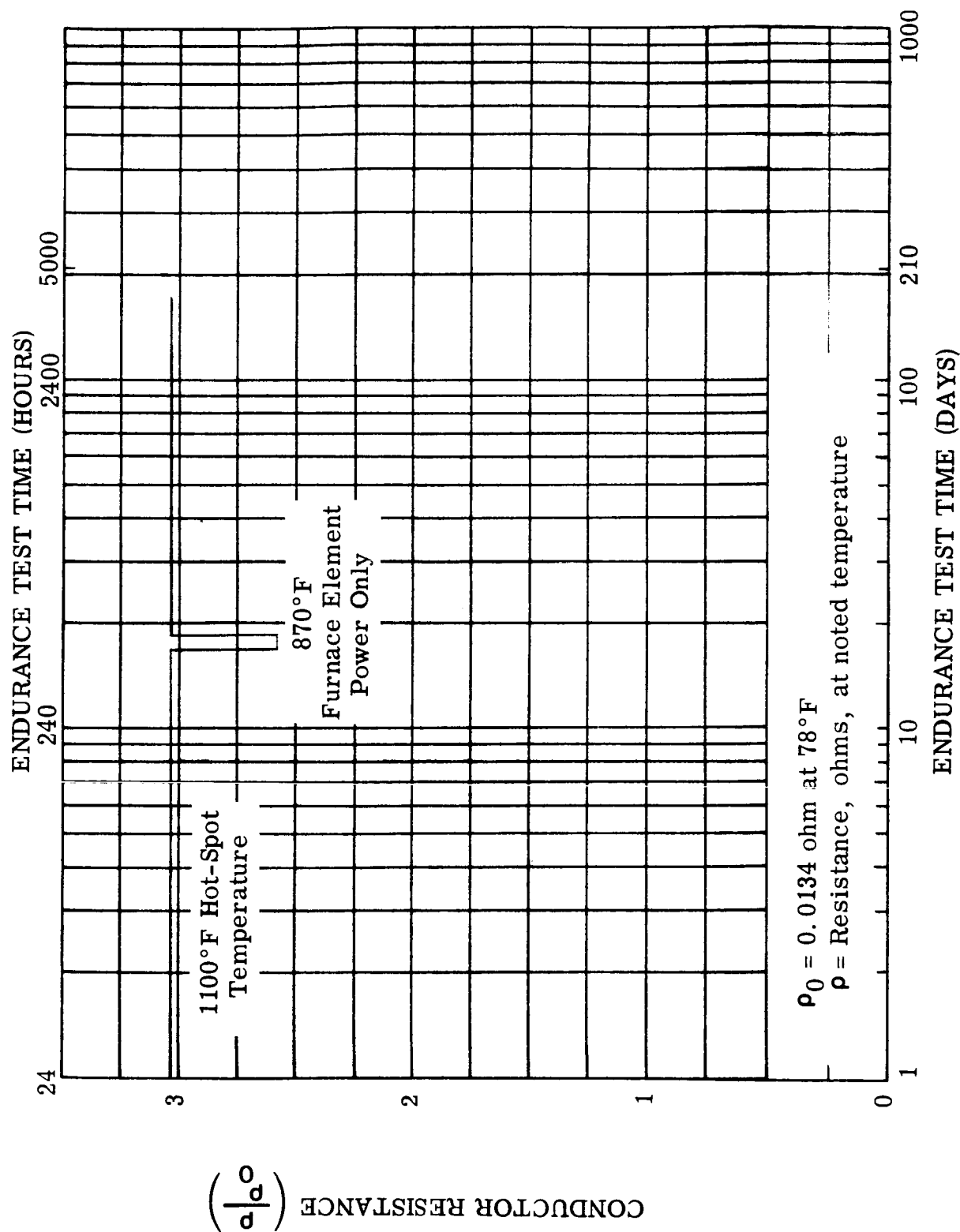


Figure IV-16. Stator Conductor Resistance Versus Endurance Test Time

FIGURE IV-16. Stator Conductor Resistance Versus Endurance Test Time at Noted Conductor Hot-Spot Temperatures

by the temperatures shown on the figure. Conductor resistance at a constant temperature has not indicated any change in more than 4000 hours of test time.

Table IV-4 is a tabulation showing the stator insulation system performance as the test progressed. Readings were taken with 500 volts d-c potential applied between each pair of phases and each phase to ground. Hot spot temperature (stator slot) was maintained in part by the furnace heater element and in part by the current through the stator windings which develops resistive heating. Slot-liner temperatures begin to decrease as soon as power is removed in order that static electrical readings can be taken. The approximate temperatures at which readings were obtained are listed in the table. Insulation resistance varies primarily as a function of temperature.

Refer to the program fifth quarterly report for additional details on stator test procedures.

c. STATUS OF 1300°F STATOR MODEL - 2nd 5000 HOUR TEST

The 1300°F stator test model design is the same as the 1100°F model except for three materials changes. Nickel-clad silver wire is being replaced by Inconel-clad silver wire, to obtain greater mechanical strength at 1300°F temperatures. Conductor wire insulation is being changed from Anadur "E" glass to Anadur "S" glass, to provide increased insulation stability and increased retention of mechanical strength at temperature. "E" glass, which is a boro-silicate glass fiber, devitrifies and loses strength rapidly at temperatures above 1200°F. "S" glass is composed of over 99 percent silicon dioxide which is stable in the temperature range anticipated for this device. Presently available encapsulation compounds are not satisfactory for use at 1300°F because of outgassing characteristics and electrical insulation strength. W-839 encapsulation compound (aluminum-orthophosphate-bonded zircon) will be replaced by a chopped boron nitride fiber cement, which is currently being developed on a Westinghouse independent program. Details of this program will be covered in the next quarterly report.

TABLE IV-4. Stator Insulation Performance

Endurance Test Time (hours)	0	1000	2000	3000	4000
(Approximate Hot Spot Temperature-°F)	(1060)	(1070)	(1065)	(1078)	(1047)
Average Insulation Resistance (ohms) with 500 V d-c Applied:					
Phase to Phase(a)	6.8x10 ⁶	6.5x10 ⁶	5.4x10 ⁶	5.9x10 ⁶	9.7x10 ⁶
Phase to Ground(b)	3.6x10 ⁶	4.3x10 ⁶	2.3x10 ⁶	2.6x10 ⁶	4.1x10 ⁶
(a) All phase readings within 10 percent of average.					
(b) All phase-ground readings within 15 percent of average.					
Rectangular nickel-clad silver conductor (0.093 inch x 0.144 inch) with Anadur E glass insulation; 99% alumina slot liners; 0.047 inch thick 99% alumina strips between phases.					

3. Program for the Next Quarter

- a) Complete 5000 hours of stator endurance testing with a hot-spot temperature of 1100°F.
- b) Perform post-endurance test electrical, physical and chemical tests as required to determine the condition of the stator model.
- c) Complete manufacture of a second stator model rated for high-vacuum, high-temperature operation at a hot-spot temperature of 1300°F.
- d) Install the second stator model and bore seal capsule in a thermal vacuum chamber and begin a 5000-hour, 1300°F hot-spot endurance test.

C. TASK 3 - TRANSFORMER

1. Summary of Technical Progress

- a) A total of 4015 endurance test hours was accumulated as of the end of the sixth program quarter.
- b) Thermal-vacuum chamber pressure at the beginning of the period was 4.8×10^{-8} torr. Pressure had decreased to 7.4×10^{-9} torr at the end of the report period.
- c) A transformer design suitable for operation in high vacuum with a 1300°F hot-spot temperature has been defined.

2. Discussion

a. TRANSFORMER INSTALLATION, CONSTRUCTION AND OPERATION AT 1100°F

Figure IV-17 is a cutaway drawing of the thermal vacuum chamber showing the transformer and two solenoids installed in the furnace hot zone. Thermocouples and power leads were brought up through the top heat shields in the same manner as with the stator. Power leads were brazed to OFHC copper bus bar feedthroughs inside the chamber, and the thermocouples were passed through hollow Kovar tube feedthroughs and brazed to the tubes outside the chamber.

The transformer design is rated at 1 KVA with 600 volts a-c on the primary winding and approximately 30 volts on the secondary winding. This 600 volt a-c single-phase design is representative of the technology for a three-phase transformer having the same phase voltage which, when coupled in a wye network with a full wave rectifier system, would provide 1400 volts d-c.

The transformer core was made from E-I style Hiperc 27 alloy laminations 0.008 inch thick, with a coating of plasma-arc sprayed Linde A compound (Al_2O_3) on one side of each lamination (same as stator laminations). The windings were formed around a ceramic spool (99.5% Al_2O_3) which provided insulation between the windings and the center leg of the core. Alumina (99.5%) end plates and channels provided insulation between the winding ends and sides and the laminations. Non-magnetic alloy strips

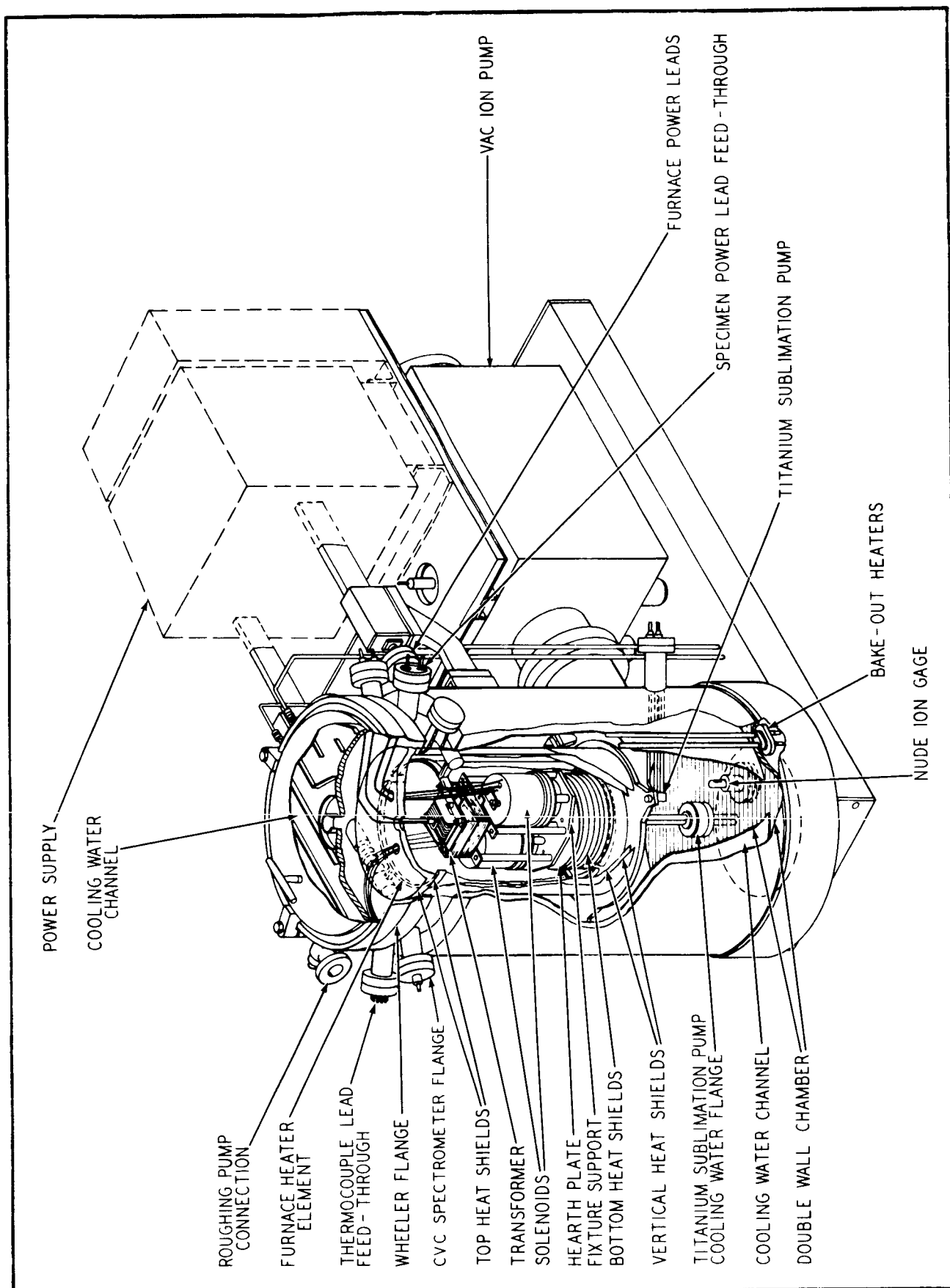


FIGURE IV-17. Cutaway View of a Vacuum Furnace Showing Installation of Two Solenoids and a Transformer

(Hastelloy Alloy "B") were used outside the laminations to provide lamination support. The laminations and support strips were held together by through-studs, ceramic washers and lock nuts. The primary winding was made from #20 gauge (0.032 dia) nickel-clad silver wire (20 percent nickel cross-sectional area) coated with Anadur insulation, and consisted of 174 turns in five layers. Flexible insulation (Burnil CM-2) 0.010 inch thick was used to separate the layers. The secondary winding was a single layer 10 turn coil made from the same type wire and insulation but in #7 gauge size (0.144 dia). Four layers of 0.010 inch thick Burnil CM-2 were installed between the outermost primary winding layer and the secondary winding. Pairs of thermocouples were installed between the primary winding and ceramic spool and between the primary and secondary windings. The stack was divided into two halves by ceramic strip spacers so that two thermocouples could be buried in ceramic tubes in the center of the core. During the period of normal transformer operation prior to the primary winding failure, the primary winding current density was 2130 amperes per square inch and secondary winding current density was 1800 amperes per square inch.

Refer to the program fourth quarterly report for additional details on transformer construction, preparations for installing the transformer in the test chamber, and initiation of the test program.

Transformer test operation was routine during the program quarter. Both windings were connected in series and supplied by an a-c voltage source to maintain a 600 volt a-c potential between each winding and ground. This mode of test was adopted in the fourth quarter after the primary winding developed a layer-to-layer short circuit which prevented normal transformer operation. Details of this are covered in the fourth quarterly report. The 1100° F test hot-spot temperature was established in the energized solenoid (Task 4), which is installed in the same test chamber. Transformer temperature was maintained at an average value of 1035° F by heat radiated from the solenoid and test chamber heater element.

Static electrical measurements were taken once each week, covering winding resistance, d-c insulation resistance, and insulation leakage current when subjected to an a-c voltage potential.

Titanium sublimation pump (TSP) bursts of two minute duration were used at intervals to evaluate the effect on the chamber base pressure. Early in the program quarter, the chamber pressure was reduced by approximately one decade after each TSP burst, but it would begin to rise to the base level within minutes after reaching its lowest values. By the end of the program quarter a two minute TSP burst was drawing the chamber pressure down into the 10^{-10} torr range, where it would remain for several hours before beginning to rise.

b. TRANSFORMER DATA AND DISCUSSION

Figure IV-18 is a plot of chamber pressure vs. endurance test time. The total time shown applies to the solenoids rather than the transformer, as time was not logged for the transformer during periods when either power or a voltage potential was not applied. The power supply for the transformer is one phase of the generator which supplies the stator. The curve shows the temporary pressure reductions that occurred when two minute titanium sublimation pump bursts were applied. It also shows the pressure decreases which accompanied the removal of power when the Variac failed and during a plant-wide power failure which occurred in the fourth program quarter. Chamber pressure was read by a Bayard-Alpert type nude ion gauge.

Figure IV-19 is a dimensionless plot of the transformer primary and secondary conductor resistance as a function of endurance test time. Neither conductor showed any change in resistance values at constant temperature during the reporting period.

Table IV-5 tabulates transformer insulation system performance during the course of endurance testing. Initially the transformer was set up to operate at a rated load of 1 KVA with 600 volts on the primary winding, approximately 30 volts on the secondary winding, and a hot-spot temperature of 1100°F (center of lamination stack). After 107 hours of endurance testing a layer-to-layer short circuit developed in the primary winding, making it impossible to load the transformer. From that point on, a 600 volt a-c winding-to-ground potential was applied to each winding. The test hot-spot temperature (1100°F) was established in the energized solenoid and the transformer temperature was established by radiation from the solenoid and the chamber heating element. The temperature balance begins to change when power is removed from the energized solenoid so that static measure-

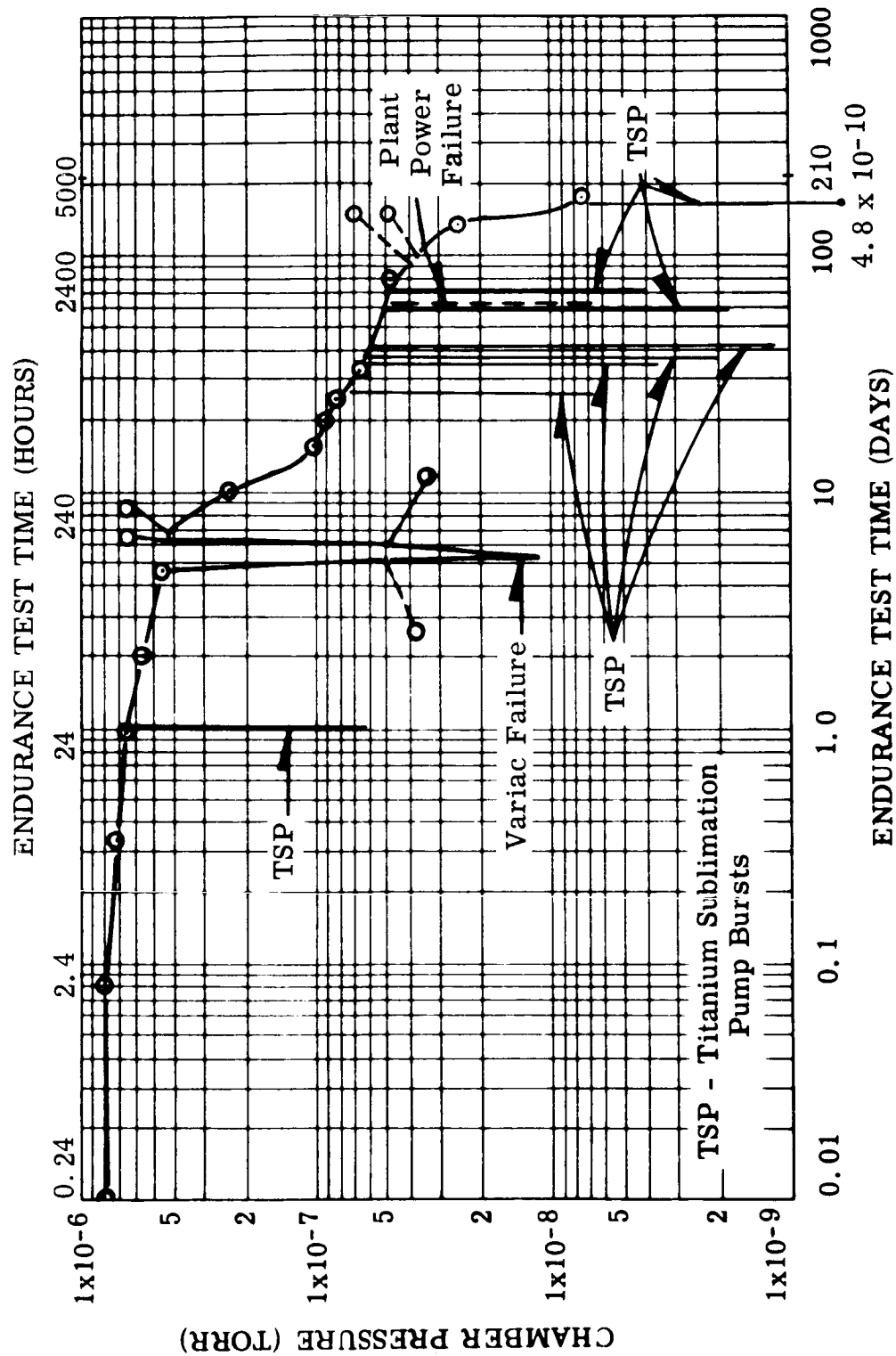


Figure IV-18. Transformer and Solenoid Chamber Pressure vs. Endurance Test Time

FIGURE IV-18. Transformer and Solenoid Chamber Pressure vs. Endurance Test Time

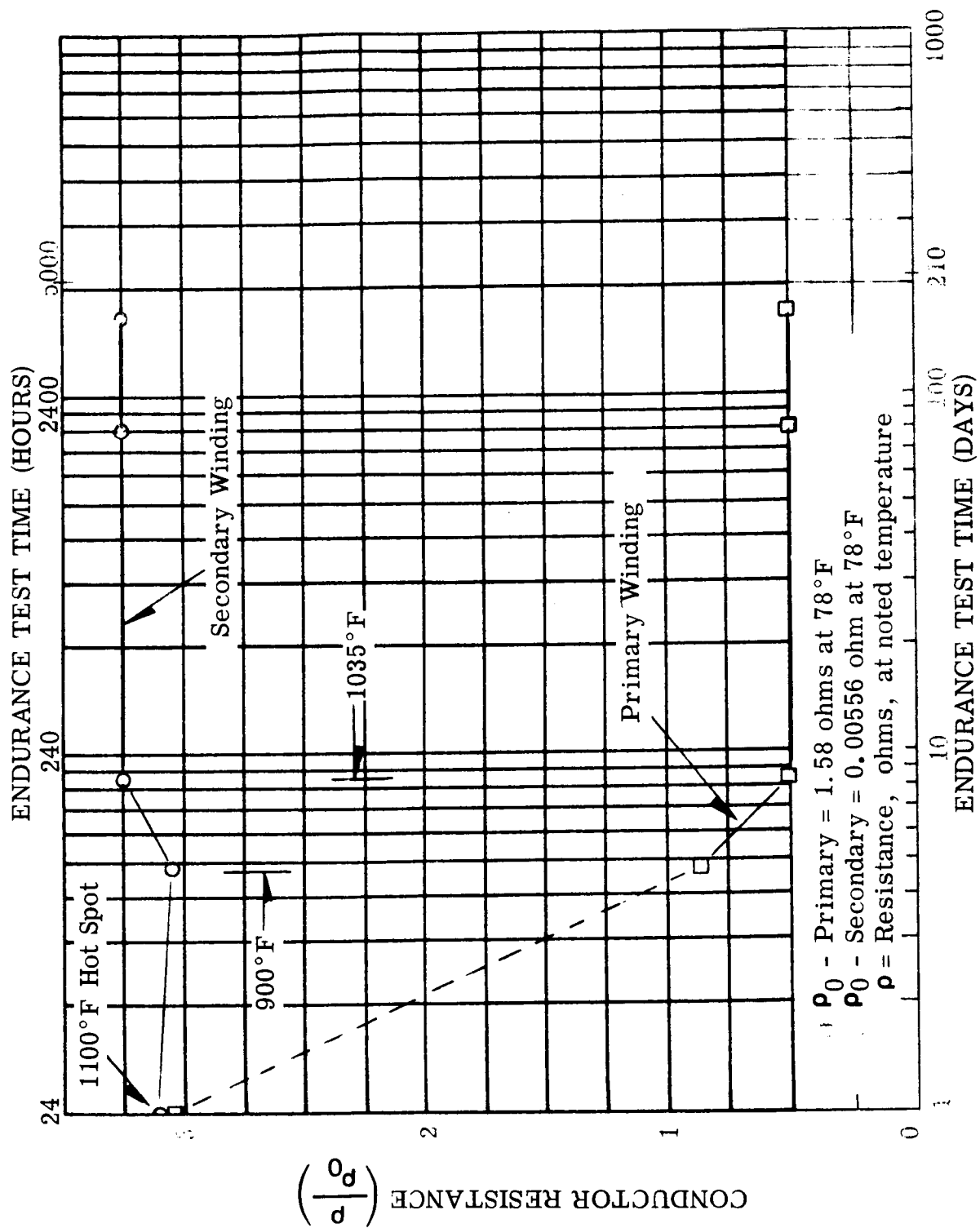


Figure IV-19. Transformer Winding Resistance Versus Endurance Test Time

TABLE IV-5. Transformer Insulation Performance

Endurance Test Time (hours)	0	1000	2000	3000	4000
(Approximate Hot Spot Temperature- °F)	(1100)	(1020)	(1035)	(1032)	(1003)
Average Insulation Resistance (ohms) with 500 V d-c Applied:					
Primary to Secondary ^(a)	1.52x10 ⁶	0.85x10 ⁶	0.8x10 ⁶	0.8x10 ⁶	0.85x10 ⁶
Primary to Ground ^(b)	11x10 ⁶	16x10 ⁶	14.7x10 ⁶	14.8x10 ⁶	24x10 ⁶
Secondary to Ground	18x10 ⁶	18x10 ⁶	14.5x10 ⁶	14.7x10 ⁶	23x10 ⁶
<p>(a) Primary winding developed a layer-to-layer short circuit after 107 hours of endurance testing.</p> <p>(b) Primary Winding - 0.032 inch diameter nickel-clad silver wire with Anadur E glass insulation-0.010 inch thick synthetic mica between layers. Secondary Winding - 0.144 inch diameter nickel-clad silver wire with Anadur E glass insulation; four 0.010 inch thick layers of synthetic mica insulation between primary and secondary windings.</p>					

ments can be taken. Approximate temperatures are shown for each insulation resistance reading. Insulation resistance varies primarily as a function of test temperature.

Refer to the fifth quarterly report for more detailed information on transformer test data.

c. STATUS OF 1300°F TRANSFORMER MODEL - 2nd 5000 HOUR TEST

The 1300°F transformer test model design is the same as the 1100°F model except for four materials changes. Nickel-clad silver wire is being replaced by Inconel-clad silver wire, to obtain greater mechanical strength at 1300°F temperatures. The winding wire insulation is being changed from Anadur "E" glass to Anadur "S" glass, for the same reasons that were

described in the 1300°F stator model write-up. Very little W-839 encapsulation compound was used on the 1100°F model, but because of high-temperature outgassing characteristics, it is being replaced by a chopped boron nitride fiber cement.

The Burnil CM-2 (3M Company) flexible sheet insulation which was used between winding layers in the 1100°F model does not have adequate electrical insulation capabilities at 1300°F. Westinghouse has been developing a flexible sheet insulation made from boron nitride fibers on an independent program. This material will be used to replace the Burnil CM-2 in the 1300°F transformer model.

3. Program for the Next Quarter

- a) Complete 5000 hours of high vacuum, high temperature testing on the transformer.
- b) Perform post-endurance test electrical, physical, and chemical tests as required to determine the condition of the transformer model.
- c) Complete the manufacture of a transformer model rated for high vacuum, high temperature operation at a hot-spot temperature of 1300°F.
- d) Install the transformer in a thermal vacuum chamber and begin a 5000 hour 1300°F hot-spot endurance test.

D. TASK 4 - SOLENOID

1. Summary of Technical Progress

- a) A total of 4039 endurance test hours was accumulated as of the end of the sixth program quarter.
- b) Thermal vacuum chamber pressure at the beginning of the period was 4.8×10^{-8} torr. Pressure had decreased to 7.4×10^{-9} torr at the end of the report period.
- c) A solenoid design suitable for operation in high-vacuum with a 1300°F hot-spot temperature has been defined.

2. Discussion

a. SOLENOID INSTALLATION, CONTRUCTION AND OPERATION AT 1100°F

The transformer installation cutaway drawing, Figure IV-17 also shows how the two solenoids were fitted into the chamber. All three components were installed at the same time.

The solenoid magnetic housing, cover and plunger are made from Hiperc 27 alloy forged material. The coil is wound on an alumina (99%) spool which provides insulation between the winding and the plunger and housing center core. Alumina end plates insulate the sides of the winding from the housing and cover. Bearing surfaces for the plunger consist of an alumina guide rod at one end of the plunger and an alumina bushing at the opposite end. The winding was formed from 1860 turns of #20 (0.032 dia) nickel-clad silver wire with an Anadur insulation system. This is the same wire that was used for the transformer primary winding.

Pairs of thermocouples were installed between the winding inside diameter and the ceramic spool, at the radial mid-winding point, between the winding outside diameter and the housing and on the housing outside diameter. All except the housing outside diameter thermocouples were installed in 99% alumina tubes.

Each solenoid is rated at 1530 ampere-turns at 28 volts d-c and a hot-spot temperature of 1100°F. Refer to the program fourth quarterly report for additional details on solenoid construction,

preparations for installing the solenoids in the test chamber, and initiation of the test program.

Solenoid test operation was routine during the program quarter. One solenoid was continuously energized with 13.0 volts d-c and 0.34 amperes, and the other was briefly energized weekly to verify movement of the plunger. The 1100°F hot-spot test temperature was established in the continuously energized solenoid. Test current density in the energized solenoid was 670 amperes per square inch.

Static electrical measurements were taken once each week, covering winding resistance, d-c insulation resistance, and insulation leakage current when subjected to an a-c voltage potential. Pick-up and drop-out voltages and currents were also measured on each solenoid, to verify that the plungers were not immobilized in one position. Average temperature in the unenergized solenoid was 1065°F.

b. SOLENOID DATA AND DISCUSSION

Each solenoid accumulated 4039 endurance test hours during the report period. One solenoid was energized continuously except during the taking of electrical readings. The other was unenergized except for periodic checks on plunger movability.

Figure IV-18 (Task 3 - Transformer) shows the chamber pressure versus test time curve which is also applicable to the solenoids. Pressure readings were taken with a nude ion gauge which is mounted in the bottom of the test chamber.

Figure IV-20 is a dimensionless plot of winding conductor resistance versus time for both solenoids. There was no change in resistance at constant temperature in either solenoid during the reporting period.

Table IV-6 is a tabulation of insulation performance for the energized and unenergized solenoids in terms of endurance test time. Readings were taken with a 500 volt d-c potential between each winding and ground. The temperature balance begins to change as soon as power is removed from the energized solenoid so that static readings can be made. Approximate temperatures at the time data were taken are shown with the insulation resistance

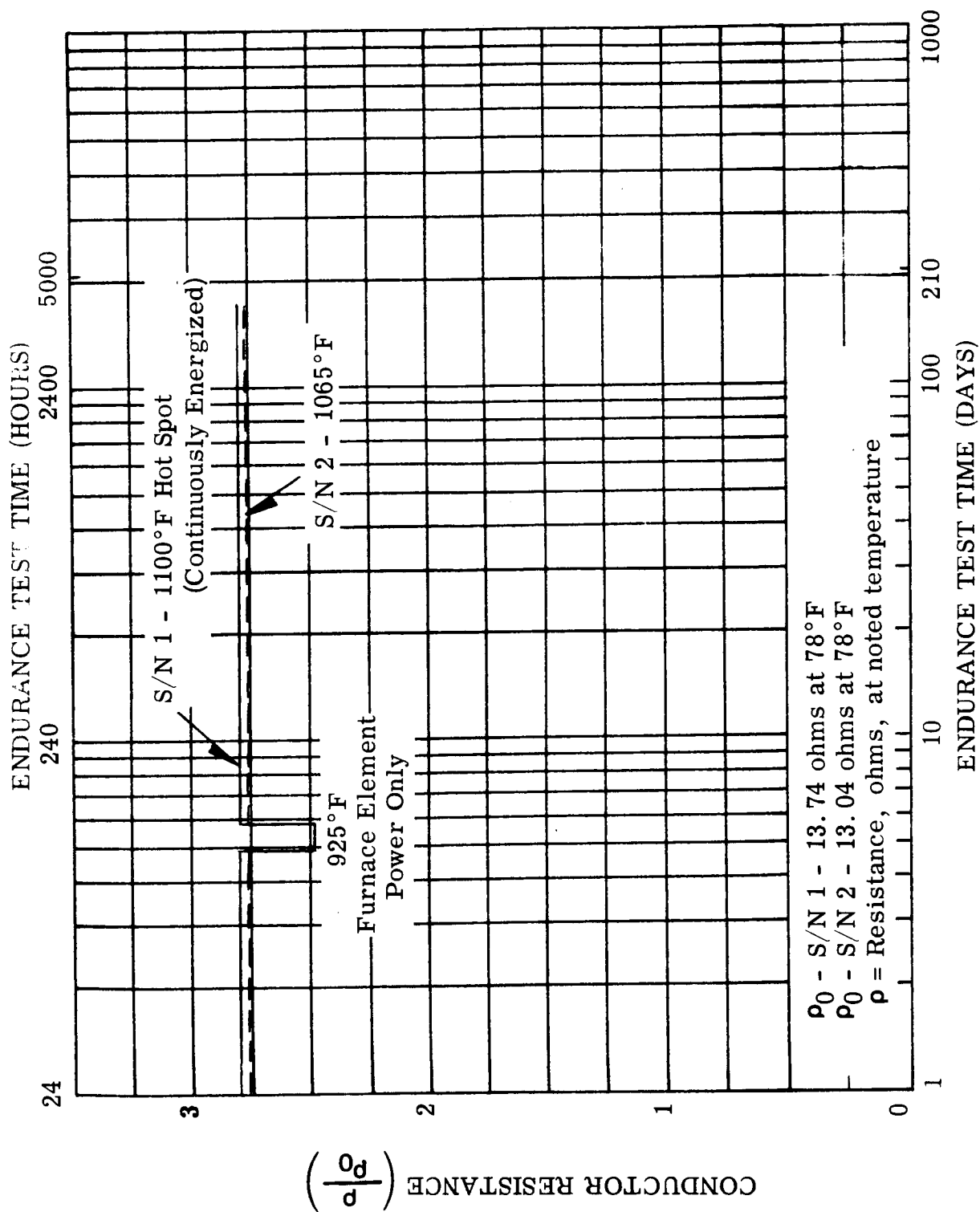


Figure IV-20. Solenoid Conductor Resistance Versus Endurance Test Time

FIGURE IV-20. Solenoid Conductor Resistance Versus Endurance Test Time

TABLE IV-6. Solenoid Insulation Performance

Endurance Test Time (hours)	0	1000	2000	3000	4000
Insulation Resistance (ohms) with 500 V d-c Applied:					
<u>S/N 1 (Energized)</u>					
Winding to Ground	10×10^6	9.5×10^6	9.0×10^6	7.3×10^6	7.2×10^6
(Approximate Hot Spot Temperature-°F)	(1103)	(1100)	(1110)	(1105)	(1085)
<u>S/N 2 (Not Energized)</u>					
Winding to Ground	21×10^6	13×10^6	13.5×10^6	14×10^6	20×10^6
(Approximate Hot Spot Temperature-°F)	(1027)	(1053)	(1070)	(1058)	(1034)
0.032 inch diameter nickel-clad silver wire with Anadur E glass insulation; 99% alumina winding spool and 99.5% alumina winding end plates.					

values. The insulation system resistance in the energized solenoid shows an apparent slight decrease in value with time as a result of an invariant electrical stress. The non-energized solenoid insulation resistance appears to vary primarily as a function of test temperature.

Solenoid temperature data was to have been reviewed for the possibility of determining apparent thermal conductivities for some of the materials. This effort has been abandoned, because the thermocouples had to be located so as to provide information on the materials being tested rather than for heat transfer purposes. The temperature gradients measured do not provide the information required for meaningful heat transfer calculations although they provide a good picture of temperature distribution in the assemblies.

c. STATUS OF 1300°F SOLENOID MODEL - 2nd 5000 HOUR TEST

The 1300°F solenoid test model design is the same as the 1100°F model except for three materials changes. Inconel-clad silver wire replaces nickel-clad silver wire and the Anadur insulation on the wire will be "S" glass in place of "E" glass. Boron nitride cement replaces W-839 encapsulating compound. The reasons for these changes are the same as those detailed in the 1300°F stator model write-up.

3. Program for the Next Quarter

- a) Complete 5000 hours of solenoid endurance testing with a hot-spot temperature of 1100°F.
- b) Perform post-endurance test electrical, physical and chemical tests as required to determine the condition of the solenoid models.
- c) Complete the manufacture of two solenoid models rated for high vacuum, high-temperature operation at a hot-spot temperature of 1300°F.
- d) Install the two solenoids in a thermal vacuum chamber and begin a 5000 hour 1300°F hot-spot endurance test.

SECTION V

REFERENCES

Reports published on this program are:

Kueser et al, P.E. , "Development and Evaluation of Magnetic and Electrical Materials Capable of Operating in the 800° to 1600°F Temperature Range", First Quarterly Report, NASA-CR-54354, March 1965.

Kueser et al, P.E. , "Development and Evaluation of Magnetic and Electrical Materials Capable of Operating in the 800 ° to 1600°F Temperature Range", Second Quarterly Report, NASA-CR-54355, June 1965.

Kueser et al, P.E. , "Development and Evaluation of Magnetic and Electrical Materials Capable of Operating in the 800° to 1600°F Temperature Range", Third Quarterly Report, NASA-CR-54356, September 1965.

Kueser et al, P.E. , "Development and Evaluation of Magnetic and Electrical Materials Capable of Operating in the 800° to 1600°F Temperature Range", Fourth Quarterly Report, NASA-CR-54357, December 1965.

Kueser et al, P.E. , "Development and Evaluation of Magnetic and Electrical Materials Capable of Operating in the 800° to 1600°F Temperature Range", Fifth Quarterly Report, NASA-CR-54358, March 1966.

References cited in this report follow and are grouped by Program and Task.

Section II

Program I - Magnetic Materials for High-Temperature Operation

References for Task 3 - Dispersion-Strengthened Magnetic Materials for Application in the 1200-1600°F Range.

1. H. P. Tripp and B. W. King, "Thermodynamic Data On Oxides at Elevated Temperatures", J. Am. Cer. Soc., V. 38, no. 12, December 1, 1955, pp. 432-437.
2. S. B. Brandstedt, "Other Iron and Nickel Base Alloys in Powder Metallurgy", Stainless Steel Powder Seminar, Detroit, Michigan, February 25, 1965, sponsored by Hoeganaes Sponge Iron Corp., Riverton, New Jersey.
3. G. W. Fischer et al, "Complex Shapes by Slip Casting", Interim Progress Report Phase I, May 1964-August 1964, Contract AF 33(657)1366, General Electric Co., Cincinnati, Ohio AD 444008.
4. K. Farrell, "Sintering of Atomized Superalloys and a Hardenable Stainless Steel", Int. J. Powder Met., V. 1, no. 3, July 1965, pp. 26-36.
5. K. Farrell, "Forging Sintered Inconel 713C Powder Compacts", Int. J. Powder Met., V. 2, no. 1, January 1966, pp. 3-5.
6. TD Nickel, Dispersion-Strengthened Nickel, Du Pont Metal Products, Production Information A-41076, E. I. du Pont de Nemours & Co., Wilmington, Delaware.
7. M. Adachi and N. J. Grant, "The Effects of Stored Energy and Recrystallization on the Creep Rupture Properties of Internally Oxidized Copper-Alumina and Copper-Silica Alloys", Trans. Met. Soc. AIME, V. 218, October 1960, pp. 881-887.
8. V. A. Tracey and D. K. Worn, "Some Observations on the Cold-Drawing and Annealing Behavior of Nickel Containing a Dispersed Phase of Thoria", Powder Metallurgy, no. 10, 1962, pp. 34-48.

9. R.W. Fraser, B. Meddings, D.J.I. Evans and V.N. Mackiw, "Dispersion-Strengthened Nickel by Compaction and Rolling of Powder Produced by Pressure Hydrometallurgy", International Powder Metallurgy Conference, June 14-17, 1965, New York, New York.
10. A.L. Mincher, W.I. Pollock, and L.J. Klinger, "Research on Dispersion-Strengthened Cobalt-Base Alloys", Third Quarterly Progress Report under AF 33(615)1680, September 1, 1965 to December 1, 1965.
11. A.S. Bufferd, Sc. D. Thesis, Dept. of Metallurgy, Massachusetts Institute of Technology, 1965.
12. J.E. White and R.D. Carnahan, "A Microplasticity Study of Dispersion Strengthening in TD-Nickel", Trans. Met. Soc. AIME, V. 230, October 1964, pp. 1298-1306.
13. G.S. Doble and R.J. Quigg, "Effect of Deformation on the Strength and Stability of TD Nickel", Trans. Met. Soc. AIME, V. 233, February 1965, pp. 410-415.
14. C.T. Sims, "Structural Stability in Ni-2ThO₂ Alloy", Trans. Met. Soc. AIME, V. 227, December 1963, pp. 1455-1457.
15. M.C. Inman, K.M. Zwilsky and D.H. Boone, "Recrystallization Behavior of Cold Rolled TD-Nickel", Trans. ASM, V. 57, 1964, pp. 701-713.

Section IV

Program III - Bore Seal Development and Combined Material Investigation Under a Space-Simulated Environment

References for Task 1 - Bore Seal Development

1. Kueser, P. E. et al, Bore Seal Technology, NASA-CR-54093, Contract 3-4162, December 1964.

2. Brown, R.J., Brush Beryllium Co., Elmore, Ohio, personal communication with R.C. McRae, EIMAC, Division of Varian, April 22, 1966.
3. Reed, L. and R.C. McRae, Evaporated Metalizing on Ceramics, American Cer. Soc. Bull. V. 44, December 1965.